REPEATED, LOW DOSE *CHLAMYDIA* INFECTIONS TRIGGER ABERRANT IMMUNE RESPONSES AND WEAKENED HOST RESISTANCE AGAINST SECONDARY CHALLENGE

by

Monica M. Surette

Submitted in partial fulfilment of the requirements
for the degree of Master of Science

at

Dalhousie University
Halifax, Nova Scotia
April 2022

Dedicated to all of the extraordinary people I have the privilege of calling my family, especially my Mom and Dad.

TABLE OF CONTENTS

LIST OF TABLES

LIST OF FIGURES

ABSTRACT

Chlamydia trachomatis infections endanger women's health, but translational gaps between animal models and human disease states persist. I compared immune responses in mice receiving repeated, low dose infections (5X) with *Chlamydia muridarum* to those generated by a conventional single, high dose infection (1X). While 5X and 1X infection schedules stimulated comparable CD4+ Th1 responses, the 5X infections concomitantly induced strong anti-inflammatory Th2 and regulatory T cell responses, as well as pro-inflammatory Th17 responses. Neutrophil infiltration, which may be associated with severe tissue damage, was substantially elevated in the 5X group. In accordance with the divergent immune responses observed in two groups of mice, mice with a prior 5X infection displayed significantly reduced bacterial clearance rates compared to those with a previous 1X infection during subsequent reinfections. En masse, I demonstrate that repeated, low dose infections produce immune responses in mice that closely resemble immune profile and outcomes in humans.

LIST OF ABBREVIATIONS AND SYMBOLS USED

ACK	ammonium-chloride-potassium
ANOVA	analysis of variance
APC	antigen-presenting cell
bp	base pair
BS	bovine serum
BSA	bovine serum albumin
Cm	*Chlamydia muridarum*
Ct	*Chlamydia trachomatis*
DC	dendritic cell
DNA	deoxyribonucleic acid
d.p.i.i.	days post initial infection
d.p.s.i.	days post secondary infection
EB	elementary body
EDTA	ethylenediaminetetraacetic acid
ELISA	enzyme-linked immunosorbent assay
FACS	fluorescence-activated cell sorting
FOXP3	forkhead box P3
FRT	female reproductive tract
gDNA	genomic deoxyribonucleic acid
GFP	green fluorescent protein
HBSS	Hank's balanced salt solution
HEPES	4-(2-hydroxyethyl)-1-piperazineethanesulfonic acid

H & E	hematoxylin and eosin
HK*Cm*	heat-killed *Chlamydia muridarum*
HRP	horseradish peroxidase
HSP	heat shock protein
ICCS	intracellular cytokine staining
IFN	interferon
IFU	inclusion forming unit
Ig	immunoglobulin
IL	interleukin
LIF	leukemia inhibitory factor
LPS	lipopolysaccharide
mg	milligram
ml	milliliters
mM	millimolar
MOMP	major outer membrane protein
MSC	mesenchymal stromal cells
ng	nanogram
NK	natural killer
OD	optical density
PBS	phosphate buffered saline
PCR	polymerase chain reaction
PDPN	podoplanin
pH	potential of hydrogen

PID	pelvic inflammatory disease
qPCR	quantitative polymerase chain reaction
RB	reticulate body
RIPA	radioimmunoprecipitation assay buffer
RPMI	Roswell Park Memorial Institute medium
RT	room temperature
SEM	standard error of mean
SPG	sucrose-phosphate-glutamic buffer
TGF	transforming growth factor
Th	T helper cell
TLR	toll-like receptor
TMB	tetramethylbenzidine substrate solution
TNF	tumour necrosis factor
Treg	regulatory T cell
tSNE	t-distributed stochastic neighbor embedding
UP	unprimed
WT	wild-type
1X	single dose infection schedule
5X	repeated, low dose infection schedule
°C	degrees Celsius
µg	microgram
µl	microliter
µm	micrometer

ACKNOWLEDGMENTS

I would like to sincerely thank my supervisor, Dr. Jun Wang, for her continued patience, support, and encouragement during my degree. Dr. Wang, I am so grateful for the opportunity to pursue this research, thank you for guiding me through this project! I would also like to express my thanks and appreciate to the members of my supervisory committee, Dr. Jeanette Boudreau and Dr. Jean Marshall, for their invaluable contributions to this work by their insight, feedback, and suggestions.

I appreciate the support of the Microbiology and Immunology Department of Dalhousie University throughout the course of my program. I am thankful for funding from the Department, as well as from the Dalhousie Medical Research Foundation I3V graduate studentship, which have made this research possible. I would like to recognize Nong Xu for his support and contributions throughout my project, especially with the qPCRs, Luminex, and ELISA! I would also like to recognize the substantial work that Derek Rowter and Renee Raudonis provide to support my flow cytometry projects.

I would like to thank my colleagues, past and present, in the lab. Anima, Julia, Dongpu, Kathy, Ashley, Moe, and Melanie: thank you for everything! I would like to express my appreciation of Melanie Tillman's time and effort with the foundational work used as a basis for this thesis. I would like to acknowledge Animamalar Mayavannan for her overall camaraderie and support for training and during animal work. I would like to emphasize that this work would not be possible without the generous use of Animamalar's skillfully purified *Chlamydia muridarum* stock. I would also like to thank Dr. Jinghua Liu for her support throughout my project, especially with the sequencing work!

I would like to sincerely thank my family for their support over the course of my degree: thank you Mom, Dad, Emily, John, Leo, and all of my wonderful aunts, uncles, and cousins for your support, encouragement, thoughtful questions, and *Chlamydia* jokes over the last few years! Each of you have helped me in more ways than I could list (even if I wrote another thesis about it) and I am so grateful for all of you!

CHAPTER 1 INTRODUCTION

1.1 Overview of *Chlamydia*

The *Chlamydiae* family contains bacteria with a diversity of species that are found as pathogens and commensals, in habitats that vary in range and extend to the bottom of the Arctic Ocean (1). *Chlamydia* is a Gram-negative coccobacillus, possessing an outer membrane with lipopolysaccharides (LPS) and major outer membrane protein (MOMP), a thin periplasmic space, and an inner membrane (2). The range of hosts that *Chlamydia* can infect is vast (3). The process of co-evolution with distinct hosts began millions of years ago for *Chlamydia* (4). Individual host species have distinct susceptibility profiles to species of *Chlamydia* despite the relative genetic similarity across the genus (5). To this end, disease outcomes are generally species specific in regard to both the host and the *Chlamydia* (6).

C. pneumoniae possesses infective potential for animal and human populations (7). Infection with *C. pneumoniae* results conjunctivitis and respiratory tract infections in equestrian, amphibian, reptilian, and marsupial species, although no zoonotic transmission of *C. pneumoniae* has been reported (3, 7). Community transmission of *C. pneumoniae* in human populations is frequently reported and can result in respiratory infections, such as bronchitis and pneumonia (8). While human disease *with C. pneumoniae* is typically mild, a third of infections can cause serious illness (8).

Chlamydia trachomatis (*Ct*) is a human specific pathogen and the resultant infections are a serious global health concern (7). *Ct* serovars are distinguished by the antigenic epitopes present in the MOMP, and specific disease states are associated with particular serovars (9). There are 18 serovars identified and the major disease states are lymphogranuloma venereum, trachoma, and genitourinary infections (7). Lymphogranuloma venereum infections are due to the L1, L2, L2a, and L3 *Ct* serovars and all are sexually transmitted (7). Trachoma is an ocular *Ct* infection caused by serovars A, B, Ba, and C; it can be transmitted vertically from mothers to their newborns to cause conjunctivitis and pneumonia (7).

Despite public health campaigns, *Ct* trachoma infections remain the leading cause of preventable blindness globally (10). Urogenital *Ct* infections are one of the most prevalent bacterial sexually transmitted infections in the world (11) and are the result of genital, rectal, and pharyngeal tissue infection by serovars B, Da, Ga, Ia, and D-K (7). Despite the homology between the serovars, lymphogranuloma venereum is considered to be more invasive due to its replication in the lymph nodes and monocytes, which can result in severe lymph tissue pathology (7). All other *Ct* serovars replicate in mucosal epithelial, squamocolumnar, or transitional epithelial cells to wreak havoc in more covert and disseminated, though clinically significant, ways (7).

C. suis and *C. cavie* are pig and guinea pig pathogens, respectively (3). These chlamydial species are most commonly associated with conjunctivitis and respiratory infections in their hosts (3). *C. muridarum* (*Cm*) is a murine specific chlamydial species with no known potential for human disease; its only hosts are hamsters and mice (3). Initially, *Cm* was considered a biovar of *Ct*, but genetic sequencing has clarified its identity as a species (6). *Cm* is used primarily for infection modelling in research settings, due to its 98% genetic similarity to the D serovar of *Ct* (5).

Other chlamydial species have a more established zoonotic potential. *C. abortus* is a pathogen for ruminants, such as cows, and can cause infection in the female genital tract (3). Infection following *C. abortus* is associated with spontaneous abortion and stillbirth, making it a pathogen of concern for agriculture and animal husbandry (3). Similarly, *C. psittaci* is an avian pathogen that results in mild ocular, respiratory, and hepatic infections in birds (3). When *C. psittaci* is zoonotically transmitted to humans, the resultant psittacosis has the capacity to cause life-threatening pneumonia in vulnerable patient populations (12).

1.1.1 *Chlamydia* life cycle

Unlike many bacteria, which conventionally exist extracellularly, *Chlamydia* are obligate intracellular parasites (2). The life cycle of *Chlamydia* is biphasic and split into an extracellular and an intracellular phase, during which the *Chlamydia* is referred to as an elementary body (EB) and a reticulate body (RB), respectively (2). While only the

larger RB is metabolically active, the small EB is responsible for facilitating host cell infection, arguably the most critical component of the lifecycle (2).

To begin its journey into the host cell, the EB interacts with mucosal epithelium (13). The EB is contained with a chlamydial outer membrane complex, which is a protein shell that includes the MOMP, as well as OmcA and OmcB, which are cysteine rich proteins (14). The size constraints of the chlamydial genome, which have been estimated to be as small as 895 open reading frames for *Chlamydia trachomatis* (*Ct*), for example, have produced considerable genetic conservation across the genus; however, there are differences in the host cell receptor attachment mechanisms across species and within their serovars (2, 9). For example, the MOMP of *Ct* and the OmcB protein of both *Ct* and *C. pneumoniae* promote attachment via their interactions with heparan sulfate-like glycosaminoglycans on the host cell (15, 16). Additionally, polymorphic membrane proteins on chlamydial outer membrane complexes contribute to adherence to host cells (9).

There is no consensus on the entry mechanism of *Chlamydia*, but there is evidence of pinocytotic, phagocytotic, and endocytic mechanisms that result in the internalization of the EB in a vacuole (17). Following attachment stabilization via electrostatic mechanisms, the EB utilizes a Type 3 secretion system (T3SS) to deliver chlamydial effectors into the cytoplasm of the host cell (9). These effectors support internalization of the EB into the host cell through manipulation of the host cytoskeleton to mediate the entry into the cell and form the inclusion body, which is the membrane lined endosome that the bacteria inhabit during the intracellular portion of its lifecycle (2). The EB inclusion body is diverted away from delivery to the lysosome and instead transported to the microtubule-organizing center, located in close proximity to the Golgi apparatus, to support the conversion into RBs (9).

The nutrients present in the Golgi area support the intracellular chlamydial processes, as the bacteria does not have a full repertoire of metabolic enzymes but does possess transport systems for energy and essential nutrients, such as tryptophan (18). The *Chlamydia* commandeers lysosomal machinery to redirect the amino acids from exogenous protein breakdown, which comes at a detriment to the protein production of

the host cell (17). This nutrient pilfering supports the replication of the RB, which occurs through binary fission; this division is estimated to occur a minimum of 6 times before the RB will asynchronously convert back to the infectious EB (19). This process takes between 24-48 hours, and once it is complete, the EB is ready to be released from the cell (9).

There is a lack of consensus, but evidence suggests that the EBs can be released from the cell through the plasma membrane via lysis, which results in cell death, or extrusion, which does not destroy the cell but releases the EB into the extracellular environment within a host membrane (20). Both mechanisms have been reported relatively equally, but there is evidence that extruded *Chlamydia* have improved survival when phagocytosed by certain cell types, such as dendritic cells (DCs) or macrophages (20).

There are certain circumstances that drive a stress response during the chlamydial life cycle, and these typically include conditions that do not permit optimal replication and growth (21). Conditions within the cell, such as deficiencies in critical nutrients or the presence of molecular mediators, as well as exposure to substances such as penicillin antibiotics, have the potential to induce the persistent state (21). During persistence, the vegetative RB form is maintained and the bacterial metabolism changes, resulting in the production of proteins such as heat shock proteins; these changes allow the bacteria to ride out the adverse environment (21, 22). If persistence occurs, the infection can remain in the intracellular form and become chronic, producing further injury to the host (23)

1.2 *Chlamydia trachomatis* epidemiology in humans

1.2.1 Epidemiological trends of *Ct*

Reports of trachoma-like disease as early as 2700 BC implicate *Chlamydia* as an ancient pathogen (4), but it was not until the 1970s that *C. trachomatis* was identified as a causal agent of sexually transmitted infections (24). An uptick of chlamydial infection reporting began in the 1990s following improvements in diagnostic technologies, and rates have been increasing annually ever since (24, 25).

According to treatment guidelines published by the Centers for Disease Control and Prevention in 2021, *Ct* infections are reported more than any other bacterial infection in the United States (25). Other data confirm that this trend is applicable to other countries in the Americas and throughout the world (26). Consistently, *Ct* infection prevalence is higher in females compared to males (25, 26), however, transmission between sexual partners is estimated to be around 65%, regardless of the sex of the partner being infected (7).

There are a range of hypotheses for the sex differences observed in *Ct* infection prevalence. The anatomical differences between sexes are thought to predominantly contribute to the disparity of infection rates, as the internal environment of the vagina is more conducive to promoting infection (26). In line with this, cervical ectopy, which occurs in some women when the endocervical epithelium extrudes to the ectocervix, is known to increase the risk of *Ct* infection (27). The use of hormonal contraceptives may enhance the risk of chlamydial infection, as there is evidence that those using oral contraceptives had significantly higher rates of infections and bacterial burdens (28). However, there is a lack of consensus on whether hormonal contraceptives will directly influence the course of infection or if they are an indicator of sexual behaviors that increase the risk of *Ct* infection (29).

In addition to the sex differences in *Ct* infection rates, reports from the United States indicate that there are also differences based on age (25). Women aged 15-24 and men aged 20-29 have the highest rates of *Ct* genital infection compared to other age groups by sex (25). Furthermore, there is heterogeneity among demographics; for example, black men and women have higher rates of *Ct* infection compared to other races in the United States (7). In Canada, there are disparities in the prevalence of *Ct* infections in First Nations communities, where the rate of sexually transmitted chlamydial infections is approximated to be up to seven times higher compared to the rest of the country (30). Another important population of consideration includes sexual minorities, specifically men who have sex with men; this subpopulation has disproportionately higher levels of *Ct* infections (31, 32). Minorities and vulnerable populations are more at risk of *Ct* infections for a range of reasons, not limited to reduced healthcare access,

socioeconomic disadvantages, and systemic oppression (33), underscoring the need for research in this field to reduce disparities in infection trends and promote health equity.

1.2.2 Clinical presentation and management of urogenital *Ct* infection

Despite their high incidence and relative ease of diagnostic detection, *Ct* urogenital infections are notorious for being asymptomatic or sub-clinically symptomatic in as many as 70% of women and 50% of men (28). For this reason, sexually transmitted *Ct* infections are referred to as "silent infections". When symptoms are present for female patients, they typically include abnormal bleeding and discharge from the vagina and cervix, painful urination, and abdominal discomfort (34). When male patients have *Ct* infection symptoms, they will most often present to clinic with urethritis, including urethral discharge and dysuria, as well as pain relating to epididymitis and prostatitis (34). Once detected, *Chlamydia* infections are easily treated with antibiotics. The current clinical guidelines suggest a 7-day course of 100 mg of doxycycline bi-daily for the treatment of *Ct* infection in non-pregnant adults and adolescents (25). If doxycycline cannot be used, alternate treatments include a single 1g dose of azithromycin or 500 mg course of levofloxacin for 7 days (25).

1.2.3 Diagnostic detection of *Chlamydia* infections

Given the high proportions of asymptomatic infection, annual screening campaigns have been heavily relied upon to detect *Ct* infections in the general population (35). The Public Health Agency of Canada and the Centers for Disease Control and Prevention are aligned in their recommendations on annual screening for *Ct* infections in people under 25 years old, pregnant women, and individuals in all age groups that meet certain risk criteria (25, 35). Furthermore, the World Health Organization has previously emphasized its recommendations on surveillance as a strategy to reduce *Ct* infections globally (11). Currently, nucleic acid amplification tests are the gold standard for diagnostic confirmation of a *Ct* infection (25).

1.2.4 Complications following *Ct* infections

Despite the availability and efficacy of treatment, the sequelae of urogenital *Ct* infections pose a significant danger. At a systemic level, *Ct* infections have been

associated with liver infection, known as perihepatitis during Fitz-Hugh-Curtis syndrome, as well as with the development of reactive arthritis and Reiter syndrome (7, 34). At the local site of infection, *Ct* infections are associated with a range of negative sexual health outcomes. Due to the impact on the tissues and host responses, *Ct* infections can increase susceptibility to human immunodeficiency virus (36), as well as human papilloma virus, which can result in increased risk of cervical cancer (37). There is also evidence that ovarian cancer may be linked to *Ct* infections (38).

However, the most significant risk for women is the ascension of *Ct* into the upper reproductive tract, leading to pelvic inflammatory disease (PID) (34). This complication is the result of the infection of the uterine, fallopian tube, and ovarian tissues by the *Chlamydia* (39). While PID includes some of the hallmark features of a local *Ct* infection, such as dysuria and worsening abdominal pain, women may also present with more systemic symptoms, such as fever, chills, and gastrointestinal disturbances (34).

Due to the ascension of the bacteria, women with PID may develop salpingitis and endometritis, which involves swelling and inflammation of the fallopian tubes and uterus, respectively (7). Among women who have had a previous episode of PID, nearly 20% will struggle with infertility (7). For some, the infertility etiology can be identified in the damage occurring in the delicate tissues of the fallopian tubes during *Ct*-induced PID, which can lead to blockages in the fallopian tubes and result in tubal factor infertility (28). Tubal factor infertility can contribute to difficulties in becoming pregnant by restricting physiological reproductive processes (28). Damage from PID following *Ct* infection also results in significantly higher rates of ectopic pregnancy due to tubal damage and changes in the molecular environment, which can induce further damage to the fallopian tubes (28, 40). Sadly, the complications following *Ct* infections can further jeopardize pregnancies even if tubal damage can be subjugated, as having a prior *Ct* infection is associated with higher risk of miscarriage, preterm birth, and stillbirth (7). Experiencing PID, infertility, pregnancy complications, and infant loss are appreciably traumatic for women and emphasize the multifaceted risk that *Ct* infections pose to women's physical and mental wellbeing.

1.2.5 Exacerbations of complications following recurrent *Ct* infection

PID and related complications are estimated to occur in 16%-50% of initial urogenital *Ct* infections (39, 41). However, repeated *Ct* infections are known to be associated with the risk of increasing complications (28, 42). This factor is clinically important, as approximately 30% of women will have a subsequent *Ct* infection following the resolution of their first infection (28). Findings from a cohort of over 33,000 women serving in the United States Army revealed a 28% increase in the risk of PID development following each *Ct* diagnosis after an initial infection (43).

It has been hypothesized that subsequent episodes of urogenital *Ct* in women that lead to PID will further inflame and damage upper genital tract tissues to result in further impairments to reproductive health (28). Many population studies have confirmed an association between the recurrent *Ct* infections and worsening complications. Findings from the longitudinal PID Evaluation and Clinical Health Study have demonstrated that women experiencing repeated PID episodes are twice as likely to have fertility problems and four times as likely to experience chronic pelvic pain compared to women who did not have recurrent PID (44). Another retrospective cohort study determined that repeated *Ct* infections significantly increase the risk of ectopic pregnancy (45). There has yet to be definitive conclusions on the mechanisms that result in the exacerbations of *Ct*-associated complications, despite the reports indicating that this phenomenon is indeed occurring and compromising the well-being of women globally.

1.3 Host responses following *Ct* infections

1.3.1 Female reproductive tract pathology following *Ct* infections

As observed in the clinical presentation of PID, the inflammatory state following *Ct* infection can result in severe tissue damage in the upper female reproductive tract (FRT), which can be observed at the gross and histological level (34). Laparoscopy procedures produce findings of overall edema and inflammation in the uterus, fallopian tubes, and ovaries, referred to clinically as endometritis, salpingitis, and oophoritis, respectively (41, 46-48). Additionally, fibrotic adhesions can be present throughout these tissues, which can substantially impair physiological reproductive function (41, 46, 48).

These findings are accentuated by purulent abscesses throughout the FRT; the most concerning among the abscesses are the tubo-ovarian forms, which can be fatal if ruptured (49). During acute PID, pyosalpinx is often observed; this refers to thick, purulent fluid with particulate matter that distends and occludes the fallopian tubes (46, 49). When the PID occurs chronically, such as during persistent or recurrent *Ct* infection, similar findings are observed; however, the pathology in the fallopian tube becomes the hydrosalpinx form, where fluid causes distension and occlusion of the salpinges (49).

While there is a wealth of animal studies with histopathology reports following chlamydial infections, there are limited reports of the microscopic changes in the human FRT following *Ct* infections. Of the few reports available, the documented histopathology is consistent with an intense inflammatory state and indicates that multiple tissue layers are impacted by the damage (50). Hyperplasia and fibrosis can be observed throughout the tissue layers of the upper FRT (41). There are also reports of neutrophilic and lymphocytic infiltrates into the tissue layers of the endometrium and the fallopian tubes (41, 46, 48). Some reports have even observed the destruction of the fallopian tube wall (47). In the cases of hydrosalpinx in women suffering from infertility, the histopathology findings have suggested atrophy and fibrosis of the fallopian tube, as well as the destruction of the cilia and microvilli (51). Despite minimal academic sources for histological changes occurring within the tissues impacted by *Ct* infections in humans, it is widely accepted that the host immune response contributes to the development of tissue pathology (7, 28).

1.3.2 Innate immune responses to *Ct* infection

1.3.2.1 Epithelial cell responses

The host response to *C. trachomatis* starts in the epithelium, where the bacteria will replicate in the epithelial cells of the urogenital tract (7). Epithelial cells have innate defenses to pathogens such as the production of antimicrobial peptides, which include defensins, cathelicidin, and lactoferrin (52, 53). To further combat the *Ct*, the infection will trigger activation of epithelial cell pattern recognition receptors, such as toll-like receptors (TLRs) via recognition of certain conserved components of chlamydial antigens (54), which would be considered pathogen-associated molecular patterns, or cell injury

components, also called damage-associated molecular patterns (55). Epithelial cells in the human FRT express TLRs, and evidence from animal studies suggests that TLR2 and TLR3 play a role in epithelial cell responses and immunity during chlamydial infection (55, 56). Other pattern recognition receptors, including CD14, play a role in detecting chlamydial LPS (57). The retinoic acid-inducible gene I-like receptors and nucleotide-binding oligomerization domain-like receptors also contribute to the host response during *Ct* infections through their detection of intracellular chlamydial RBs (57).

In vitro studies with human tissue have demonstrated that infection with *Ct* will result in secretion of interleukin (IL)-1, IL-6, IL-8, CXCL1, and granulocyte-macrophage colony stimulating factor (GM-CSF) in the epithelium two to three days after the initial infection (58). Additionally, a recent study using a human organoid model demonstrated that epithelial cells will also produce the cytokines leukemia inhibitory factor (LIF) and tumor necrosis factor (TNF), as well as confirming the expression of the aforementioned cyto- and chemokines (59).

Chemokine and cytokine secretion occurs following pattern recognition receptor activation by chlamydial components and although a single, critical receptor activation cascade has yet to be identified, many signaling pathways have been identified to be active following *Ct* infection (57). The goal of producing and secreting these molecular mediators is to recruit and activate immune cells for more directed bacteriostatic and bactericidal responses against *Ct* (60).

1.3.2.2 Local tissue responses

While the epithelial cell layers are the initial targets of *Ct*, the bacteria will progress into deeper tissue layers as the infection progresses (61). Stromal fibroblasts, which are a connective tissue cell type, will secrete molecules such as IL-1, GM-CSF, IFN-γ and eotaxin in response to infection, which further supports inflammation and immune cell activation (61). There is evidence that *Ct* can infect stromal cells throughout the FRT, including the endometrium (62, 63). Some reports suggest that the molecular mediator production and secretion from fibroblasts is higher relative to the epithelium,

due to a lack of shedding of fibroblasts, thus indicating a potential role for stromal cells mediating tissue pathology during *Ct* infection (61).

Fibrosis, or scarring, is a clinically significant outcome following chronic tissue damage and repair; this process is modulated largely by stromal cells (64). Mesenchymal stromal cells (MSC), which are synonymous with fibroblasts, are known to express factors related to tissue injury and repair during this process (64, 65). There are MSCs present in human fallopian tube and uterine tissues, and these have the potential to expand rapidly when required (66). The factors produced by MSCs include classic expression products involved in angiogenesis, collagen deposition, and matrix remodeling, such as trophic growth factors, proteinases, collagenases, cytokines, and chemokines, as well as protein products such as collagen, elastin, fibronectin, fibrins, and glycosaminoglycans (64, 67).

It is likely that many of the products secreted by fibroblasts could impact pathogenetic processes following *Ct* infection. This is clear in some cases, such as that of matrix metalloproteinases, as their production is an indicator for *Ct* infection complications (68). Other MSC products have profiles that indicate a potential for contributing to *Ct*-related pathology but have not yet been directly connected. For example, in addition to epithelial cells, MSCs are also able to express LIF (59, 69). LIF has the potential to modulate angiogenic and cell migration processes (69). There is evidence that LIF can be produced by a variety of cell types during inflammation and some studies have indicated that inappropriate LIF expression can contribute to inhibition of cell differentiation (70). Maladaptive LIF expression may also be a factor in predisposing one to ectopic pregnancy, which is a significant concern following *Ct* infection (34, 71). Furthermore, the transition of epithelium to mesenchyme is modulated in part by LIF; this process has been theorized to occur following *Ct* infection and could account for some of the features of *Ct* sequelae (59, 72).

There are also reports of the expression of podoplanin (PDPN), a surface glycoprotein, by MSCs during inflammation at the local site of an infection (73). PDPN expression has been shown to support cell migration and platelet aggregation (73). PDPN

is able to interact with CD11b-expressing cells, which appears to enhance inflammation and result in tissue pathology via escalated apoptosis, extracellular matrix remodeling, and enzymatic tissue destruction (74). There is also evidence from cardiovascular studies that the inhibition of PDPN abrogates some of the pathological tissue remodeling potential associated with its expression (74). Despite their role during infection, inflammation, tissue repair, and fibrosis, there is a paucity of literature on these processes as they pertain to *Chlamydia* literature, so the responses and impacts of *Ct* infection on female genital tract stromal cells and their products has yet to be fully characterized.

1.3.2.3 Neutrophil responses

Due to a variety of signaling cascades, neutrophils will infiltrate the site of infection and they are among the first immune cell types to do so (75). IL-8 is the primary chemoattractant for neutrophils during *Ct* infections in humans (58), but the chemokines CXCL1-CXCL3 and CXCL5-CXCL7 are also capable of neutrophil recruitment (76). Additionally, neutrophil chemoattraction can also be mediated by formyl peptides, leukotriene B_4, and complement components, such as the anaphylatoxins C3a and C5a (76). Neutrophilic defenses against pathogens are well characterized, and can include phagocytosis, secretion of inflammatory cytokines, and extrusion of their cellular contents to result in a sticky extracellular trap (77). Neutrophils are also known for their ability to degranulate and release antimicrobial peptides, proteolytic enzymes, and reactive oxygen and nitrogen species, ROS and RNS respectively (78).

There are conflicts in the literature regarding the specific role that neutrophils play during chlamydial infections. Previous research indicates that neutrophils are able to help control the spread of *Chlamydia* infection and the extent of bacterial burden within the first two weeks of infection (79). *Chlamydia* has evolved to interfere with neutrophil functioning, perhaps due to their role in infection control; chlamydial protease-like activating factor permits the infection of neutrophils by *Ct*, which prevents neutrophil apoptosis, thereby improving the survival of the bacteria and disrupting appropriate adaptive immune priming (80, 81). In line with this, Frazer and colleagues have reported that *Cm* strains that are unable to interfere with neutrophil apoptosis produce infection

states in mice that feature ephemeral neutrophil functioning, reductions in inflammatory molecules, and a striking lack of reproductive tissue pathology (80).

The association with neutrophils and chlamydial tissue pathology may be attributed to the normal functioning of neutrophils. Neutrophilic inflammatory and antimicrobial products are effective for controlling and destroying pathogens, but they are generally cytotoxic and have the capacity to damage host cell tissues (78). Indeed, neutrophilic products, such as matrix metalloproteinases, have been shown to be involved in the development of female reproductive tract pathology following chlamydial infections (82). In line with this, there is animal research associating a reduction in neutrophil infiltration and inflammation with corresponding decreases in the extent of tissue damage following chlamydial infection (83). The role of neutrophils during tissue pathology development is most convincing when considering studies that prohibit neutrophilic involvement. Particularly, neutrophil depletion during chlamydial infection in animal models consistently results in remarkable reductions in reproductive tissue pathology (84, 85).

There are other considerations in the capacity of neutrophils to modulate tissue damage. There are reports of distinct neutrophil subsets occurring in mice following *S. aureus* infections, which include pro-inflammatory (N1), pro-regulatory (N2), and undifferentiated (N0) neutrophils and can be identified by their expression of the CD11b integrin (86). Thus, it is physiologically possible for particular neutrophil phenotypes to direct the formation of tissue damage following *Ct* infection. Furthermore, there is a role for neutrophils during the development of fibrosis after chronic inflammation (87). Upregulation of neutrophilic involvement has been associated with fibrosis in many pulmonary conditions, due in part to their ability to enhance inflammation and secrete destructive products (87). At this time, there are no available reports on the impact of neutrophil subsets or neutrophil-mediated fibrosis on *Ct* infection, indicating an expanse of potential research avenues.

When considered comprehensively, it appears that temporal factors, duration, direction, and intensity of neutrophilic involvement are the determining factors for the capacity of neutrophils to both support infection defense and inadvertently promote tissue

damage. These reports come from animal studies, although the limited literature regarding human histology following chlamydial infections fits in well with these assumptions. In one study of FRT histopathology following *Ct* infection, there were reported observations of neutrophilic accumulation around infected cells and infiltrating into the epithelium; however these findings are limited due to their observational nature (50). Although there is convincing data and a wealth of intriguing hypotheses, there is not yet a defined paradigm for the mechanism of neutrophilic direction of tissue pathology complications due to *Ct* infection.

1.3.2.4 Other modulators of innate immunity and adaptive immunity priming

As a result of signaling from infected cells, immune cells will be recruited to the site of infection. Professional antigen presenting cells (APCs), such as DCs, have the capacity to phagocytose extracellular *Chlamydia*, which supports priming of the adaptive response (88). However, *Ct* is able to infect DCs, which can promote the secretion of IL-1, IL-6, and TNF, as well as IL-8, IL-12, and IL-18 (89).

Macrophages are another type of APC, and they are readily involved in the innate response to *Ct* infection (75). The presence of tissue resident monocytes and macrophages within the reproductive tract allows for their activation, primarily by LPS and heat shock proteins (cHSPs) from *Chlamydia* (90). Additionally, circulating monocytes will be recruited to the site of infection, primarily via CCL2 and CCL7, thereupon differentiating into macrophages, as well as certain dendritic cell subsets (91). Macrophages are defined by their predilection for phagocytosis and capacity for adaptive immune priming (92). It is possible for macrophages to have different phenotypes, and there is animal study evidence that inflammatory macrophages (M1), which are characteristically activated by IFN-γ and chlamydial LPS, can control bacterial burdens during *Chlamydia* infections more effectively than macrophages that have been alternatively activated with IL-4 (M2) and those that have not differentiated (93).

Macrophages can also be infected with *Chlamydia*, leading to adaptive priming and secretion of IFN-ß, IL-1ß, IL-6, and IL-10, this was found to be due to TLR2 signaling in an animal model and further enable ROS/RNS production to control *Chlamydia* (94). In spite of this, the role of infected macrophages is not yet entirely clear;

Ct infection of macrophages can maladaptively direct T cell death and may also enable chlamydial persistence (75).

Natural killer (NK) cells, a subset of innate lymphocytes, will also infiltrate into the *Ct* infection site (75, 95). NK cells are attracted and recruited into the mucosal epithelium by molecules such as CCL5, CXCL10, IL-12, and IL-18, among others (75, 96). Like neutrophils, NK cells are not thought to play a significant and direct role in controlling the infection; instead, they are thought to be critical for modulating adaptive responses (97). In line with this, it is well established that NK cells can produce IFN-γ during *Ct* infections, which is necessary for CD4+ T cell polarization (98, 99). Indeed, a recent report suggests that NK cells direct the interactions of DCs, although this was demonstrated during respiratory infection with *C. pneumoniae* and may not necessarily be the case during urogenital *Ct* infection (100). Furthermore, recent work in animal models of *Ct* suggest that when the contribution of NK cells is distinguished from that of other innate lymphocytes, there is a potential role for innate lymphoid cell 3, a helper-like innate lymphoid subset, in controlling the very early stage of the infection (101). Thus, the complexity of the innate effector contributions during chlamydial infection represents an important component of the host response that necessitates continued investigation in the context of *Chlamydia*.

Other innate effectors, such as mucosal-associated invariant T cells, remain completely uncharacterized for their role in chlamydial infections. These cells have the capacity to recognize bacterial components and display tissue-specific cytokine production profiles (102). In line with this, a recent report of human FRT mucosal-associated invariant T cell functioning in response to *E. coli* suggests that these cells are inclined to produce IL-17 and IL-22, which could contribute to CD4+ T helper cell response polarization and impact the epithelial cell responses if this occurred during *Ct* infection (103). Such emerging reports emphasize the physiological capacity of mucosal-associated invariant T cells to influence the outcomes of urogenital *Ct* infections.

The recruitment of innate adaptors, as well as the responses of infected tissues, modulate the priming and development of adaptive immunity. Classically, epithelial, stromal, and dendritic cells would present chlamydial antigens through major

histocompatibility class I (MHC-I) molecules to CD8+ cytotoxic T lymphocytes; however, this process is reduced during *Ct* infection (104). Recent research suggests that *Ct* can interfere with some of the cellular pathways, particularly those involving endosomes, resulting in ineffective MHC-I functioning (105). This muddies the waters of chlamydial literature, as other studies have demonstrated that *Ct* has no direct impacts on the MHC-I pathway in its quest to avoid detection by the host (106); these conflicts underscore the deficits in characterizing the complex host responses to *Chlamydia*. Regardless of the direct mechanistic impacts of *Ct* on MHC-I, it is known that NK cell activation will occur following any disturbance of MHC-I expression, which indicates another avenue of NK cell involvement in facilitating polarization and memory cell responses during chlamydial infections (96, 97).

APCs, including DCs, neutrophils, and macrophages, will present phagocytosed antigens via the MHC-II pathway to naïve CD4+ T cells (107), and there is evidence that peptides from lysosome-degraded MOMP is a major source of this antigen presentation (108). Similarly to MHC-I, there is evidence that chlamydial manipulation will reduce the expression of MHC-II as an ongoing attempt to outmaneuver the host immune response (109). Still, there are reports of effective MHC-II expression by dendritic cells in animal models, which enable the development of protective immunity (110, 111). To this end, there is evidence that DCs play a critical role in their expression of MHC-II and co-stimulatory molecules, such as ICOSL, ICAM-1, and B7-1, during the activation of cell mediated immunity (89, 111).

1.3.2.5 Summary statements of innate responses

Ct infects epithelial and stromal cells, which triggers innate defenses and immune cell recruitment (61). Recruitment, expansion, and infiltration of neutrophils, macrophages, natural killer cells, and dendritic cells follows to provide innate protection during early *Ct* infection and begin the priming of adaptive responses (75). However, certain innate immune cells, such as neutrophils, are likely to be implicated in modulating host-mediated tissue damage following *Ct* infection (112).

1.3.3 Adaptive responses to *Ct* infection

1.3.3.1 Cell-mediated immunity

Due to the priming of the adaptive immune response, cell mediated immunity will become activated to contribute to infection clearance and to develop a memory response against *Ct* (28). The two cellular phenotypes involved in cell-mediated immunity include CD4+ and CD8+ T cells (113). CD4+T cells are able to differentiate to suit the defenses needed for a range of pathogens; their secretion of various cytokines, chemokines, and other molecular mediators supports the development of a memory response and enhances the responses of CD8+ T cells and B cells (113). CD8+ T cells are often referred to as killer or cytotoxic T cells due to their effector functions; these cells will secrete inflammatory cytokines, such as TNF and IFN-γ, and are involved in the control of intracellular pathogens via the destruction of infected host cells (113). Furthermore, CD8+ T cells are known for their memory subsets, which include effector memory cells throughout the body and central memory cells in certain lymphoid tissues (113).

In regard to chlamydial infection, there is underwhelming evidence for a substantial protective role by CD8+ T cells, despite their ability to kill cells infected by an intracellular parasite (114, 115). There is some evidence that CD8+ T cells contribute to the priming of a CD4+ T cell response during *Ct* infection (116). Generally, the effect that CD8+ T cells do have on immunity appears to be indirect (116, 117), but there is evidence that these cells can contribute to pathology. A recent report by Zhou and colleagues demonstrated that *Chlamydia* primed CD8+, but not CD4+, T cells could enable the development of FRT tissue damage (118). While this finding has not been replicated in humans, it supports the reports of human studies that have not found a protective role for CD8+ T cells (114, 115). Conversely, the CD4+ T cell response is essential for protective immunity and infection resolution (114, 119, 120).

1.3.3.2 CD4+ T cell responses

The CD4+ T helper response is made up of several arms, and the major subsets include T helper (Th) 1, Th2, Th17, T follicular helper cells (Tfh) and regulatory T cells (Tregs) (121). Each of the responses occurs following the polarization of an

undifferentiated CD4+ T cell with specific cytokines (121). Typically, APCs are the primary, although not the only source, of extrinsic cytokines necessary for the differentiation of naïve CD4+ T cells (122). The Th1 response is polarized by IL-12 and interferon (IFN)-γ, while the Th2 response is polarized by IL-2 and IL-4 (121). The Th17 response has an extended repertoire of polarizing cytokines, which include IL-1ß, IL-6, IL-21, IL-23, and transforming growth factor (TGF)-ß (121). Some redundancy is present for IL-21 which also polarizes the Tfh response, as well as for IL-2 and TGF-ß, which induces the differentiation into Tregs (121). The ability of certain cytokines are able to polarize more than one arm of the CD4+ Th response is thought to enhance the heterogeneity of the immune response (121).

The polarizing cytokines will propagate intracellular signaling, thereby promoting or inhibiting specific transcription factors necessary for the differentiation into specific Th subsets (123). The transcription factor Tbet defines the Th1 response, GATA3 defines the Th2 response, and RORγt facilitates the Th17 response (123). Differentiation into the Tfh subset is mediated by the transcription factor Bcl6, whereas the transcription factor Foxp3 is active for Treg polarization (123). Each of the responses has a unique niche in immunity and produces cytokines relevant to the susceptibility of the pathogens they are directed against. Th1 is known for expression of IFNγ for defense against intracellular viruses and bacteria (123). Extracellular pathogens are target of both the Th2 and Th17 responses; Il-4, IL-5, and IL-13 are produced during the Th2 response to protect against large parasites, while Th17 cells will express IL-17 and IL-22 for defense against fungi and bacteria (123). The Tfh response is distinct in that it does not serve to protect from specific pathogens, instead is notable for its facilitation of germinal centers via IL-21 production, a critical aspect of antibody production by B cells (121). Similarly, Treg responses are critical for the dampening of inflammatory responses through the production of IL-10 (121).

It is well established that the Th1 arm of the CD4+ T helper cell responses are associated with infection control and clearance during chlamydial infections; this concept has been demonstrated in human and animal studies (114, 119, 120, 124-127). This is primarily due to the production of IFN-γ, which impacts the metabolism of the *Ct* within

the cell (22, 114). When cells are exposed to IFN-γ, the expression of indoleamine-2,3 dioxygenase (IDO1) will be upregulated; the IDO1 enzyme directs the conversion of the amino acid tryptophan to kynurenine (128). *Ct* lacks the biosynthetic pathways needed to produce tryptophan, thus an environmental tryptophan deficiency interrupts the chlamydial life cycle (128).

There is evidence that other cell types, such as NK cells and activated CD8+ T cells also can contribute some degree of IFN-γ during chlamydial infections; however, the amounts produced are not enough to contribute meaningfully to clearance and instead bolster the overall IFN-γ response (99, 117). In the few studies that have not found a direct association between IFN-γ and *Chlamydia* from the local site of infection, there has still been evidence of a protective role in limiting the propagation of the bacteria systemically (129), underscoring the protective nature of this response. The caveat of IFN-γ during *Ct* infections is that the exposure must be at high enough concentrations for a continuous amount of time for a bactericidal effect; anything less will result in chlamydial persistence, which can cause chronic infection states that damage host tissues (128).

Other subsets of the CD4+ T helper cell responses do not have a clear consensus on their roles in supporting protective immunity or in mediating the development of tissue damage. The findings of Hawkins and colleagues reinforced the protective function of the Th1 response but found that Th2 responses are unable to contribute to infection clearance in a mouse model of *Chlamydia* infection (120). However, some findings in humans indicate that CD4+ Th2 responses are upregulated in the blood and endometrium of *Ct*-infected women (130). This finding was augmented by work in an animal model, as eosinophils primed by the CD4+ Th2 response to *Ct* infection secreted IL-4 and were associated with reduced reproductive tract pathology (63). In contrast to these findings, there is a wealth of reports that link Th2 effector cytokines with modulating damaging fibrosis in pulmonary and liver conditions (131). Thus, there remains a need to characterize the immunity and the direct involvement of the CD4+ Th2 response on *Ct* associated tissue pathology.

There is a fair amount of evidence that Th17 responses are associated with tissue damage following chlamydial infection, as their depletion during infection has been shown to minimize reproductive tissue damage (132). Given the possibility of Th17 responses mediating tissue damage, one might expect that the inhibitory effects of Tregs would abrogate this effect, though this does not appear to be the case (133). Indeed, reports indicate that there appears to be a feedback axis between Tregs and Th17, as the depletion of Tregs in a mouse model of Chlamydia will result in lower Th17 cell levels, as well as diminished numbers of infiltrating neutrophils and the extent of tissue pathology (83).

Despite the current paradigms in the literature regarding the roles of various CD4+ Th subsets during chlamydial infection, some conflicts in understanding remain. For example, a report that Morrison and colleagues demonstrated that CD4+ T cell depletion did not change the course of a *Ct* infection in a mouse model (134). The lack of consensus within the field indicates that more work is needed to fully characterize the impact of cell-mediated responses and to completely relate them to human conditions following chlamydial infections.

1.3.3.3 Humoral immunity

There have been continuous adjustments made to the understanding of the role for B cells and the humoral response during chlamydial infections (135). In previous decades, there was conflicting evidence from animal research regarding the impact of antibodies during chlamydial infection; it was not clear if IgM was meaningfully contributing to clearance during initial infections (136). Furthermore, although there were measurable levels of antibodies directed against *Chlamydia* following primary infections, there was not a consensus on whether the presence of IgG or IgA was robustly protective during subsequent exposures (137). Despite these findings, other reports suggested that antibody responses were critical to the control of the infection, as antibody depletion results in increased bacterial burdens (137).

In more recent years, animal models of chlamydial infections have shifted the opinions on humoral immunity (135). The popular humoral immunity paradigm suggests that direct B cell contributions are not striking during primary infection, but they are

important to protection during secondary infections (139-141). These findings primarily support the concept that interactions between B cells and other cell types support the development of protective immunity, particularly through the priming of CD4+ Th1 responses by B cells (139, 140). Furthermore, there is evidence that both neutrophils and NK cells can contribute to the impact of humoral immunity through *Chlamydia* destruction via antibody dependent cellular cytotoxicity (141), thus demonstrating the need for B cell involvement during chlamydial infections.

In terms of human infection, there is limited evidence for the role of B cells and antibody production, as it is not feasible to remove confounding factors during observational studies of chlamydial infections in the clinic. A recent epidemiological study has concluded that there is a correlation between the number of chlamydial exposures and the expansion of an enduring antibody titer, yet this did not appear to protect from re-infection (142). This appears to be consistent with previous reports, and so the role of humoral immunity during *Ct* infections in humans remains poorly characterized (140).

An important consideration of humoral immunity is the direction of pathogenic host responses; some reports indicate an association between antibodies directed against certain chlamydial antigens with tissue damage in the host (143). cHSPs, such as cHSP60, are associated with atherosclerosis and cardiovascular tissue damage following *C. pneumoniae* respiratory infection (144, 145). A potential explanation for this phenomenon is well-conserved similarities between human and chlamydial HSPs, and it is theorized that this could result in some degree of cross-reactivity for host tissues following chlamydial infections (143). There is ongoing research into to whether anti-chlamydial antibodies may be contributing to tissue damage processes during *Ct* infection, but there is currently not a firm agreement as to whether or not this is the case (143).

1.3.3.4 Summary statement of adaptive responses

The activation of CD4+ T helper cell responses improves the disease state following *Ct* infection; the polarization of the Th1 response results in the production of IFN-γ, which results in impaired replication of the *Ct* and control of the infection (114).

Yet, this could result in a persistence of the *Chlamydia*, and a chronic infection state (128). The role of B cells is unclear, and while they may contribute to some degree of protection during secondary infections, they may also mediate tissue pathology (135, 143).

1.3.4 Summary of proposed mechanisms of tissue pathology resulting from *Ct* infection

Host mechanisms following *Ct* infection are hypothesized to inflict tissue damage, while concomitantly endeavoring to resolve the infection. However, there is not yet a successful characterization of the exact mechanisms. Potential paradigms of host-mediated tissue damage include the hypersensitivity, persistence, infection ascension, and cell-mediated damage (28, 143).

The hypersensitivity paradigm of *Ct*-related pathology development was initially thought to be due to type IV delayed hypersensitivity, which is mediated through sensitized T cells (143). However, due to inconclusive evidence and ongoing research, this paradigm was reassessed to include a potential for cross-reactive antibodies directed against certain chlamydial antigens, such as cHSP60 (143). This theory is supported in part by the detection of anti-cHSP60 IgG and IgA in humans that were also directed against human HSP60 (146). Conversely, it is hypothesized that the infected epithelial cells are the initial contributors to the development of inflammation during the cellular paradigm of tissue damage (147). This inflammation leads to the infiltration of destructive lymphocytes and granulocytes to mediate the damage to the host tissue; this is consistent with the findings of gross pathology inflammation and histopathology reports of cellular infiltrates in damaged tissue (50).

Clinical findings have determined that *Ct* can bypass the endocervix and infect the upper genital tract (148). Thus, the model of ascension postulates that because of the spreading of the infection, significant inflammation and fibrosis will follow (28). Similarly to ascension, the paradigm of persistent infection is thought to induce an over vigilant immune state due to the lingering pathogen (28).

While they have been made distinct, there is a possibility that features from some or all of these paradigms may interact to produce the extensive FRT damage following *Ct* infection. It is essential for the mechanism of this tissue damage to be characterized in order to develop clinical interventions that inhibit the pathological capacity of these processes.

1.4 Animal models of chlamydial infections

1.4.1 Species used for chlamydial research

Due to the ethical constraints of human research, animal models of chlamydial infection have been widely utilized in an attempt to characterize the Ct infection and its complications. These include infections in rodents, rabbits, guinea pigs, pigs, and non-human primates (149). As *Ct* is an etiologic agent of sexually transmitted infections in humans, it is frequently used for infections in research; however, some models may use other chlamydial species, such as *Cm* in mice and *C. caviae* in guinea pigs (149). Additionally, the infection can be initiated via a range of techniques, including intravaginal and transcervical inoculation, as well as species specific models (149).

Due to their appreciable biological homology to humans and innate sensitivity to urogenital *Ct* infection, nonhuman primate models of chlamydial infection have been developed (150). Studies utilizing grivet monkeys, olive baboons, and pigtailed macaques have demonstrated promising results, as the primates develop disseminated reproductive tract inflammation that is akin to the PID state in human women (150). The ethical constraints of using nonhuman primates, as well as the resources required, reduce the practicality of these models (149). Pigs have been used as alternatives to nonhuman primates (151). Porcine models incorporate similar immunity, physiology, and hormonal states to humans (151). Furthermore, there is evidence that porcine infection with the pathogen *C. suis*, which is genetically similar to *Ct*, results in sequelae also seen in humans, such as infertility (151). However, some of the size and cost concerns that prevent the use of nonhuman primates for basic science research impact pig models similarly (149). To mitigate the animal size issue, some investigators have found success with the use of guinea pigs (151). Historically, *C. caviae* was used in guinea pig models, but there is evidence that *Ct* infection modelling is possible for these animals (152).

1.4.2 Mouse models of chlamydial infections

The mouse species, *Mus musculus*, has been extensively used for disease research in many fields and they are frequently utilized to study chlamydial disease, especially for basic studies (149). The mouse model is advantageous for many reasons, but especially because they are financially feasible and genetically altered strains are commercially available (149). Furthermore, the use of mice can be versatile, as chlamydial infections can be done with *Cm* or *Ct*; although mice are the natural host for *Cm*, the species is very similar to serovar D of *Ct* (149).

Rodent models of *Chlamydia* conventionally involve estrous cycle synchronization with progesterone, which reduces the potential for confounding factors from varying hormone states between animals (149). Furthermore, the use of progesterone can ensure a stronger *Chlamydia* infection, given the expansion of epithelial cells within the genital tract following progesterone treatment (153). Although *Cm* models use progesterone treatment to rule out confounds and diminish variability, *Ct* infections in rodents require progesterone to produce the same upper genital tract features as *Cm* infection will (149). Notably, it is necessary to transcervically infect *Ct* into the mouse upper genital tract during research to produce tissue pathology and complications; intravaginal infection alone will not result in ascension (149). This is in contrast to *Cm* infections, which can occur intravaginally and still go on to cause a productive infection (154).

Both *Cm* and *Ct* infections will result in bacterial shedding, although to difference degrees (149). Furthermore, both infection models are able to produce varying degrees of upper reproductive tract pathology in female mice (149). It is very well established that chlamydial infection in mice, especially with *Cm*, will result in processes observed in humans, such as hydrosalpinx, infiltrating neutrophils, damage to tubal structures, and infertility (155, 156). Furthermore, previous work has determined that infection resolution during *Cm* and *Ct* models depends on CD4+ Th1 immunity (119, 120, 124-127). This similarity is intriguing due to the obligate tryptophan requirements present in *Ct* that are bypassed by other mechanisms in *Cm* (134). There is not yet an explanation

for why *Cm* is susceptible to Th1 responses, but it is consistently reported nonetheless (149).

Yet, there are known differences in the conclusions regarding the development of protective immunity in the *Cm* and *Ct* models. Following a primary *Cm* infection, there is the development of protective, cell-mediated immunity that can promote rapid infection clearance upon secondary infection; this is not observed in *Ct* murine infections (154). Conversely, mouse models of *Ct* have demonstrated that the infection can be contained with only innate immune cells, but this has not been demonstrated for *Cm* infection (157). It is only when mice are infected repeatedly with *Ct* that they will eventually develop some degree of adaptive immunity (134). Thus, there are necessary considerations when comparing the conclusions of *Cm* and *Ct* mouse model studies.

1.4.3 Limitations of mouse models

Nearly every animal model of disease will have limitations, and there are several in the mouse model of *Chlamydia* that are relevant to consider. Generally, animal studies will initiate chlamydial infections through a single infection (158); however, it is established that reinfection with *Ct* is an alarming public health concern in human populations (25). In line with this, there is known variability in infection states, immune kinetics, and host outcomes following both *Cm* and *Ct* infections in mice, therefore some of the findings from animal studies cannot be readily related to human states (149, 154).

Another notable feature of chlamydial infections in mouse models is the ability of most animals to resolve the *Chlamydia* infection on their own (149, 154); this has not been reliably observed in humans and anti-microbial treatment remains as a standard in management of *Ct* infections (25). Most critically, mice are known to consistently develop partial protective immunity to *Cm*, as well as a degree of cross protection to *Ct (*149, 154). This is evidenced by reports of shorter infection and less shedding during secondary infections in mice, as well as observations of the direct impact of CD4+ T cell responses (134). For these reasons, it is not feasible to fully connect the observed disease states in mice to that of human chlamydial disease, although the similarities in sequelae emphasize their value.

1.5 Rationale

As described, human disease states with *Ct* can result in severe complications that are destructive to female health outcomes (7). The development of improved clinical management for tissue damage resulting from *Ct* infection, or an immunization strategy to prevent the spread of infection, have the potential to ease the burden of this pathogen (159). Yet, effective management of tissue fibrosis and efficacious vaccines have not come to fruition, primarily due to the lack of clarity in fully elucidating the human response to urogenital *Ct* infection and the resultant tissue damage. In spite of extensive animal research in chlamydial pathology, which has provided critical insight into the pathophysiology and host immune responses to infection, this knowledge deficit remains (149, 159).

Previous studies have utilized mouse models of *Chlamydia* infection with a range of inoculative doses, although there remains to be a consensus on the impact of IFU dosage on bacterial shedding, tissue pathology, immune responses, and infection clearance rates (149, 160-163). Typically, large doses of *Chlamydia* IFUs are used to ensure productive infection in animals during research (160) but it is unlikely for a human to receive a single, high IFU dose of *Chlamdyia*, then go weeks or months without another *Ct* exposure. Indeed, estimated chlamydial quantities in human semen secretions contain relatively low IFUs (164); still, no study has established the infectious dose of *Ct* in humans due to obvious and appropriate ethical considerations.

Furthermore, research on human sexual behavior suggests that at around half of sexually active adults in the United States will engage in sexual activity with a partner at least once a week (165). Given these statistics, as well as those that highlight that asymptomatic nature of urogenital *Ct* infection (28), it is plausible that low dose chlamydial exposures in human may happen repeatedly before the infection is detected. Thus, it is relevant to study infection modelling that features recurrent exposure to low IFU doses of *Chlamydia*.

To date, there is no evidence in the literature of attempts to model chlamydial infection in mice with different inoculative dose schedules that are cumulatively equivalent to each other. As previous research has not factored these concepts into their

investigation, it is reasonable to compare a repeated, low dose model of chlamydial infection with a single, high dose model, as is classically utilized (160). Dr. Jun Wang's lab has undertaken the development of a comparative model of *Chlamydia* infection using a single, high dose (1X) of 6×10^5 IFU of *Cm*, or five low doses (5X) of 1.2×10^5 IFU of *Cm* that are collectively equivalent to the single dose (Figure 1.1). This work seeks to identify whether there is divergence in host responses and outcomes following repeated low dose infections with *C. muridarum* in a mouse model, compared to single, high dose infections that are conventionally used.

1.6 Hypothesis

I hypothesize that repeated exposure to *Chlamydia* will result in a hyperactive inflammation state that dysregulates neutrophil recruitment and effector functions, contributing to host-mediated tissue damage.

1.7 Aims

The initial aim of this project is to assess the impact of single and repeated *Chlamydia* infections on immune cell kinetics. The second aim is to identify the mechanisms, both molecular and cellular, contributing to tissue pathology. The third aim is to clarify the impact of primary repeated, low dose *Chlamydia* infections on protective immunity during subsequent reinfection.

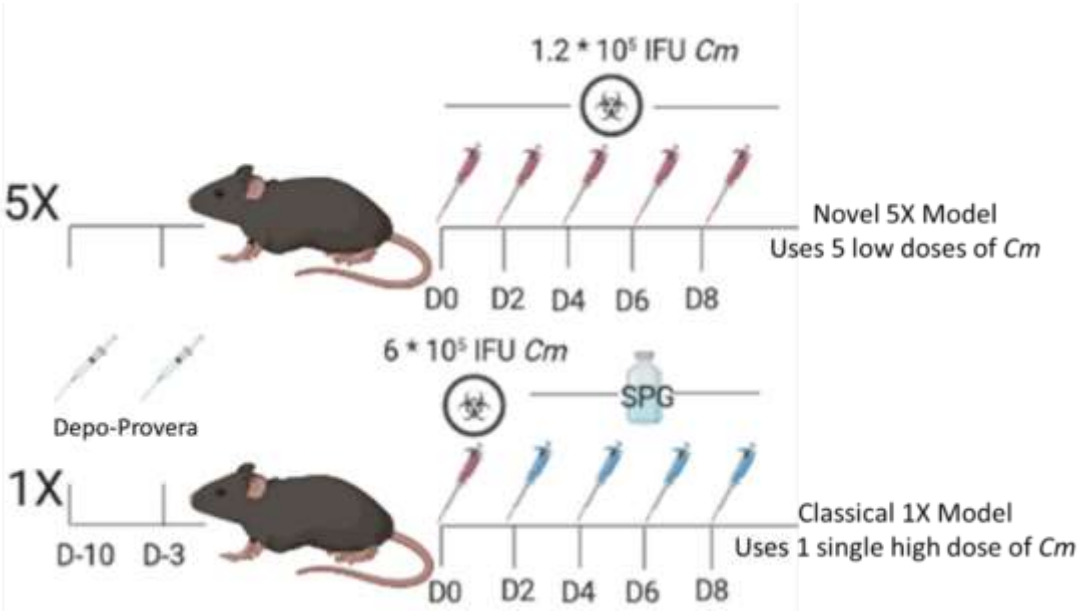

Figure 1.1: Diagram of the experimental schedule for single (1X) and repeated (5X) infections. Murine estrous cycles are synchronized with Depo-Provera ten and three days before the initial infection. Mice in the 5X group are intravaginally infected with 1.2×10^5 IFU of *Cm* every other day, for a total of 5 infections. These are cumulatively equivalent to the single high dose of 6×10^5 IFU of *Cm* that the 1X mice are intravaginally infected with. Sucrose phosphate glutamate buffer is used as a vehicle control in the 1X group on the four time points that 5X animals are receiving their low dose infections.

CHAPTER 2 MATERIALS AND METHODS

2.1 *Chlamydia muridarum* (*Cm*)

The *Cm* used during for this work was prepared as described previously (83). A stock of monolayer-derived *Cm* with a titer of 1.611×10^5 infection forming units (IFU)/µL, stored in sucrose-phosphate-glutamic (SPG) buffer (Table 2.1), was used for all *in vivo* infections.

2.2 *In vivo* investigations

2.2.1 Animals

Animals were housed in specific pathogen-free conditions in the *in vivo* facility of the Isaac Walton Killam (IWK) Health Centre in Halifax, Nova Scotia, as well as the Carleton Animal Care Facility of Dalhousie University. C57BL/6 mice of a CD45.1 background (The Jackson Laboratory, Maine, USA) were bred in-house within the facility and will be referred to as 'wild-type' (WT) for the purpose of this thesis. Forkhead box P3 (Foxp3)-IRES-eGFP knock-in (Foxp3-GFP) mice of a CD45.2 background were kindly provided by Dr. Mohamed Oukka of Harvard Medical School (Massachusetts, USA) and bred in-house. All *in vivo* work was performed with females between the ages of 6-12 weeks at the time of initial infection. All experimental protocols were approved by the Dalhousie University Committee on Laboratory Animals in accordance with the Canadian Council of Animal Care guidelines.

2.2.2 *In vivo Cm* infection

For *in vivo Cm* infection modelling, the murine estrous cycles were synchronized using 2.5 mg subcutaneous injections of Depo-Provera (Pfizer Canada, Kirkland, QC) suspended in phosphate buffered saline (PBS) (Table 2.1) at three and ten days before the initial infection. Animals were anesthetized with inhalational isoflurane prior to the injections.

To infect mice with *Cm*, animals were anesthetized with isoflurane, then the 10 µL dosage of *Cm* was delivered intravaginally. For the 5X group, the 10 µL dose contained 1.2×10^5 IFU of *Cm* diluted in SPG, and the infections occurred every other day

Table 2. 1: List of buffers, media, and other reagents used during *in vivo* and *in vitro* experiments.

Buffer or Medium	Ingredient & Supplier	Amount/L
Ammonium-chloride-potassium buffer (ACK) pH 7.3	NH_4Cl; BioShop	16.6 g
	$KHCO_3$; BioShop	2 g
	EDTA; Bioshop	0.04 g
Complete RPMI medium (cRPMI)	Fetal bovine serum; Sigma Aldrich	100 mL
	HEPES buffer; Wisent Bio Products	1 mL
	Penicillin/streptomycin; Thermo Fisher	1 mL
	L-glutamine; Thermo Fisher	1 mL
ELISA coating buffer pH 9.6	Na_2CO_3; BioShop	1.59 g
	$NaHCO_3$; BioShop	2.93 g
Fluorescence-activated cell sorting buffer (FACS)	Phosphate buffered saline; in-house	995 mL
	Inactive bovine serum; Sigma Aldrich	5 mL
Phosphate buffered saline (PBS)	NaCl; BioShop	8 g
	KCl; BioShop	0.2 g
	Na_2HPO_4; BioShop	1.15 g
	KH_2PO_4; BioShop	0.2 g
Sucrose-phosphate-glutamic buffer (SPG) pH 7.2	Sucrose; BioShop	75.3 g
	KH_2PO_4; BioShop	0.42 g
	K_2HPO_4; BioShop	1.25 g
	Monosodium glutamate; BioShop	0.92 g

for 8 days (days 0 through 8). For the 1X group, the 10 µL dose contained 6.0×10^5 IFU of *Cm* diluted in SPG, which was delivered on day 0, and 10 µL of SPG was used as a vehicle control on days 2, 4, 6, 8.

2.2.3 Vaginal swabbing

Intravaginal swabbing was done throughout the infection to assess bacterial burden. Calcium alginate nasopharyngeal swabs (Puritan Medical Products, Maine, USA) were inserted into the vagina of the mice, rotated clockwise 3 times, then counter-clockwise 3 times. Swabs were placed into 1.5 mL tubes containing 350 µL of SPG with a sterilized 4 millimeter glass bead, then the length of the swab was cropped to a length conducive to tube closure and the tubes were stored on ice. Then, each tube was vortexed for 30 seconds and rotated at 4°C in a ManSci Inc. Lab Revolution tube revolver. After spinning for an hour, 100 µL of the *Cm*-SPG sample was aliquoted directly into 500 µL of DNAzol (Molecular Research Center Inc., OH, USA) and stored at 4°C for genomic (g)DNA isolation. The remaining sample was aliquoted and stored at -80°C.

2.2.4 Splenocyte isolation

Single-cell suspensions were isolated from spleens extracted at sacrifice by pulverizing the organ between 2 sterile glass slides into a Petri dish with 10 mL of Roswell Park Memorial Institute 1640 medium (RPMI) (Wisent Bio Products) with 5% bovine serum (BS) (5% BS-RPMI), then the slides were rinsed with an additional 10 mL of 5% BS-RPMI. The suspension was transferred to a 50 mL conical tube, then the dish was washed with another 10 mL of 5% BS-RPMI, which was also transferred to the tube. The cells were pelleted via a 525×g centrifugation at 4°C for 10 minutes in a Beckman Coulter Allegra X-12R centrifuge, then the supernatant was discarded. The pellet was resuspended by vortex mixing, then 5 mL of ammonium-chloride-potassium (ACK) lysis buffer (Table 2.1) was used for red blood cell (RBC) lysis. After a 5 minute incubation at RT, the reaction was halted with 20 mL of 5% BS-RPMI, then the splenocytes were filtered through a 40 µm cell strainer (Sarstedt, Germany). A 10 µL aliquot of cells was taken from sample and diluted with Trypan Blue (Gibco, Oakville, ON), then counted with a hemocytometer (Hasser Scienfitic, Horsham, PA) and a Leica DML microscope or a TC10 automatic cell counter (Bio-Rad, Saint-Laurent, Québec). Cells were re-

suspended in culture medium or fluorescence-activated cell sorting (FACS) buffer (Table 2.1) at a concentration of 5×10^6 cells/mL.

2.2.5 Blood collection and processing for serum isolation

Serum was extracted from blood samples collected at sacrifice to establish antibody responses. A 23-gauge needle (Becton, Dickinson, and Company, NJ, USA) was used to puncture the submandibular vein, then 250 µL of blood was collected into a 1.5 mL Eppendorf tube. The blood was allowed to clot at room temperature for 30 minutes, then the samples were centrifuged for 30 minutes at 21,000×g at 4°C in a Thermo Scientific Sorvall Legend Micro 21R benchtop centrifuge. The serum component was extracted by a micropipette, then stored at -80°C until further use.

2.2.6 Lymph node cell isolation

Single-cell suspensions were isolated from lumbar, iliac, and sacral lymph nodes. The nodes were excised at sacrifice using two fine forceps to remove the organs from the connective tissues. Depending on size, an average 2-3 nodes were collected from each animal. The nodes were crushed between glass slides and filtered through a 40 µm cell strainer (Sarstedt) into a 50 mL conical tube, as described in 2.2.3. Then, the strainer was rinsed with an additional 5 mL of 5% BS-RPMI and centrifuged at 525×g for 20 minutes at 4°C in an Allegra X-12R centrifuge. The cells were counted and re-suspended as described for splenocyte isolation.

2.2.7 Bone marrow cell isolation

To generate single-cell suspension from bone marrow tissues, femur bones from euthanized animals were stripped of tissues and opened at both ends to expose the marrow. A 20-gauge needle (Becton, Dickinson, and Company) and a syringe containing 5 mL 5% BS-RPMI was used to flush the marrow from the bone cavity into a Petri dish containing another 5 mL of 5% BS-RPMI. The strand of marrow was taken up with the needle and syringe to disrupt the connective tissues and release the cells, then the 10 mL suspension was transferred to a 50 mL conical tube. Another 10 mL of 5% BS-RPMI was used to rinse cells from the plate and transfer them into the tube. Then, the cells were

centrifuged, ACK-buffer lysed, filtered, counted, and re-suspended as described for splenocyte isolation.

2.2.8 Genital tract cell processing

2.2.8.1 Single cell suspension

Genital tracts, including the cervix, uterine horn, oviducts, and ovaries, were excised at sacrifice. To isolate single cells, whole tissues were transferred to 2.5 mL of Hanks Balanced Salt Solution (HBSS) (Wisent Bio Products) and minced with surgical scissors, then 25 units each of collagenase I, collagenase II, and collagenase IV (Sigma Aldrich) were added. Samples were inverted to mix, then incubated at 37°C while shaking. For kinetics experiments, samples were incubated 75 minutes then filtered with 5%BS-RPMI, ACK-buffer lysed, counted, and resuspended as described for splenocyte isolation.

To enhance cell recovery and minimize cell death for sorting and phenotyping experiments, samples were incubated for 35 minutes, then cells were collected by centrifuge filtration through a 40 µm cell strainer (Sarstedt) while spinning at 525×g for 5 minutes at 4°C in the Allegra X-12R centrifuge. The incubation was continued for another 40 minutes by scraping the remaining tissues off the filter and combining with the HBSS + collagenase supernatant, while the isolated cells were resuspended in 2 mM ethylenediaminetetraacetic acid (EDTA) in HBSS. Following the 2nd incubation, the filter centrifugation step was repeated for 10 minutes and included a 10 mM EDTA in HBSS filter rinse. After the filtration, the supernatant was discarded and the cell pellet was re-suspended in 5% BS-RPMI to be counted and processed as described for splenocyte isolation.

2.2.8.2 Tissue homogenates

Genital tracts were excised as described in above. Each tract was split vertically at the endocervix into 2 halves and weighed, then each half was placed into a 1.5 mL Eppendorf tube containing 150 µL of radio-immunoprecipitation assay buffer (RIPA) buffer (Sigma Aldrich) with cOmplete™ protease inhibitor (Sigma Aldrich) and stored on ice. Stainless steel beads ranging in size from 0.9 to 2.0 millimeters (Next Advance

Inc., Troy, NY, USA) were measured out with the manufacturer-provided scoop, then half of a scoop of beads was added to each of the tubes. Samples were homogenized in a Bullet Blender Storm 24 Pro homogenizer (Next Advance Inc.) for 4 minutes on a speed of 12 and repeated as needed until the tissues were fully homogenized. Between steps, the samples were kept on ice for as long as possible to prevent protein degradation.

Following the homogenization process, a Thermo Scientific Sorvall Legend Micro 21R benchtop centrifuge was used for a primary centrifugation of 1,000×g for 10 minutes at 4°C (low speed spin) to collect approximately 100 µL of supernatant for to estimate bacterial burden. The remaining homogenate was centrifuged at 21,000xg for 10 minutes at 4°C (high speed spin) for assaying chemokines and cytokines. The remaining supernatant was collected and stored at -80°C until further use.

2.3 *In vitro* investigations

2.3.1 Bacterial burden quantification of isolated gDNA by quantitative Polymerase Chain Reaction (qPCR)

For qPCR quantification of the bacterial loads, 100 µl of samples taken from vaginal swabs were incubated at 4°C in 500 µL of DNAzol (Molecular Research Center Inc.) for cell lysis. Following the DNAzol reaction, 250 µL of 100 % ethanol was added, the tubes were inverted to mix, and were then incubated at RT for 5 minutes. Samples were centrifuged in a Thermo Scientific Sorvall Legend Micro 21R benchtop centrifuge at 14,800×g at 4°C for 15 minutes. The supernatant was discarded and 750 µL of 70% ethanol was used to wash the gDNA pellet, then the samples were centrifuged at 14,800×g at 4°C for 5 minutes. This 70% ethanol wash was repeated, then the remaining supernatant was blotted away with a Kim Wipe. The gDNA pellet was solubilized with 100 µL of 8 mM sodium hydroxide. To attain a pH of 7.2, 3.2 µL of 1 M HEPES buffer (Molecular Research Center Inc.) was added to the samples prior to storage at -20°C.

The extracted gDNA was quantified via qPCR. The *Cm* gDNA, was diluted tenfold in UltraPure™ DNase and RNase free distilled water (Thermo Fisher). A previously quantified stock of *Cm* gDNA, with a titer of 4.75×10^6 IFU, was diluted tenfold once, then was serially diluted fivefold and used to create a standard curve with a

minimum of 7.6 IFU to a maximum of 95,000 IFU of *Cm*. The qPCR reaction mix for each sample contained 5 µL of RT^2 2X SYBR Green ROX fast supermix (Quiagen, Maryland, USA), 2 µL of the UltraPure ™ distilled water, 0.25 µL of forward primer (5'-CGC CTG AGG AGT ACA CTC GC-3'), and 0.25 µL of reverse primer (5'-CCA ACA CCT CAC GGC ACG AG-3'). The forward and reverse primers used were specific to the *Cm* MoPn strain 16S rRNA and were diluted tenfold prior to use.

The 7.5 µL of the master reaction mix and 2.5 µL of the diluted gDNA from the samples, the quantified stock *Cm*, or UltraPure ™ distilled water were combined in a RNAase-, DNAase-, DNA-, and PCR inhibitor-free, 96 well qPCR plates (Bio-Rad, USA), then covers were applied to the plate. An Allegra X-12R centrifuge was used to centrifuge the plate at 525×g for 10 minutes at 4°C to remove bubbles and draw residual liquid to the bottom of the wells of the plate, then a Bio-Rad CFX96 Touch Real-Time PCR Detection System was used to apply the following qPCR cycle: 95°C for 2 minutes, followed by 40 cycles of 95°C for 10 seconds, then 60°C for 20 seconds. After 40 cycles there was 10 seconds of 95°C, then 31 seconds of 65°C, 5 seconds of 95°C, and ended by 10 minutes at 10°C. Bio-Rad CFX Maestro software was used for standard curve creation and data analysis.

2.3.2 Histopathology

Histopathological assessment of oviduct cysts was utilized to determine tissue damage in the upper genital tract. Upon sacrifice, whole or partial genital tracts were excised, stored in histological cassettes, and fixed with 1% formalin. Samples were paraffin embedded, sectioned, and stained with hematoxylin and eosin (H & E) by the IWK Pathology department. A Leica DM2500 microscope was used to collect digital images of the pathology present around the oviducts. Images were analyzed for the cross-sectional cyst diameter in microns, using the largest cyst present around the oviduct, with NIH ImageJ software developed by Schneider and colleagues (166).

2.3.3 Flow cytometry

Surface, intracellular, and intranuclear cell markers were stained with fluorescent antibodies to establish the immune responses following infection. Following staining,

fixed samples were stored away from light at 4°C until flow cytometry acquisition. OneComp eBeads™ and UltraComp eBeads™ (Thermo Fisher) were stained with individual antibodies and used for compensation controls. Sample acquisition was performed using the FACS Fortessa (BD Biosciences). FCS Express 7 software (De Novo Software, Pasadena, CA USA) was used for analyzing and transforming flow cytometry data.

2.3.3.1 Flow cytometry for surface antigen staining

Following processing, cells were resuspended in PBS and were plated 1×10^6 cells/well in a 96 well V-bottom plate (Sarstedt). Following centrifugation at 755×g for 5 minutes at 4°C in an Allegra X-12R centrifuge and flicking the plate to remove the supernatant, samples were resuspended for viability staining in 50 µL of fixable viability dye eFluor™ 506 (Thermo Fisher) diluted 1:1000 in PBS, then incubated in the dark for 30 minutes at 4°C. After incubating, samples were rinsed with 200 µL of FACS buffer, then the centrifugation and supernatant removal was repeated. Fc domains were blocked with a 20-minute incubation at 4°C using 50 µL of FACS buffer containing 10% rat serum. The FACs buffer rinse, centrifugation, and supernatant removal step was repeated, then 50 µL of the FACS antibody staining cocktail (Table 2.2) was added. Samples were incubated without light for 20 minutes at 4°C. The FACS buffer rinse, centrifugation, and supernatant removal step was repeated twice. For surface staining, all cells were fixed with 200 µL of FACS buffer with 1% formalin prior to storage away from light at 4°C.

2.3.3.2 Cytokine amplification and intracellular flow cytometry

To amplify cytokine signalling for intracellular flow cytometry staining, cells suspended in cRPMI were stimulated with 2 µg/mL ionomycin (Thermo Fisher) and 50 ng/mL Phorbol 12-myristate 13-acetate (PMA) (Sigma Aldrich). Cytokine secretion was inhibited with 10 µg/mL Brefeldin-A (BioLegend, CA, USA). After a 4 hour incubation at 37°C, amplified cells were stored overnight at 4°C prior to flow cytometry staining.

Following amplification, surface antigens on cells were stained as described above in 2.3.5.1. Then, 200 µL of IC Fixation Buffer (Thermo Fisher) was added to each of the samples, which were then incubated for 1 hour at RT. Following the incubation

period, samples were centrifuged at 600×g at RT for 5 minutes to discard the IC Fixation buffer, then washed twice with 200 µL of Permeabilization Buffer (Thermo Fisher) and centrifuged for supernatant discard. Samples were re-suspended 50 µL of 0.002% anti-mouse CD16/32 (ThermoFisher) in Permeabilization Buffer (Thermo Fisher) and incubated at RT for 15 minutes while protected from light. Another 100 µL of Permeabilization Buffer (Thermo Fisher) was added and the samples were centrifuged at 600×g for 5 minutes at RT, then the supernatant was discarded. The samples were resuspended in 100 µL of intracellular staining cocktail (Table 2.2), then incubated at RT for 20 minutes while covered from light. The Permeabilization Buffer (Thermo Fisher) rinse, centrifugation, and supernatant removal step was repeated twice, then the samples were resuspended in 200 µL of FACS buffer.

2.3.3.3 Intranuclear flow cytometry staining

Surface antigens on cells were stained as described above in 2.3.5.1., then 200 µL of Fixation/Permeabilization Buffer (Thermo Fisher) was added to each of the samples prior to incubation for 1 hour at 4°C. Following the incubation period, samples were processed as described above in 2.3.5.2, using 100 µL of the intranuclear staining cocktail (Table 2.2).

2.3.4 Cell culture for *ex vivo* antigen recall

To quantify recall responses, cells isolated from spleens, lymph nodes, bone marrow, and genital tracts were re-suspended in complete (c)RPMI medium (Table 2.1) and plated 1×10^6 cells/well (200 µL) in a 96 well U-bottom tissue culture dish (Sarstedt). Cells from a given sample were plated in triplicate for each stimulation condition. Culture stimulation conditions included media alone, total dilutions at 1/50 (4.8×10^6 IFU/mL), 1/100 (2.4×10^6 IFU/mL), and 1/200 (1.2×10^6 IFU/mL) of *Cm* that had been heat-killed at 65°C for 30 minutes (HK*Cm*), or 1 ng/well of anti-mouse CD3 (Bio X Cell, Lebanon, NH). Cultures were incubated at 37° C for 72 hours, then were centrifuged for 20 minutes at 525×g at 4°C in the Allegra X-12R centrifuge for the separation and collection of the supernatant, which was stored at -20°C for future use.

Table 2.2: List of anti-mouse, fluorochrome conjugated, primary monoclonal antibodies used for flow cytometry experiments.

Target	Conjugate	Catalogue Number	Manufacturer	Volume/Test
CD3	Brilliant Violet 650™	100229	BioLegend	0.167 µL
CD3	PerCP-Cyanine5.5	45-0031-82	Thermo Fisher	0.25 µL
CD4	Alexa Fluor® 700	100430	BioLegend	0.1 µL
CD4	APC	17-0042-83	Thermo Fisher	0.5 µL
CD4	FITC	11-0042-85	Thermo Fisher	0.25 µL
CD8a	PE	12-0081-85	Thermo Fisher	0.33 µL
CD11b	APC	17-0112-82	Thermo Fisher	0.125-0.25 µL
CD11c	PerCP-Cyanine5.5	45-0114-82	Thermo Fisher	0.25 µL
CD19	PE-Cyanine7	25-0193-82	Thermo Fisher	0.042 µL
CD31	Brilliant Violet 711™	740690	BD Biosciences	0.125 µL
CD45	Brilliant Violet 421™	103134	BioLegend	0.062 µL
CD45R	eFluor™450	48-0452-82	Thermo Fisher	0.5 µL
CD185	APC/Fire™ 750	145534	BioLegend	2.5 µL
IL-4	PE	12-7041-82	Thermo Fisher	1 µL
IL-17A	APC	17-7177-81	Thermo Fisher	1 µL
Foxp3	PE	12-5773-82	Thermo Fisher	1 µL
F480	Brilliant Violet 650™	123149	BioLegend	0.167 µL
I-A/I-E	Brilliant Violet 785™	107645	BioLegend	0.033 µL
IFNγ	PE-Cyanine7	25-7311-41	Thermo Fisher	1 µL
Ly6C	PE	560592	BD Biosciences	0.083 µL
Ly6G	FITC	11-9668-82	Thermo Fisher	0.2-0.25 µL
Podoplanin	PE/Dazzle™ 594	127420	BioLegend	0.25 µL
TCRβ	APC eFluor™780	47-5961-82	Thermo Fisher	0.25 µL

2.3.5 Enzyme linked immunosorbent assay (ELISA)

2.3.5.1 Indirect ELISA

The indirect ELISA protocol was used to determine antibody levels in serum samples. Coating solutions were prepared by diluting 500 IFU of HK*Cm* per sample or 5 µg of one of the isolated *Cm* antigens per sample in 0.05 M $NaHCO_3$ ELISA coating buffer (Table 2.1). High-binding, 96-well microplates (ELISA plates) (Grenier Bio-One) were coated with 50 µL containing 500 IFU/well of HK*Cm* or 5 µg/well of the isolated *Cm* antigens; TC0912C, -0582, and -0047 (167). A 2012 report characterized the TC0912C and TC0582 as pathogenic antigens, and the TC0047 antigen as non-pathogenic (167). Coated ELISA plates were incubated overnight at 4° C to facilitate binding of the pathogen/antigen coat.

Within 24 hours, the unbound coat was washed off 3 times with 200 µL of 0.1% Tween20 (Sigma Aldrich) PBS (PBST) (Table 2.1) using a BioTek plate washer. The wash was removed by dumping and blotting the plates with paper towel. The wells of the plates were blocked with 200 µL of PBST with 2% bovine serum albumin (BSA) (Sigma Aldrich) and incubated at room temperature for 2 hours. During this time, serum samples were diluted serially in PBST with 2% BSA across a 96-well V-bottom test plate (Sarstedt), starting at 1:50. Following the incubation, the 3-cycle wash and dumping step was repeated, then 100 µL of diluted sample or PBST, as a negative control, was loaded into the wells. The plates were incubated overnight at 4°C.

On the third day, the diluted samples and negative controls were removed from the plates with a 5 cycle PBST washing and dumping step. Secondary antibodies of goat anti-mouse IgG1, IgG2a, IgG2b, and IgA conjugated to horseradish peroxidase (HRP) (Novus Biologicals, Colorado, USA) were diluted 1:50,000 in PBST with 2% BSA, then 100 µL of the diluted secondary antibody was added to each of the wells of their respective plates. After a 2-hour incubation at RT, the plates were washed 7 times with PBST and the wash was removed by dumping, then 50 µL of 1X tetramethylbenzidine substrate solution (TMB) (Thermo Fisher) was added to all wells. The plates were incubated in the dark for 8 minutes, then 50 µL of 2M H_2SO_4 was used to end the reaction and stabilize the colour. The OD of each of the wells was measured at 450 nm

within 15 minutes of stopping the reaction using a Biotech Synergy HT plate reader with Gen5 2.03 software.

2.3.5.2 Sandwich ELISA

Cytokines were measured in *ex vivo* antigen recall supernatant samples via a sandwich ELISA. Capture antibodies directed against mouse IL-10, -13, 17A, TNFα, and IFNγ (Thermo Fisher) were diluted in 1X assay diluent (Thermo Fisher) according to manufacturer instructions. ELISA plates were coated with 50 µL/well of diluted capture antibody and incubated overnight at 4°C.

The unbound capture antibodies were washed off with a BioTek plate washer using the 3-wash cycle with 200 µL of PBST. After discarding the wash and blotting the plates, 200 µL of 1X assay diluent (Thermo Fisher) was used to block the plates during a 2-hour incubation at RT. During this time, the supernatant samples were diluted as needed with 1X assay diluent: twofold for IL-10 and TNF, fourfold for IL-13 and -17A, and tenfold for IFN-γ. Lyophilized standards of a known concentration (Thermo Fisher) were reconstituted with 1X assay diluent (Thermo Fisher) and serially diluted twofold for a total of 8 standard dilution points. Following the incubation, the 3-cycle wash and dumping step was repeated, then 100 µL of diluted sample, the known standards, or PBST, as a negative control, was loaded into the wells. The plates were incubated overnight at 4°C.

On the third day, the plates were washed with a 5 cycle PBST washing and dumping step. Biotin-conjugated, secondary detection antibodies for each of the cytokines (Thermo Fisher) were diluted in 1X assay diluent (Thermo Fisher) according to manufacturer instructions, then 50 µL of the diluted detection antibodies were added to their respective plates. After a 2-hour incubation at RT, the plates were washed 5 times with PBST, the wash removed by dumping, and 50 µL of 1X streptavidin-horseradish peroxidase (SAV-HRP) (Thermo Fisher) was added to each of the wells. The plates were incubated at room temperature for 20 minutes, then the unbound SAV-HRP was removed by a 7-cycle PBST wash. The final wash was discarded by dumping and blotting, then 50 µL of 1X TMB (Thermo) was added to all wells. The plates were incubated in the dark until the 7th well of the serially diluted standard developed colour, then 50 µL of 2M

H_2SO_4 was used to end the reaction and stabilize the colour. The OD of each of the wells was measured at 450 nm within 15 minutes of stopping the reaction using a Biotech Synergy HT plate reader with Gen5 2.03 software.

2.3.6 Chemokine and cytokine Luminex assay

The molecular mediators present in the high-speed spin, homogenized genital tracts were quantified via a 36-plex ProcartaPlex assay with Luminex technology (Thermo Fisher). Included in the kit were beads specific to CCL2 (MCP-1), CCL3 (MIP-1α), CCL4 (MIP-1ß), CCL5 (RANTES), CCL7 (MCP-3), CCL11 (eotaxin), CXCL1 (GRO-α), CXCL2 (MIP-2α), CXCL5 (ENA-78), CXCL10 (IP-10), G-CSF, GM-CSF, IFN-α, IFN-γ, LIF, M-CSF, TNF, IL-1α, IL-1ß, IL-2, IL-3, IL-4, IL-5, IL-6, IL-9, IL-10, IL-12p70, IL-13, IL-15, IL-17A, IL-18, IL-22, IL-23, IL-27, IL-28, and IL-31. Following the thawing of the homogenate supernatants on ice, the samples and controls were prepared, assayed, and acquired according to the manufacturer's protocol. The fluorescent signals from the assay plate were detected with a Bio-Plex200 system (Bio-Rad, CA).

In order to normalize the 36plex assay data, total proteins present in the homogenate samples were measured using a bicinchoninic acid assay (Thermo Fisher). The homogenates were diluted tenfold with dilution buffer from the kit. The commercially available albumin protein standard was prepared according to the manufacturer instructions by serially diluting twofold for a total of 8 standard dilution points, with concentrations ranging from 0 to 2000 µg/mL. A V-bottom plate (Sarstedt) was used to combine the diluted samples and standards with the bicinchoninic acid working reagent; each sample or standard was plated in duplicate. The samples were mixed well, incubated at 37°C for 30 minutes, and then the absorbance of each of the wells was measured at 562 nm using a Biotech Synergy HT plate reader with Gen5 2.03 software. The values from the albumin standards were used to create a standard curve in order to quantify the protein concentrations of the homogenates.

2.4 Statistics

Prism 5 and Prism 9 software (GraphPad, La Jolla, CA) was utilized for statistical analysis and visualization of data. Analysis involving a single variable and two groups was conducting using an unpaired t test. Analysis involving two independent variables and two or more groups was conducted using a 2-way ANOVA with a Bonferroni *post hoc* test. Analysis for infection clearance survival curves were conducing using a Mantel-Cox test and a Gehan-Breslow-Wilcoxon test. All data are presented as mean ± standard error of mean (SEM), excluding infection clearance survival curves, which as presented as mean only. Significance is indicated by a P value < 0.05 as *, P value <0.01 as **, P value <0.001 as ***, and P value <0.0001 as ****.

CHAPTER 3 RESULTS

3.1 Differential outcomes in pathology, but not bacterial load, follow repeated and single *Cm* infections

Due to the possibility of repeated exposure to *Ct* in humans, which is not accounted for in conventional animal research of *Chlamydia*, preliminary work on a model of low dose *Cm* infections in mice was undertaken in the past decade by preceding trainees in the Wang Lab. Mice were infected with either a single, high 3×10^5 IFU dose of *Cm* (1X), to represent the infection models used classically, or five repeated, low 6×10^4 IFU doses of *Cm* (5X), to correspond to potential infection states in humans. Infected mice were followed to comprehend the natural course of infection following each of the dosage schedules. Vaginal swabbing, chlamydial gDNA isolation, and quantification by qPCR was utilized to estimate the bacterial loads from each of the animals, while tissue pathology was assessed using oviduct cyst measurement, which is a standard marker of tissue damage used in the field of *Chlamydia* research (168).

The results of these investigations demonstrated that the infections following 1X and 5X exposure to *Cm* result in comparable bacterial shedding over the course of the infection; there were similar initial burdens and rates of clearances between the groups (Figure 3.1). However, histopathology assessment of the oviduct cyst dilations revealed that 5X infected mice had significantly larger oviduct cyst dilations compared to those identified in 1X infected animals (Figure 3.2), indicating a higher degree of tissue damage in the 5X group following *Cm* infection. The deviation in tissue pathology outcomes between the 1X and 5X groups, despite apparent similarities in infection control, underscored the potential of the 5X infection schedule to augment the understanding of chlamydial disease states in humans, and to characterize the concepts that remain without consensus in the field.

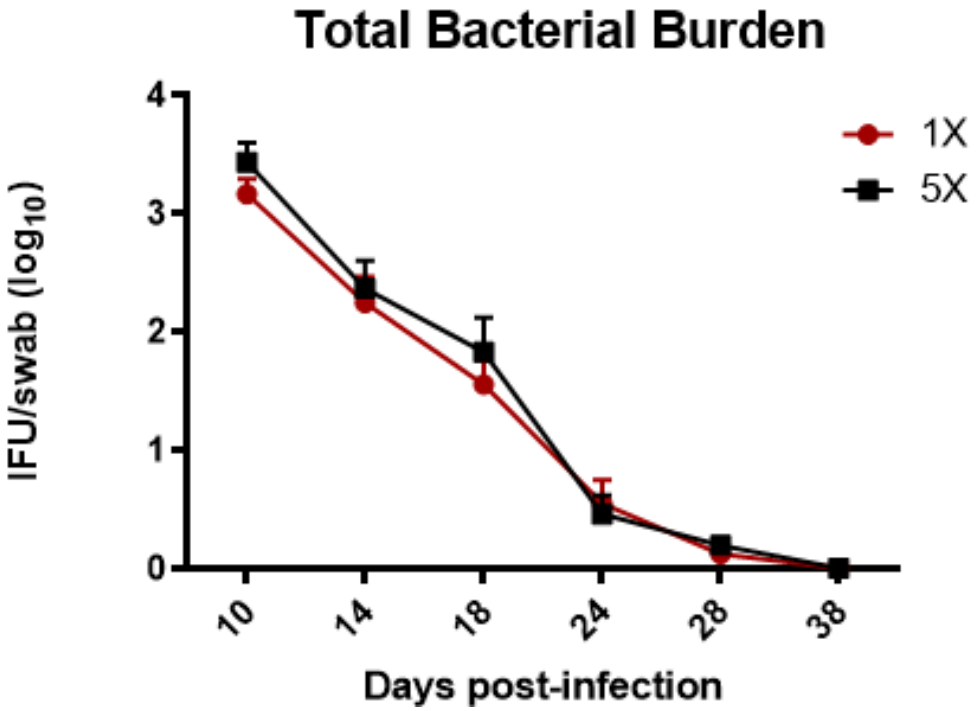

Figure 3.1: Vaginal bacterial shedding is comparable following 1X and 5X *Cm* infections. C57BL/6 mice were intravaginally infected with one 3×10^5 IFU dose of *Cm* (1X) (n=14) or five, low 6×10^4 IFU doses of *Cm* that are cumulatively equivalent to the 1X dose (5X) (n=13). Vaginal swabs were collected from infected animals, then chlamydial DNA was isolated and quantified by quantitative PCR. Log_{10}-transformed bacterial burden data from 2-3 pooled experiments was produced from work conducted by Melanie Tillman and are presented as mean ± SEM using a two-way ANOVA test with a Bonferroni *post hoc* test.

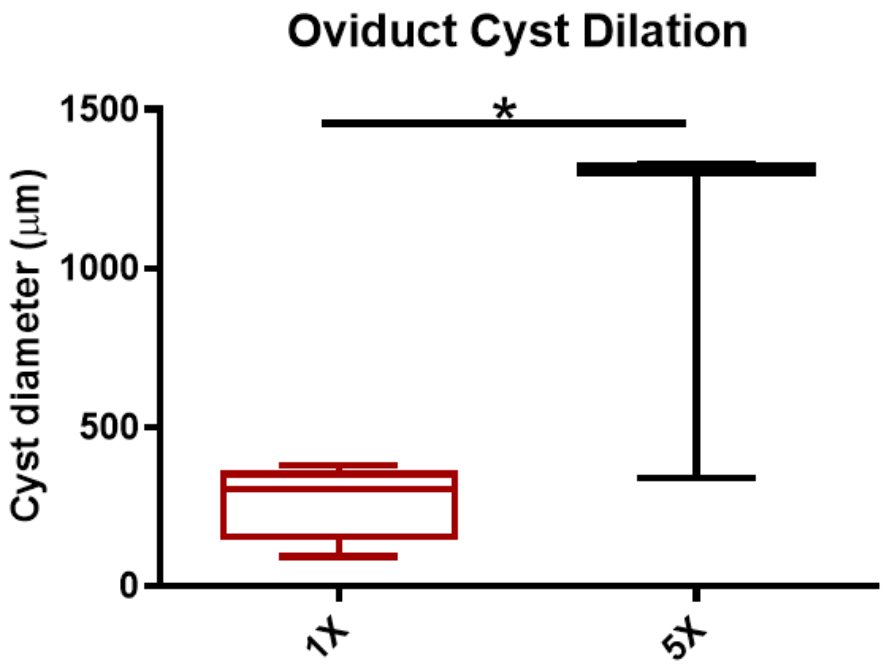

Figure 3.2: Oviduct pathology following *Cm* infection is exacerbated in 5X-infected mice. C57BL/6 mice were intravaginally infected with one 3×10^5 IFU dose of *Cm* (1X) (n=4) or five, low 6×10^4 IFU doses of *Cm* that are cumulatively equivalent to the 1X dose (5X) (n=3). Genital tracts from infected animals were processed for histology at 50 days post-initial infection, then analyzed for oviduct cyst dilation as a measure of tissue damage via Fiji image analysis software. The largest cyst dilation, calculated from histological samples under 5X or 10X magnification, was chosen for analysis. Data was produced from experiments conducted by Melanie Tillman and are presented as a box plot with whiskers from minimum to maximum values; *$p< 0.05$ using a t-test.

3.2 1X and 5X *Cm* infections induce distinct immune kinetic profiles

As previous work using the single and repeated infections model has indicated that there are differences in oviduct pathology, but not bacterial burden, following single and repeated infections, we were interested in investigating whether the 1X and 5X infection schedules induced differential host responses. To accomplish this, mice were infected with either the 1X or 5X dosage schedule, then tissue samples were taken at days 10 and 30, then immune kinetics for neutrophils, T cells, and B cells were determined via flow cytometry. Tissue samples from uninfected animals were included as a baseline control, in order to calculate the fold change from baseline.

No differences between the 1X and 5X animals were observed in the spleen for any of the cell types. However, the influx of neutrophils was markedly higher in the genital tract of the 5X group compared to the 1X group. Neutrophil levels in the 5X genital tract were elevated at 10 days post-initial infection (d.p.i.i.) and became significantly higher compared to the levels in the 1X genital tract at 30 d.p.i.i. (Figure 3.3). The significantly lower levels of neutrophils in the bone marrow of 5X animals compared to those of 1X animals at 30 d.p.i.i. is consistent with this change and implies the increased departure of neutrophils from the bone marrow to the local site of infection in the 5X mice (Figure 3.3).

Despite the robust neutrophilic kinetics, the influx of T and B cells into the genital tract were remarkably reduced in the 5X group compared to the 1X group. The levels of both T and B cells were significantly lower in the 5X group genital tracts at 30 d.p.i.i. (Figure 3.4; Figure 3.5). In the bone marrow, T cells were significantly reduced in the 5X group at 30 d.p.i.i. (Figure 3.4), and the B cell levels followed a similar pattern, despite non-significance (Figure 3.5). Together, these data suggest that the 1X and 5X infections induce distinctive host immunity kinetics, which become apparent at later timepoints.

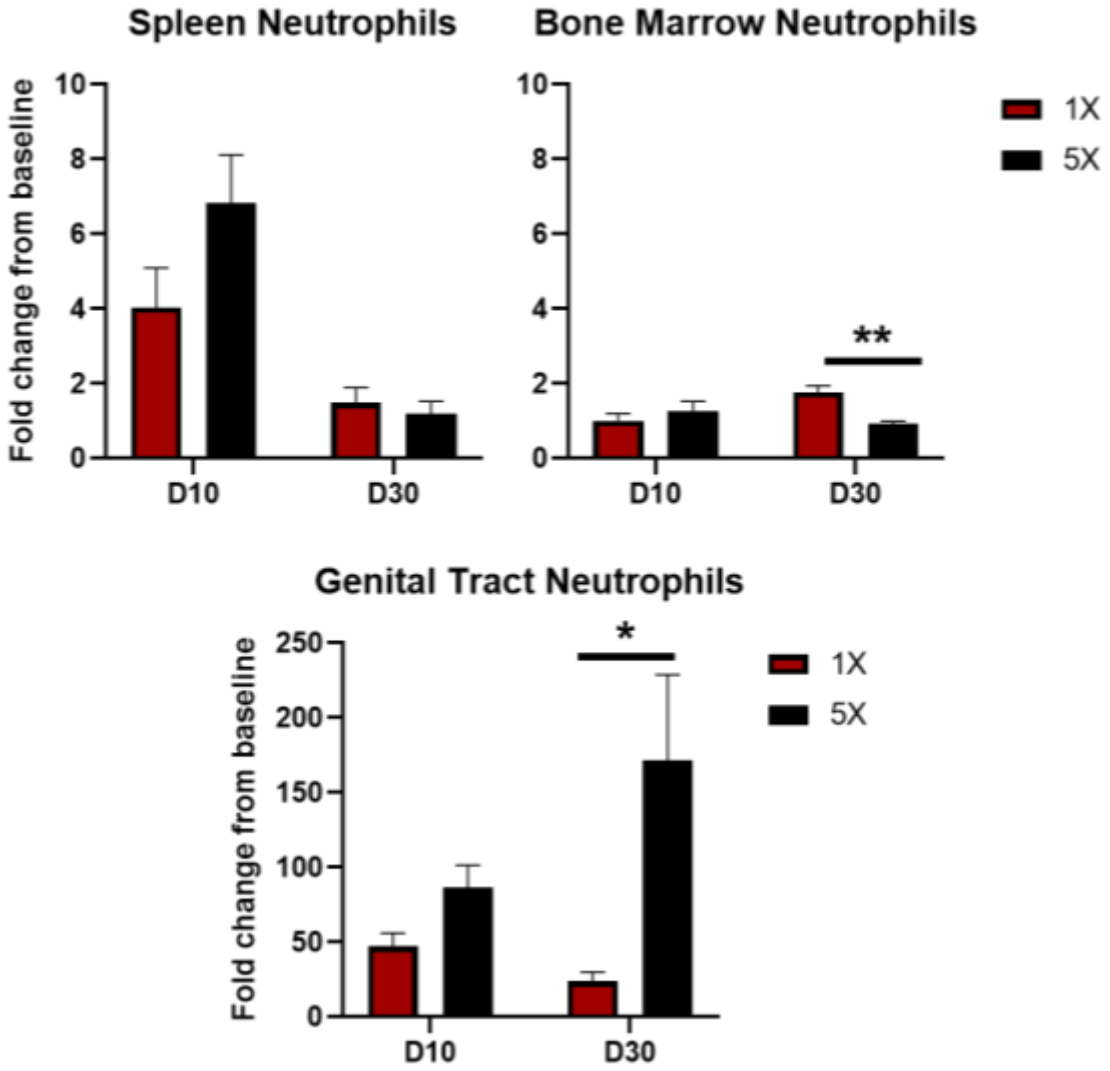

Figure 3.3: 5X *Cm* infections trigger significant neutrophilic influx compared to 1X infection. C57BL/6 CD45.1 mice were intravaginally infected with one dose of *Cm* (6×10^5 IFU; 1X) or five low doses of *Cm* that are cumulatively equivalent to the 1X dose (1.2×10^5; 5X). The fold change of neutrophils from baseline in the spleen, bone marrow, and genital tract (n=4-5 mice/timepoint) at days 10 and 30 post-initial infection were determined by flow cytometry. Data are presented as mean ± SEM; *P≤0.05, **P≤0.01 using a two-way ANOVA test with a Bonferroni *post hoc* test.

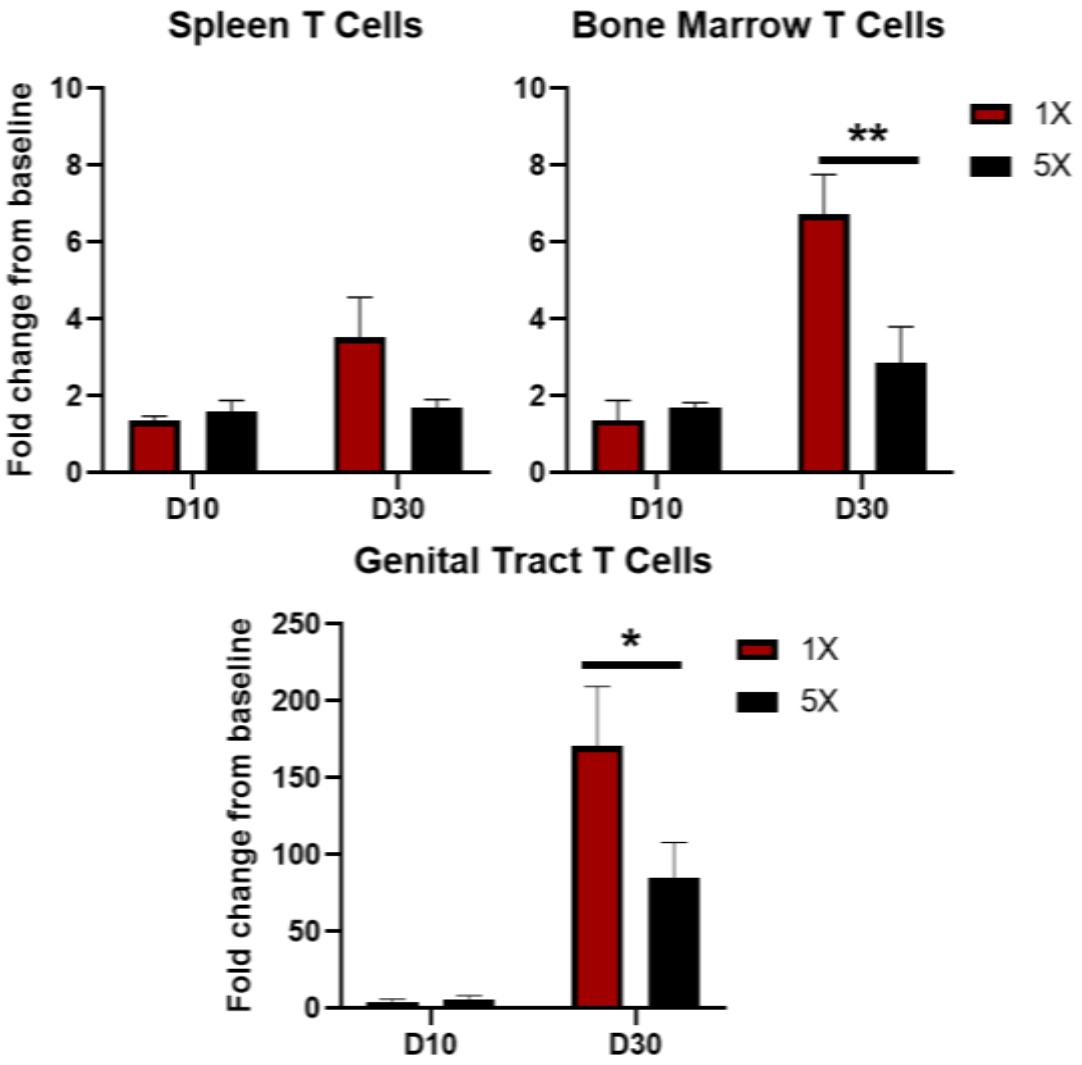

Figure 3.4: 5X *Cm* infections induce reduced T cell influx compared to 1X infection. C57BL/6 CD45.1 mice were intravaginally infected with one dose of *Cm* (6×10^5 IFU; 1X) or five low doses of *Cm* that are cumulatively equivalent to the 1X dose (1.2×10^5; 5X). The fold change of T cells from baseline in the spleen, bone marrow, and genital tract (n=4-5 mice/timepoint) at days 10 and 30 post-initial infection were determined by flow cytometry. Data are presented as mean ± SEM; *P≤0.05, **P≤0.01 using a two-way ANOVA test with a Bonferroni *post hoc* test.

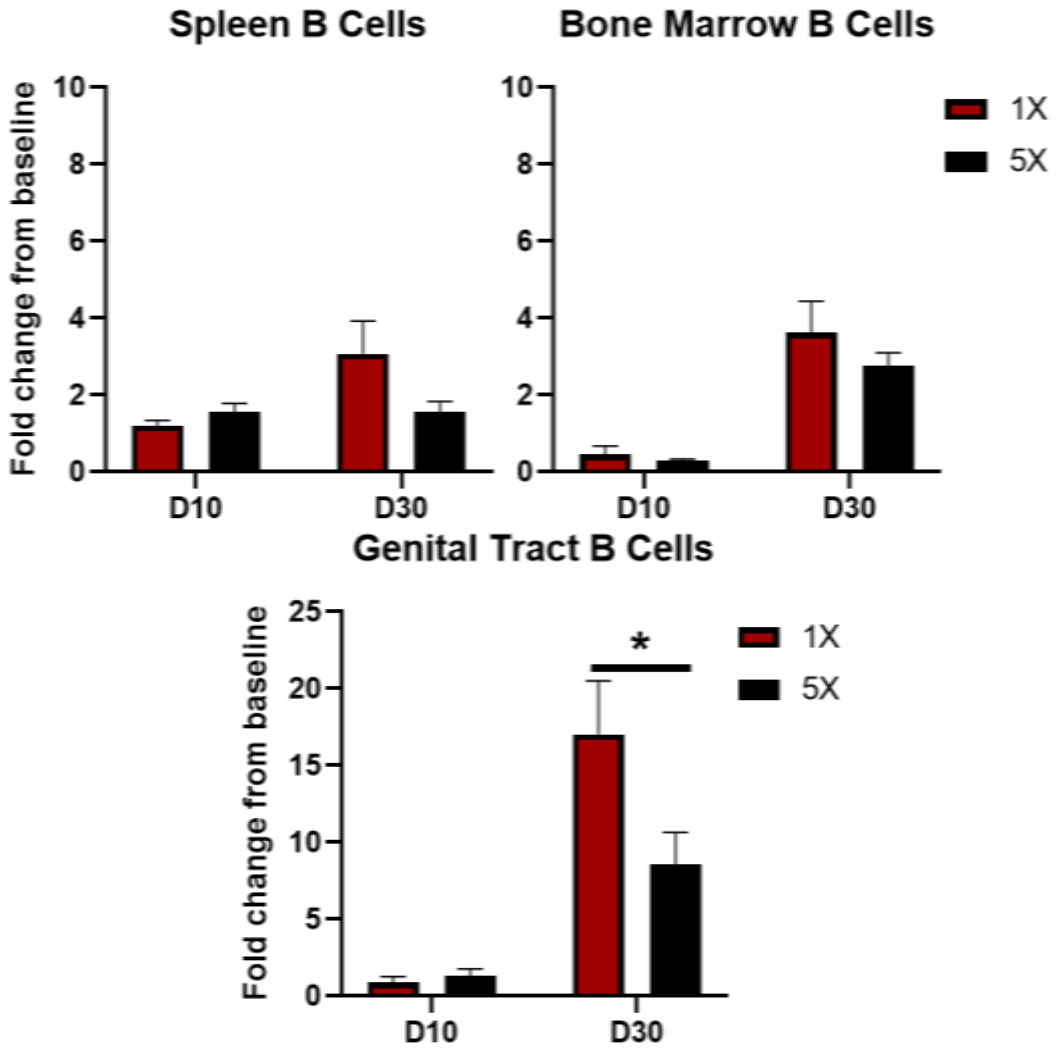

Figure 3.5: 5X *Cm* infections induce reduced B cell influx compared to 1X infection. C57BL/6 CD45.1 mice were intravaginally infected with one dose of *C. muridarum* (6×10^5 IFU; 1X) or five low doses of *C. muridarum* that are cumulatively equivalent to the 1X dose (1.2×10^5; 5X). The fold change of B cells from baseline in the spleen, bone marrow, and genital tract (n=4-5 mice/timepoint) at days 10 and 30 post-initial infection were determined by flow cytometry. Data are presented as mean ± SEM; *P≤0.05 using a two-way ANOVA test with a Bonferroni *post hoc* test.

To ascertain if there were any divergences that were not revealed with traditional gating strategies, FCS Express 7 data transformation functions were utilized. The flow cytometry data from the genital tracts of 1X and 5X mice at 30 d.p.p.i. were merged, then transformed with a t-distributed stochastic neighbor embedding (tSNE) overlay. The spread of the data reflected the overall observations of enhanced neutrophil influx into the genital tract of the 5X mice (Figure 3.6B) compared to that of the 1X mice (Figure 3.6A); neutrophils were identified based on their Ly6G expression (Figure 3.7). Furthermore, the tSNE density plots revealed the differences that were not limited to neutrophils, T cells, and B cells.

Based on the clustering of the expression density, the 1X and 5X genital tract cell environments diverge from each other (Figure 3.6). Population E appears to be enriched in the 1X (Figure 3.6A), but not the 5X genital tract (Figure 3.6B). Conversely, populations A, B, C, D, F, and G were obviously pronounced in the 5X genital tract (Figure 3.6B) but were absent or reduced in the 1X genital tract (Figure 3.6A), though no statistically significant differences could be identified. While these populations have yet to be fully characterized, they display unique profiles in terms of relative marker expression (Figure 3.7). There were especially remarkable visual distinctions in Ly6C and CD11c expression between the populations, although no analysis was conducted to determined whether the expression was significantly divergent (Figure 3.7). The tSNE transformed 30 d.p.p.i. data reinforces the observations of diverging immune responses to repeated, low dose *Cm* infections when compared to those following the convention single dose model of *Cm* infection.

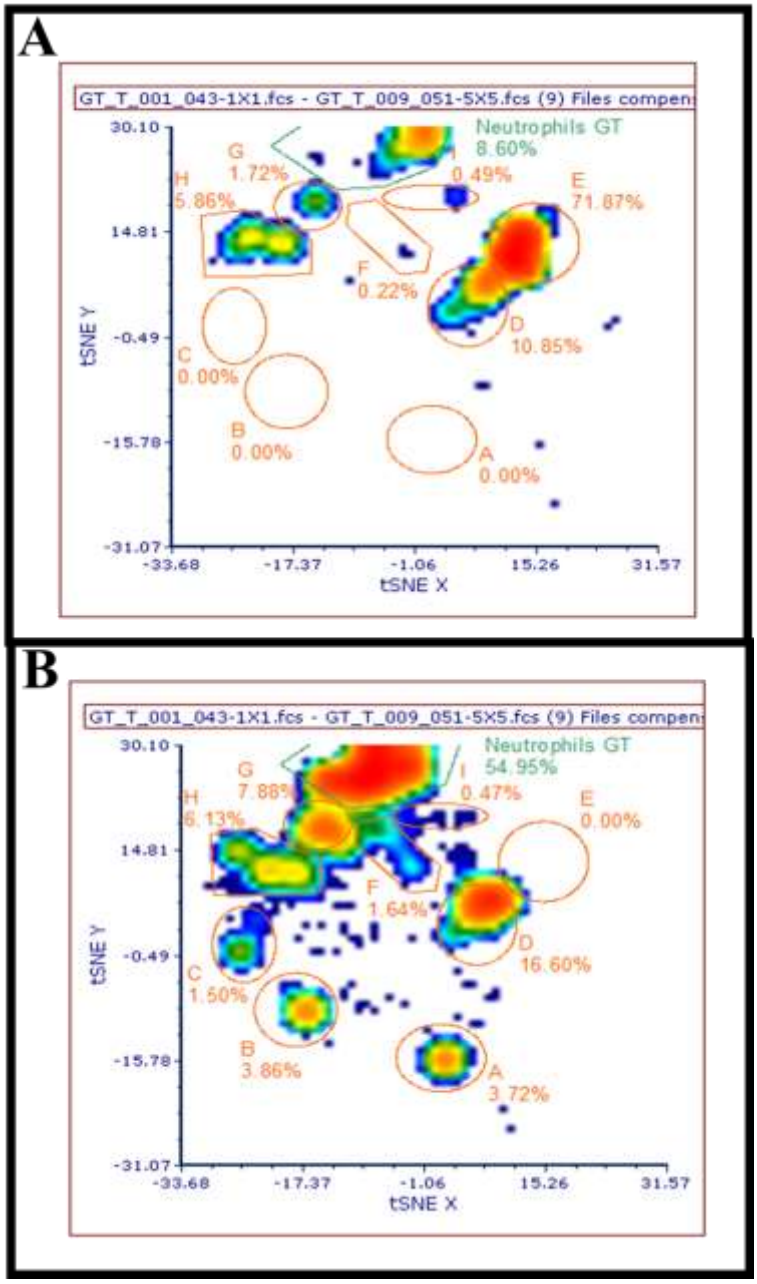

Figure 3.6: 1X and 5X *Cm* infections induce distinct immune profiles. C57BL/6 CD45.1 mice were intravaginally infected with one dose of *Cm* (6×10^5 IFU; 1X) or five low doses of *Cm* that are cumulatively equivalent to the 1X dose (1.2×10^5; 5X). Genital tract samples from 1X (n=4 mice) and 5X (n=5 mice) infected mice were assessed for their expression of Ly6G, Ly6C, CD11b, CD11c, TCR-ß, B220, and CD19 at 30 days post-initial infection via flow cytometry. Data are presented as a merged 1X (A) or 5X(B) cell marker expression profile density with a t-distributed stochastic neighbor embedding (tSNE) transformation. Distinct cell populations, both identified or uncharacterized, are circled and include their estimated frequencies.

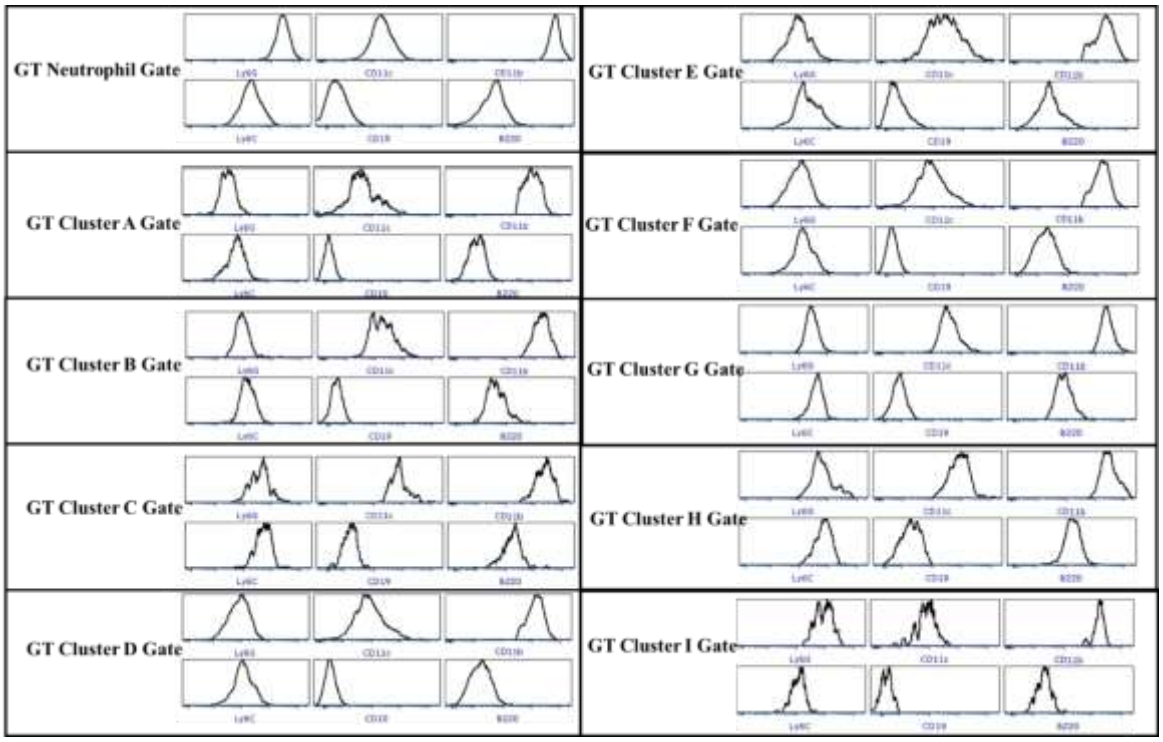

Figure 3.7: 1X and 5X *Cm* infections induce distinct immune profiles that display unique marker expression. C57BL/6 CD45.1 mice were intravaginally infected with one dose of *Cm* (6×10^5 IFU; 1X) or five low doses of *Cm* that are cumulatively equivalent to the 1X dose (1.2×10^5; 5X). Genital tract samples from 1X (n=4 mice) and 5X (n=5 mice) infected mice were assessed for their expression of Ly6G, Ly6C, CD11b, CD11c, TCR-ß, B220, and CD19 at 30 days post-initial infection via flow cytometry. Data are presented as histograms of relative marker expression from the identified or uncharacterized distinct cell populations present in the t-distributed stochastic neighbor embedding (tSNE) transformation in Figure 3.6.

3.2.1 Neutrophil phenotype subsets are polarized at the local site of infection during 5X, but not 1X, infections

Given that distinct neutrophil kinetics were generated from the 1X and 5X infections, we investigated whether there was an impact on the neutrophil phenotype primed by the infection schedules. Previous work with *S. aureus* infections in mice has demonstrated the existence of multiple neutrophilic profiles; pro-inflammatory (N1), pro-regulatory (N2), and undifferentiated (N0), which can be distinguished based on CD11b expression levels (86). To identify the populations in flow cytometry data, N1 neutrophils were designated as $Ly6G^{hi}CD11b^{int}$, N2 neutrophils as $Ly6G^{hi}CD11b^{hi}$, and N0 neutrophils as $Ly6G^{int}CD11b^{int}$ (Figure 3.8A).

There was differential neutrophil polarization present in the genital tract; 5X, but not 1X, infected mice had significantly higher levels of N1 pro-inflammatory neutrophils at 30 d.p.p.i (Figure 3.8B). This significant elevation was not present on at other time points (Figure 3.8B). Furthermore, there were no significant differences observed between the groups for the N0 or N2 neutrophils in the genital tract (Figure 3.8B). This effect was not observed systemically, as splenic neutrophils were primarily of the undifferentiated N0 phenotype (Figure 3.8B), indicating that the modulators of polarization are likely present in infected tissues.

3.2.2 PDPN expression is upregulated following 5X infections

Due to the immune cell population differences between the groups after the first 30 days of *Cm* infection, we were keen to determine whether any stromal changes were occurring. We included a fluorescent antibody directed against mouse PDPN, which can be expressed by fibroblasts during inflammation and has been shown to contribute to host-mediated tissue damage (73, 74). At 23 d.p.p.i, we observed upregulated PDPN expression in the genital tract of 5X animals (Figure 3.9). This cannot be explained by the total cell numbers present in the pooled samples for each group, as the frequency (Figure 3.9A) and average amount of cells expressing PDPN (Figure 3.9B) reveal higher PDPN levels in the 5X genital tract. While the sample size precludes statistical analysis, it appears that the repeated *Cm* infections could be initiating a shift in the dynamics of the tissue repair machinery that does not occur following the single *Cm* infection.

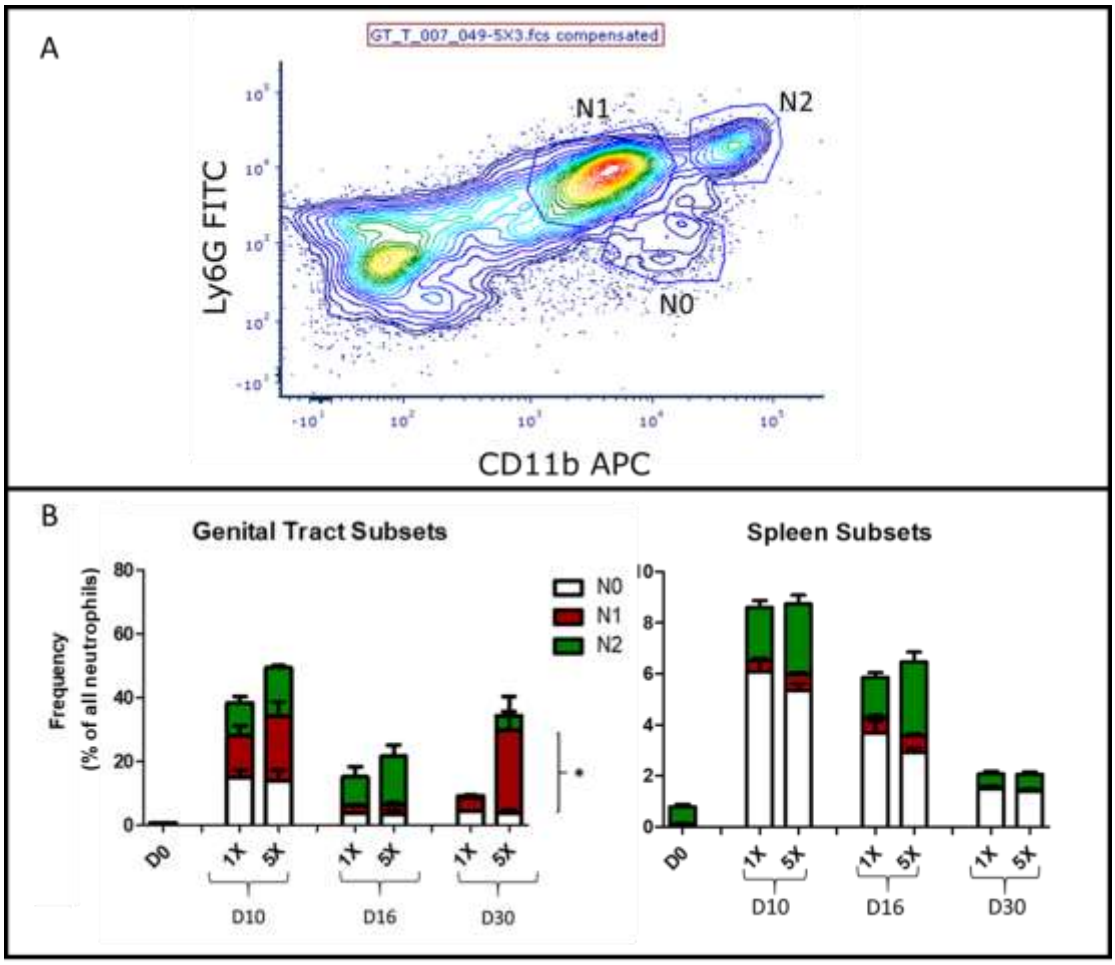

Figure 3.8: 5X *Cm* infections induce pro-inflammatory neutrophil subset differentiation in the genital tract, but not the spleen. C57BL/6 CD45.1 mice were intravaginally infected with one dose of *Cm* (6×10^5 IFU; 1X) or five low doses of *Cm* that are cumulatively equivalent to the 1X dose (1.2×10^5; 5X). The frequency of pro-inflammatory N1 neutrophils, designated as $Ly6G^{hi}CD11b^{int}$, pro-regulatory N2 neutrophils, designated as $Ly6G^{hi}CD11b^{hi}$, and undifferentiated N0 neutrophils, designated as $Ly6G^{int}$ $CD11b^{int}$ (A), in genital tracts and spleens (n=4-5 mice/timepoint) at days 0, 10, 16, and 30 post-initial infection were determined by flow cytometry (B). Data are presented as mean ± SEM; *P≤0.05, using two-way ANOVA test with a Bonferroni *post hoc* test.

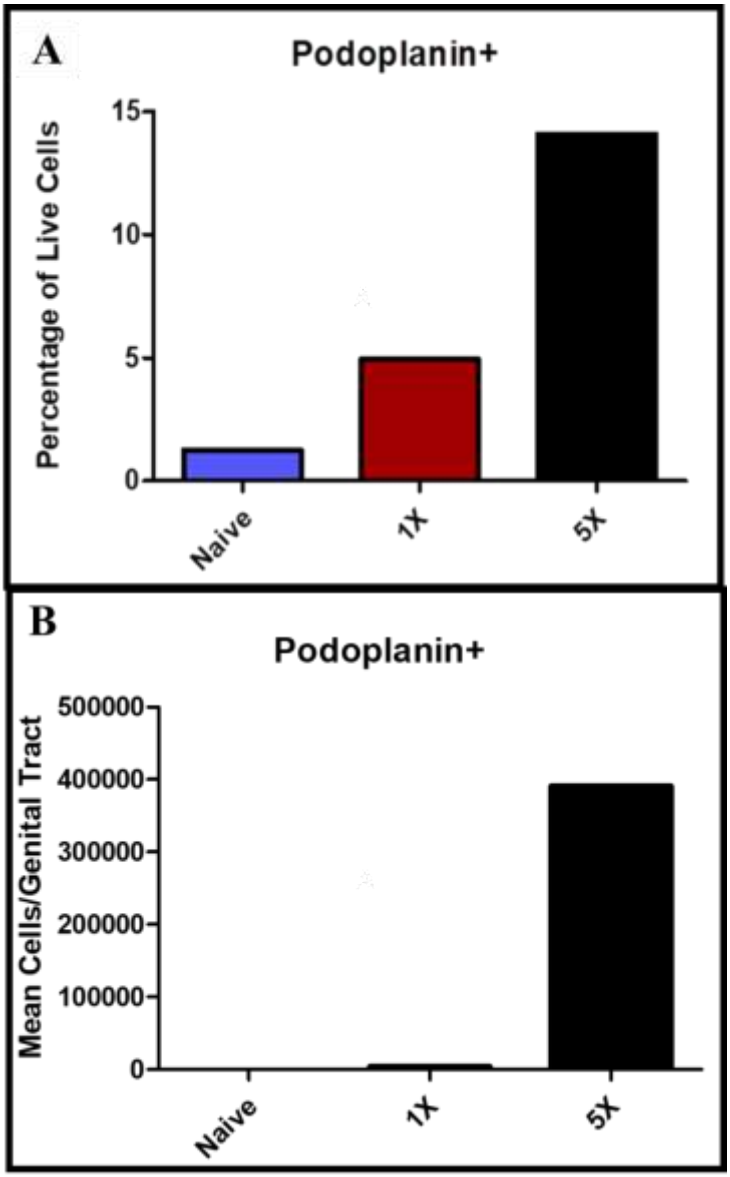

Figure 3.9: 5X *Cm* infections enhance PDPN expression compared to levels in 1X infection and naïve animals. C57BL/6 CD45.1 mice were intravaginally infected with one dose of *Cm* (6×10^5 IFU; 1X) (n=4 mice) or five low doses of *Cm* that are cumulatively equivalent to the 1X dose (1.2×10^5; 5X) (n=4 mice). A naive group of C57BL/6 CD45.1 mice (n=10) were included as a control. The frequency of PDPN expressing cells (A) and the average number of PDPN expressing cells per genital tract (B) (n=1 pooled sample/group) at day 23 post-initial infection was determined by flow cytometry. Data are presented as the mean only, due to the n of 1.

3.3 1X and 5X *Cm* infections induce distinct molecular mediator environments at the local site of infection

As we observed divergences in the immune cell kinetics and local tissue responses following single and repeated infections, we were keen to understand what host factors could be mediating the differential responses. To this end, we homogenized the genital tracts of 1X and 5X infected animals at 23 d.p.p.i., then assayed supernatant from the homogenates using a Luminex assay that could quantify the concentrations of 36 different cytokines and chemokines. Homogenate supernatant from naïve mice was included as a control.

The Luminex assay corroborated the findings observed for the divergence in the responses between the 1X and 5X group; there were obvious differences in the molecular mediator expression profiles (Figure 3.10). Based on the relatively darker colors corresponding to higher molecule concentration, there was enhanced expression of IL-1ß, IL-6, IL-18, IL-22, CXCL1, CXCL2, CCL2, CCL3, CCL4, CCL7, M-CSF, and eotaxin in the 5X group compared to levels in the 1X and naïve groups (Figure 3.10). IL-9 appeared to be downregulated in the 5X group, as both the 1X and naïve groups had higher levels that appeared to be comparable to each other. Conversely, in the 1X group, only CXCL5 (ENA-78) was upregulated compared to the 5X and naive groups (Figure 3.10).

There were some similarities between the 2 groups of infected animals. Compared to the naïve mice, both the 1X and 5X mice had higher levels of LIF, CCL5, and CXCL10 that appeared to be comparable to each other (Figure 3.10), indicating molecules that may be upregulated for both models of the infection. However, for the molecules IL-1α, IL-2, IL-4, IL-5, IL-15, IL-17A, and IL-31 (Figure 3.10), there were no obvious differences between any of the groups. Furthermore, there was no signal detected for IL-3, IL-10, IL-12p70, IL-13, and IL-28 and IFN-γ (data not shown). Despite the lack of data for some of the molecules, the pattern of mediator profile variations further emphasizes the deviation in host response in the repeated *Cm* infection model.

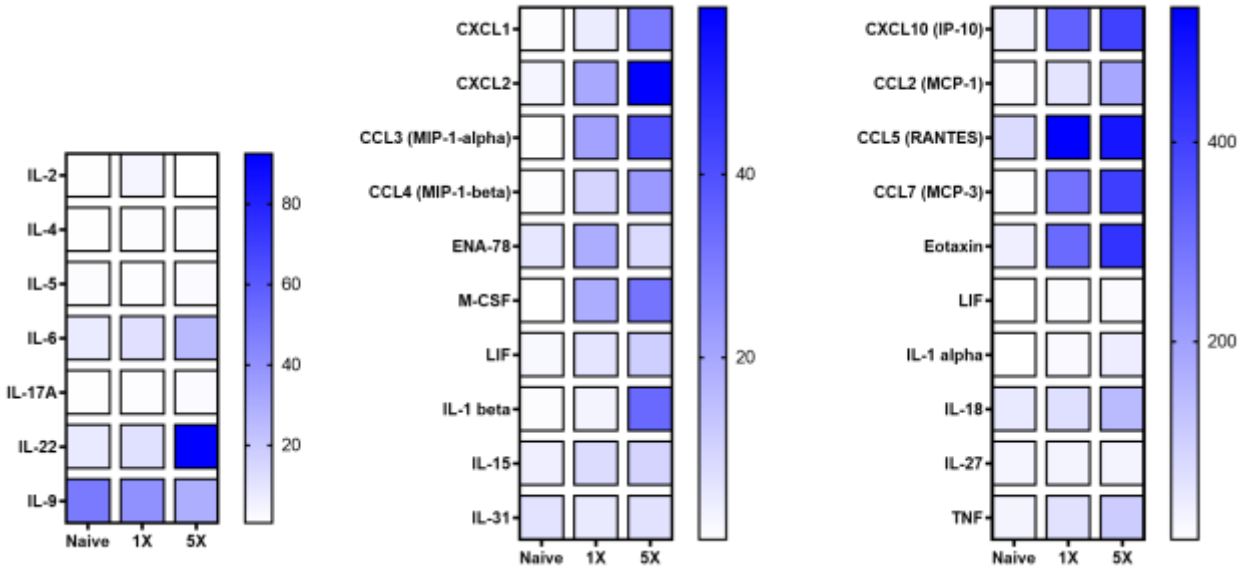

Figure 3.10: 1X and 5X *Cm* infections induce distinct mediator environments. C57BL/6 CD45.1 mice were intravaginally infected with one dose of *Cm* (6×10^5 IFU; 1X) or five low doses of *Cm* that are cumulatively equivalent to the 1X dose (1.2×10^5; 5X). Genital tract samples from 1X (n=4 mice) and 5X (n=5 mice) infected mice at 23 days post-initial infection were homogenized and supernatant from the homogenates were assayed in a cytokine/chemokine array using Luminex technology. The homogenate supernatants from naïve mice (n=6) were included as a control. Data are presented as a heat map of the average molecule concentration for each group, with relatively higher concentrations being a darker blue compared to lower concentrations.

3.4 *In vitro* cytokine production reveals 1X and 5X infections prime distinct CD4+ T cell responses

Based on the distinctive immune and neutrophil polarization profiles generated by the single and repeated infection models, we wanted to assess whether the divergence extended to other polarization-driven immune responses, such as the CD4+ T helper cell response. To pursue this, unseparated splenocytes and lymph node-derived lymphocytes isolated from 1X and 5X infected mice at 23 d.p.p.i. were cultured for 72 hours with anti-mouse CD3 antibody, HK*Cm* diluted 1:100, or with media as a negative control. Supernatants from the cultures were assayed via sandwich ELISA to quantify production of the IFN-γ, TNF, IL-13, IL-7A, and IL-10 cytokines by the splenocytes or lymph node derived lymphocytes. The presence of IFN-γ and TNF was used to determine a CD4+ Th1 response. The production of IL-13 and IL-17A was used to indicate a CD4+ Th2 and CD4+ Th17 responses, respectively. IL-10 was used a marker for the CD4+ Treg response.

The CD4+ Th1 responses from splenocytes and lymphocytes was not entirely clear and was sometimes conflicting. IFN-γ production by splenocytes in response to HK*Cm* was not impacted by whether the *Cm* infection occurred once or five times (Figure 3.11). Conversely, production of IFN-γ was significantly higher in lymph node-derived lymphocytes isolated from 1X animals compared to 5X infected animals (Figure 3.12). There was minimal production of IFN-γ in response to stimulation with anti-mouse CD3 or media by both splenocytes and lymphocytes from the 1X and 5X animals (Figure 3.11; Figure 3.12). The TNF produced by splenocytes was significantly higher in the 5X group compared to the 1X group in response to HK*Cm* stimulation; however, there was minimal production of TNF following anti-mouse CD3 and media stimulation (Figure 3.11). Stimulation with HK*Cm* elicited the highest production of TNF by lymphocytes, although there were no differences between the amounts produced by 1X and 5X animals for any of the stimulation settings (Figure 3.12).

Splenic production of IL-13 indicated an enhanced CD4+ Th2 response, as the levels of IL-13 were significantly higher in the 5X group compared to the 1X group (Figure 3.11). Furthermore, the stimulation by HK*Cm* generated appreciably more IL-13

production compared to stimulation by anti-mouse CD3, and media stimulation did not result in IL-13 production (Figure 3.11). IL-13 produced by lymph node-derived lymphocytes did not reveal significant differences between the 1X and 5X groups (Figure 3.12). The highest levels of IL-13 were produced in response to lymphocytic stimulation with anti-mouse CD3 (Figure 3.12). HK*Cm* and media stimulation of lymphocytes produced similar levels of IL-13, with the 1X group producing noticeably more of the cytokine, although the differences were insubstantial (Figure 3.12).

The splenic production of IL-17A following anti-mouse CD3 stimulation was strikingly higher in the 5X animals compared to the 1X animals, demonstrating that the CD4+ Th17 response is primed by 5X infection (Figure 3.11). HK*Cm* and media stimulation did not result in any IL-17A being produced by splenocytes (Figure 3.11). There were no significant differences between the groups for the production of IL-17A by lymph-node derived lymphocytes from any of the stimulations (Figure 3.12).

Similar patterns were present for the CD4+ Treg response in both the spleen and lymph nodes, based on IL-10 production. Anti-mouse CD3 stimulation of splenocytes resulted in significantly more IL-10 being produced in the 5X group compared to the 1X group (Figure 3.11). The highest levels of IL-10 were produced by splenocytes following HK*Cm* stimulation, despite the differences between the groups being insignificant and the IL-10 produced following media stimulation was unremarkable (Figure 3.11). As with the splenocyte data, significantly more IL-10 was produced by 5X lymph-node derived lymphocytes compared to those from 1X infected animals, however, this was in response to HK*Cm* stimulation (Figure 3.12). Stimulation of lymphocytes with anti-mouse CD3 and media resulted in minimal production of IL-10 from both 1X and 5X infected animals (Figure 3.12). Despite differences between the spleen and lymph node cytokine levels, when considered collectively, this data indicates that the 1X and 5X infections drive unique CD4+ T helper response profiles.

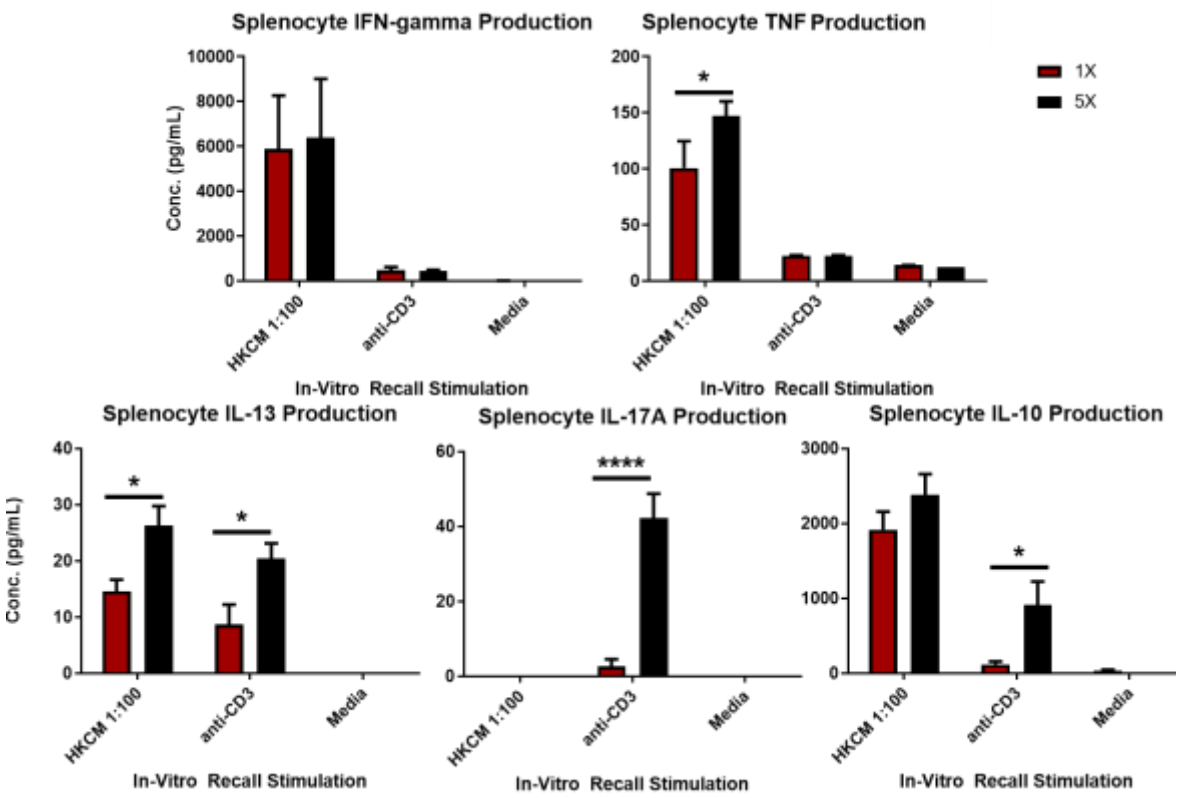

Figure 3.11: Splenocyte stimulation indicates differential cytokine environments are induced by 1X and 5X *Cm* infections. C57BL/6 CD45.1 mice were intravaginally infected with one dose of *Cm* (6×10^5 IFU; 1X) or 5 low doses of *Cm* that are cumulatively equivalent to the 1X dose (1.2×10^5; 5X). Splenocytes (n=3-5 mice/group pooled; n=3 technical replicates/group/stimulation) isolated at 23 days post-initial infection were stimulated with media, heat killed *Cm* (HKCM), or anti-mouse CD3 antibody for 72 hours. Supernatants collected from the culture stimulations were assayed in a sandwich ELISA to measure production of IFN-γ, TNF, IL-13, IL-7A, and IL-10. Data are presented as mean ± SEM; *P≤0.05, ****P< 0.0001 using a two-way ANOVA test with a Bonferroni *post hoc* test.

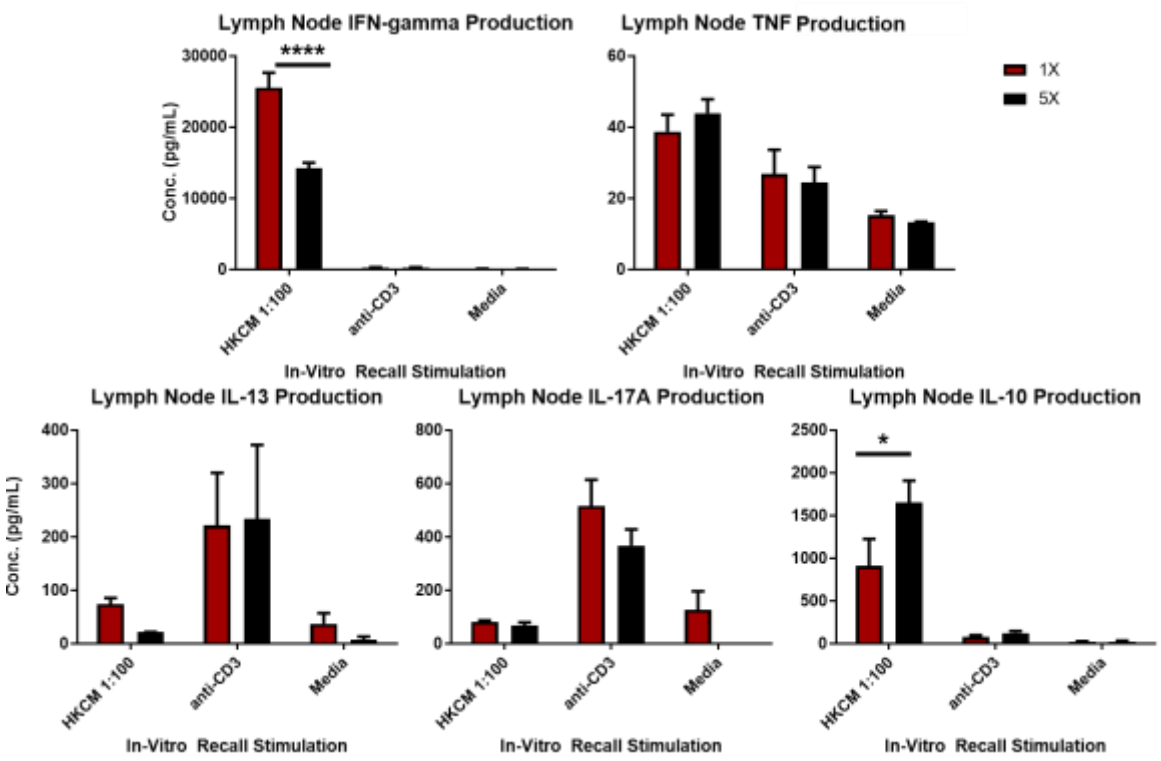

Figure 3.12: Lymphocyte stimulation indicates differential cytokine environments are induced by 1X and 5X *Cm* infections. C57BL/6 CD45.1 mice were intravaginally infected with one dose of *Cm* (6×10^5 IFU; 1X) or 5 low doses of *Cm* that are cumulatively equivalent to the 1X dose (1.2×10^5; 5X). Lymph node derived lymphocytes (n=3-5 mice/group pooled; n=3 technical replicates/group/stimulation) isolated at 23 days post-initial infection were stimulated with media, heat killed *Cm* (HKCM), or anti- mouse CD3 antibody for 72 hours. Supernatants collected from the culture stimulations were assayed in a sandwich ELISA to measure production of IFN-γ, TNF, IL-13, IL-17A, and IL-10. Data are presented as mean ± SEM; *P≤0.05, ****P< 0.0001 using a two-way ANOVA test with a Bonferroni *post hoc* test.

3.5 1X and 5X infections prime distinct CD4+ T cell responses, indicated by antibody isotypes

Previous reports have established IgG2a and IgG2b as indicators of a Th1 response, while IgG1 is associated with Th2 responses (169). Based on this, we utilized the presence of the isotypes to further clarify the divergent CD4+ T helper cell responses primed by the 1X and the 5X infection schedules. Serum taken from 1X or 5X infected mice at 30 d.p.i.i. was assayed via an ELISA to determine the relative levels of IgG antibody isotypes directed against individual *Cm* antigens representing a chlamydial infection: TC0047, -0582, and 0912c. A 2012 report characterized the TC0912C and TC0582 as pathogenic antigens, and the TC0047 antigen as non-pathogenic (167). Serum collected from naïve animals was used as a control.

Overall, there was a pattern of higher levels of IgG2a directed against all 3 antigens in the 1X group compared to the 5X group (Figure 3.13). This difference was significant for IgG2a directed against TC0047 in serum diluted 1:50 and 1:100 (Figure 3.13). A similar pattern was observed for IgG2b directed against TC0582 in the serum of 1X infected animals compared to those in the 5X group (Figure 3.14). However, these differences were only significantly higher in the 1X group for anti-TC0582 IgG2b in serum diluted 1:50, and the levels of IgG2b directed against TC0912c and TC0047 appeared to be comparable between the groups (Figure 3.14). IgG1 produced against TC0582, TC0912c, and TC0047 was visibly elevated in the 5X group compared to the 1X group (Figure 3.15). The IgG1 levels in the 5X group were significantly elevated against TC0582 for serum diluted 1:50 and 1:200, as well as against TC0047 in serum diluted 1:50 and 1:100 (Figure 3.15).

When considered collectively, the antibody isotype results suggest that the 5X infection generates more IgG1 and reveals a predominant CD4+ Th2 response. Conversely, the patterns of IgG2a driven by the 1X infection implies a predominant CD4+ Th1 response. In addition to the IgG isotypes, serum IgA was also assayed. IgA directed against any of the 3 antigens was absent or weakly present (Figure 3.16).

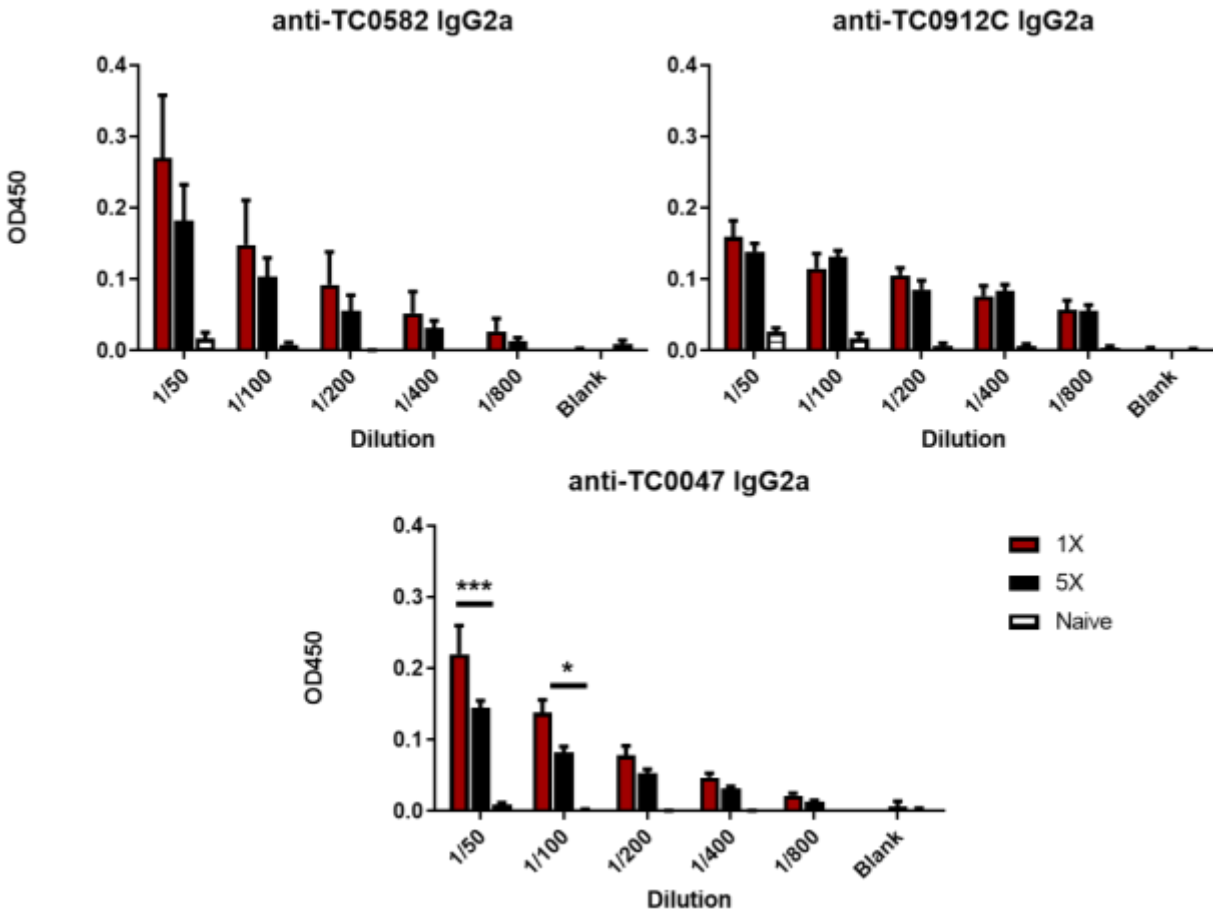

Figure 3.13: Serum IgG2a levels indicate 1X *Cm* infection primes Th1 responses. C57BL/6 CD45.1 mice were intravaginally infected with one dose of *Cm* (6×10^5 IFU; 1X) or 5 low doses of *Cm* that are cumulatively equivalent to the 1X dose (1.2×10^5; 5X). Serum collected (n=4-mice/group) at day 30 post-initial infection was serially diluted and assayed in an indirect ELISA to determine the IgG isotype, IgG2a, present against 3 antigens representing chlamydial infection, TC0582, TC0912c, and TC0047. Data was corrected to account for background signals, are presented as mean ± SEM; *P≤0.05, **P≤0.01, ***P≤ 0.001, using a two-way ANOVA test with a Bonferroni *post hoc* test.

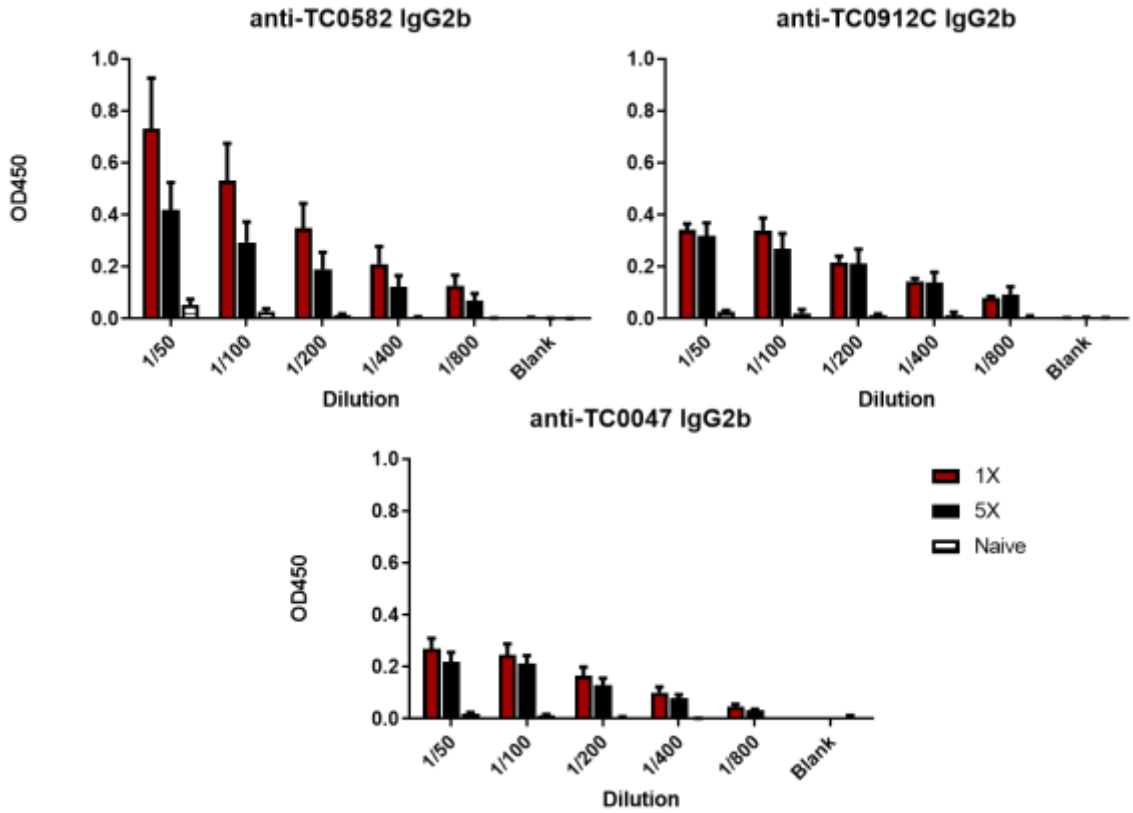

Figure 3.14: Serum IgG2b levels indicate 1X *Cm* infection primes Th1 responses. C57BL/6 CD45.1 mice were intravaginally infected with one dose of *Cm* (6×10^5 IFU; 1X) or 5 low doses of *Cm* that are cumulatively equivalent to the 1X dose (1.2×10^5; 5X). Serum collected (n=4-mice/group) at day 30 post-initial infection was serially diluted and assayed in an indirect ELISA to determine the IgG isotype, IgG2b, present against 3 antigens representing chlamydial infection, TC0582, TC0912c, and TC0047. Data was corrected to account for background signals, are presented as mean ± SEM; *P≤0.05, **P≤0.01, ***P≤ 0.001, using a two-way ANOVA test with a Bonferroni *post hoc* test.

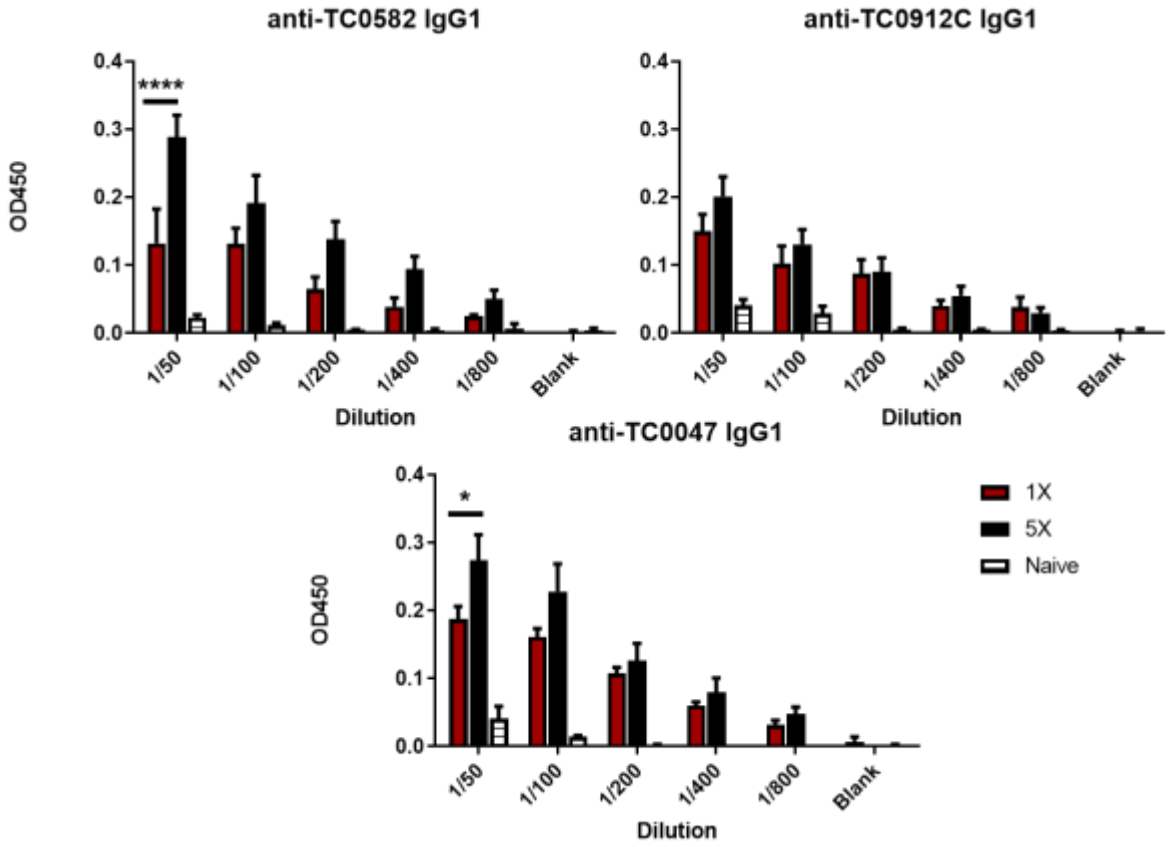

Figure 3.15: Serum IgG1 levels indicate 5X *Cm* infections prime Th2 responses. C57BL/6 CD45.1 mice were intravaginally infected with one dose of *Cm* (6×10^5 IFU; 1X) or 5 low doses of *Cm* that are cumulatively equivalent to the 1X dose (1.2×10^5; 5X). Serum collected (n=4-mice/group) at day 30 post-initial infection was serially diluted and assayed in an indirect ELISA to determine the IgG isotype, IgG1, present against 3 antigens representing chlamydial infections, TC0582, TC0912c, and TC0047. Data was corrected to account for background signals, are presented as mean ± SEM; *P≤0.05, **P≤0.01, ***P≤ 0.001, using a two-way ANOVA test with a Bonferroni *post hoc* test.

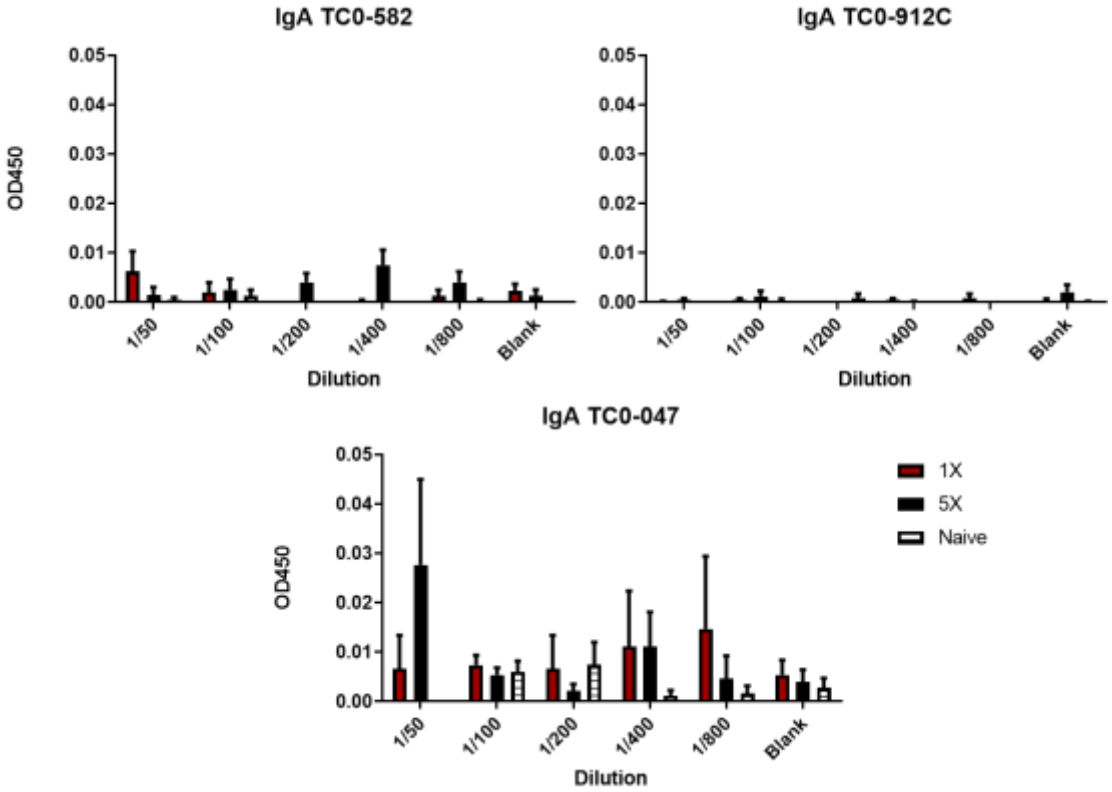

Figure 3.16: 1X and 5X *Cm* infections do not induce systemic IgA responses. C57BL/6 CD45.1 mice were intravaginally infected with one dose of *Cm* (6×10^5 IFU; 1X) or 5 low doses of *Cm* that are cumulatively equivalent to the 1X dose (1.2×10^5; 5X). Serum collected (n=4-mice/group) at day 30 post-initial infection was serially diluted and assayed in an indirect ELISA to determine the amount of IgA present against 3 antigens representing chlamydial infections, TC0582, TC0912c, and TC0047. Data was corrected to account for background signals, are presented as mean ± SEM; *P≤0.05, **P≤0.01, ***P≤ 0.001, using a two-way ANOVA test with a Bonferroni *post hoc* test.

3.6 Primary 1X and 5X *Cm* infections produce differential levels of immune protection during subsequent *Cm* challenge

Given that the 1X and 5X infection models do not generate identical immune responses, we were keen to clarify whether these trends would persist and further deviate during subsequent infection and unveil long-term impacts to immunity. To determine the impacts of the 1X and 5X models on subsequent infections, 1X and 5X infected animals were given time to fully clear their primary infections, which was confirmed by qPCR by 52 d.p.i.i. At 74 and 81 d.p.i.i., Depo Provera was used to re-synchronize their estrous cycles. Both groups were re-challenged with the 1X dose 6.0×10^5 IFU of *Cm* diluted in SPG at 84 d.p.i.i. and followed for 7 days. As a control and to underscore potential differences between secondary and primary infections, a third group of animals that had no previous infection were also infected with the 1X *Cm* dose (unprimed, 1X-UP).

To determine whether previous 1X or 5X infection impacted the capacity of acquired protective immunity, vaginal swabs were taken from the 1X and 5X mice during the 7 day subsequent infection, as well as from the 1X-UP group. The qPCR quantified bacterial burden suggested weaknesses in the capacity of the 5X group to control the subsequent infection; the bacterial load was significantly elevated compared to the 1X group at 6 days post secondary infection (d.p.s.i.) (Figure 3.17). Furthermore, the 1X mice had a significantly reduced bacterial burden beginning at 3 d.p.s.i.; this significant divergence from the control group was delayed by an additional 2 days for 5X infected mice (Figure 3.17). The impact of the prior infection was especially meaningful when considering infection resolution, as significantly fewer 5X infected animals were able to fully clear their subsequent infections compared to those in the 1X group (Figure 3.18). While these divergences demonstrate a diminishment of protective immunity driven by past 5X *Cm* infection, it is obvious that both 1X and 5X *Cm* infections enable some degree of memory response, as the 1X-UP animals had significantly elevated bacterial loads during their primary infection compared to both groups during their subsequent infections, albeit at different days since the initial re-challenge of the 1X and 5X previously infected mice (Figure 3.17).

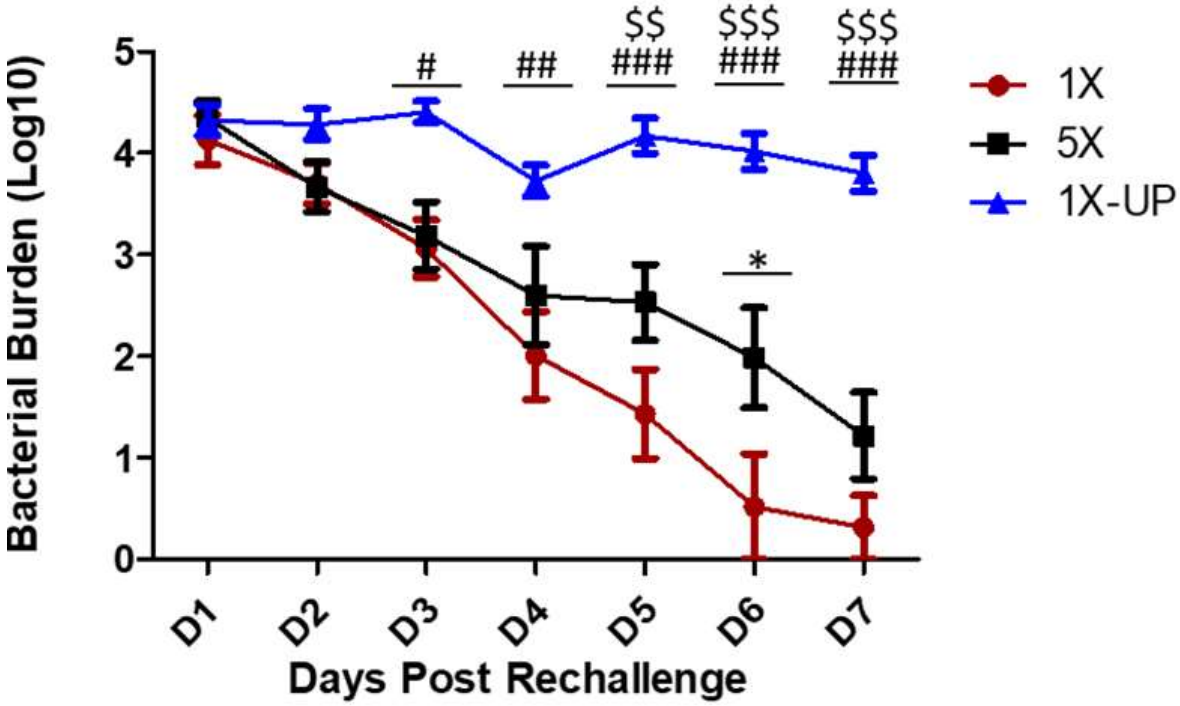

Figure 3.17: Prior 5X *Cm* infections weaken infection control during subsequent *Cm* infection. C57BL/6 CD45.1 and Foxp3-GFP mice were intravaginally infected with one dose of *Cm* (6×10^5 IFU; 1X) (n=5 mice/CD45.1; n=4 mice/Foxp3-GFP) or 5 low doses of *Cm* that are cumulatively equivalent to the 1X dose (1.2×10^5; 5X) (n=6 mice/CD45.1; n=4 mice/Foxp3-GFP), then allowed to clear the infection prior to a single 1X dose re-challenge. An unprimed group (n=5 CD45.1; n=3 Foxp3-GFP) were also infected with the single 1X dose as a control (1X-UP). Vaginal swabs were collected for 7 days post-re-challenged infection. *Cm* gDNA was isolated from the swabs and quantified via qPCR to assess the levels of bacterial burden. Data are presented as mean ± SEM; *P≤0.05 for differences between prior 1X and 5X infections using a two-way ANOVA test with a Bonferroni *post hoc* test; #P≤0.05, ##P≤0.01, ###P≤ 0.001 for differences between prior 1X and unprimed 1X infections using a two-way ANOVA test with a Bonferroni post hoc test; $$P≤0.01, $$$P≤ 0.001 for differences between prior 5X and unprimed 1X infections using a two-way ANOVA test with a Bonferroni *post hoc* test.

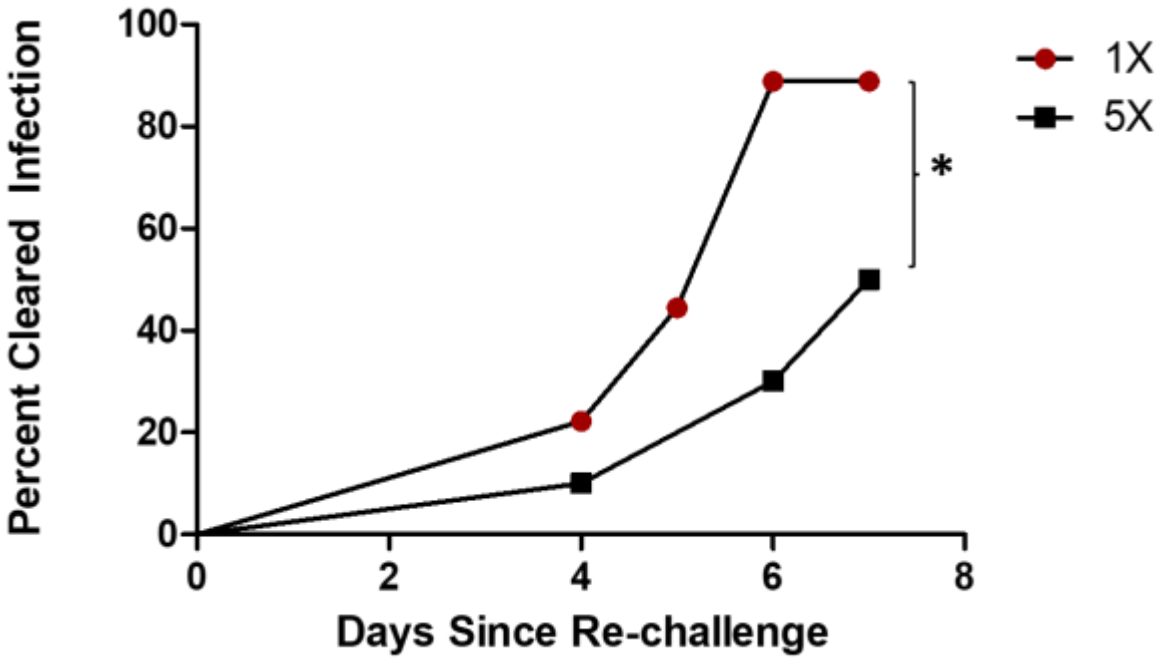

Figure 3.18: Prior 5X *Cm* infections weaken bacterial clearance during subsequent *Cm* infection. C57BL/6 CD45.1 and Foxp3-GFP mice were intravaginally infected with one dose of *Cm* (6×10^5 IFU; 1X) (n=5 mice/CD45.1; n=4 mice/Foxp3-GFP) or 5 low doses of *Cm* that are cumulatively equivalent to the 1X dose (1.2×10^5; 5X) (n=6 mice/CD45.1; n=4 mice/Foxp3-GFP), then allowed to clear the infection prior to a single 1X dose re-challenge. Vaginal swabs were collected for 7 days post-re-challenged infection. *Cm* gDNA was isolated from the swabs and quantified via qPCR to assess the levels of bacterial burden. Data are presented as the mean percent of animals that have cleared the infection; *P≤0.05, using a Mantel-Cox test and a Gehan-Breslow-Wilcoxon test.

3.7 Oviduct cyst pathology is present during subsequent *Cm* infections

Due to the reduced capacity of the 5X mice to control the subsequent infection, we decided to explore whether the tissue pathology was also impacted. The genital tracts of the 1X and 5X animals were excised after 7 days of the subsequent infection and sent for histological processing. The genital tracts of the 1X-UP infected animals were also included as a control, as the lack of tissue damage developing over the 7 days of infection makes their oviducts comparable to that of naïve mice. There were no statistically significant differences between the groups (Figure 3.19). Furthermore, there was a range of cyst dilations in both of the groups with a prior *Cm* infection, suggesting variable degrees of tissue damage present within the groups and indicating that some degree of tissue damage will develop regardless of the infection schedule (Figure 3.19). It is possible to appreciate that the mean cyst dilation of mice with a prior 5X infection is visibly elevated relative to that of mice with a prior 1X infection (Figure 3.19). Additionally, the range of increases in cyst dilation of the prior 5X infected mice extends well beyond that of the mice with a previous 1X infection (Figure 3.19). This could imply an impact of maladaptive responses.

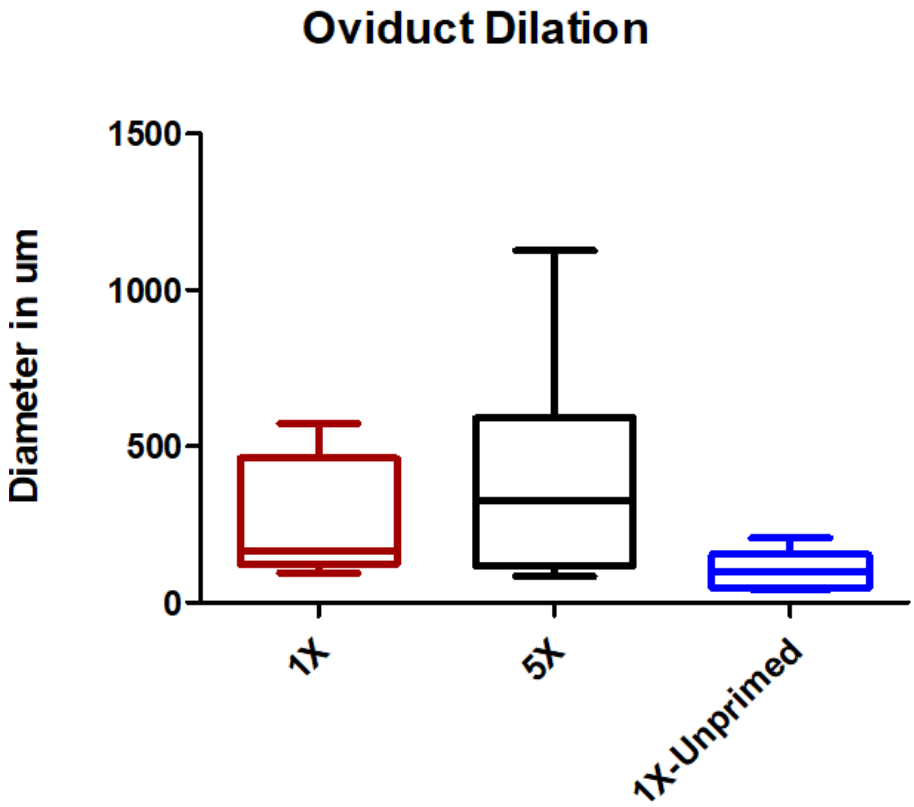

Figure 3.19: Prior 1X and 5X *Cm* infections produce observable tissue pathology. C57BL/6 CD45.1 mice were intravaginally infected with one dose of *Cm* (6×10^5 IFU; 1X) (n=5 mice) or 5 low doses of *Cm* that are cumulatively equivalent to the 1X dose (1.2×10^5; 5X) (n=6 mice), then allowed to clear the infection prior to a single 1X dose re-challenge. An unprimed group of CD45.1 mice (n=5) were also infected with the single 1X dose as a control. Genital tract samples were processed for histology, then analyzed for oviduct cyst dilation to assess the level of tissue damage at the local site of infection via Fiji image analysis software. Data are presented as a box plot with whiskers from minimum to maximum values of the largest oviduct cyst present in each tract; using a one-way ANOVA test with a Bonferroni *post hoc* test.

3.8 Prior 1X and 5X *Cm* infections prime differential CD4+ T cell responses during subsequent *Cm* infection

As the divergent bacterial burdens were present in the 5X group, we were curious to know what the impact of previous infection was on the host immune response. To this end, we isolated cells from the spleens and lymph nodes of animals with prior 1X and 5X infections at day 7 of their re-challenge infection. The cells were permeabilized and stained with intranuclear fluorescent antibodies specific to the Foxp3 transcription factor. Cells from 1X-UP animals were included for comparison. Another set of permeabilized cells from 1X and 5X animals with a prior *Cm* infection were stained with intracellular antibodies against the cytokines IFN-γ, for the CD4+ Th1 response, IL-4, for the CD4+ Th2 response, and IL-17A, for the CD4+ Th17 response. Additional data was generated from splenocytes isolated from animals with prior 1X and 5X infections at day 7 of their re-challenge infection, which were cultured for 72 hours with HK*Cm* diluted 1:50, 1:100, and 1:200, anti-mouse CD3 antibody, or with media as a negative control. Supernatants from the cultures were assayed via sandwich ELISA to quantify production of the IFN-γ, TNF, IL-13, IL-17A, and IL-10 cytokines, in order to determine the extent of CD4+ T helper responses as previously described.

There were not significant differences in the levels of intracellular cytokines between the 1X and 5X mice (Figure 3.20A and B). A very low frequency of splenocytes and lymph node-derived lymphocytes had detectable levels of intracellular cytokines (Figure 3.20A and B). Both the 1X and 5X prior infection impacted the CD4+ Treg response during the subsequent infection, compared to the response generated by the unprimed mice during their initial challenge (Figure 3.21A and B). There were no differences in the absolute number of cells expressing Fox3P in the spleen and lymph nodes of the 1X and 5X mice during their subsequent infection (Figure 3.21A and B). There were significantly fewer Tregs in the spleen of 1X infected mice compared to 1X-UP mice, but this difference was not present between the 5X and 1X-UP groups (Figure 3.21A). Furthermore, both the 1X and the 5X mice had significantly fewer Tregs in their lymph nodes compared to 1X-UP mice, with the extent of the reduction being more

substantial for the 5X mice (Figure 3.21B). This demonstrates yet another avenue of divergence in the host responses following single and repeated *Cm* infections.

Sandwich ELISA analysis of the splenocyte supernatant revealed that prior 1X, but not 5X, infection bolsters the CD4+ Th1 response. The IFN-γ and TNF produced in response to splenocyte stimulation with HK*Cm* was markedly reduced in the 5X group compared to the 1X group, significantly so for IFN-γ produced following stimulation with all 3 dilutions of HK*Cm* and for TNF produced after exposure to 1:50 and 1:100 diluted HK*Cm* (Figure 3.22). The amounts of IFN-γ and TNF produced following anti-mouse CD3 stimulation was substantially lower compared to the levels produced following HK*Cm* stimulation, and the differences between the groups were not present (Figure 3.22). The levels of IL-13, IL-17A, and IL-10 produced following all 3 dilutions of HK*Cm* and anti-mouse CD3 were lower, though not significantly so, in the 5X group compared to the 1X group (Figure 3.22). Despite the lack of differences in the CD4+ Th2, Th17, and Treg responses, this data clearly indicates a weakening of the CD4+ Th1 response during subsequent infections following a repeated, low dose infection.

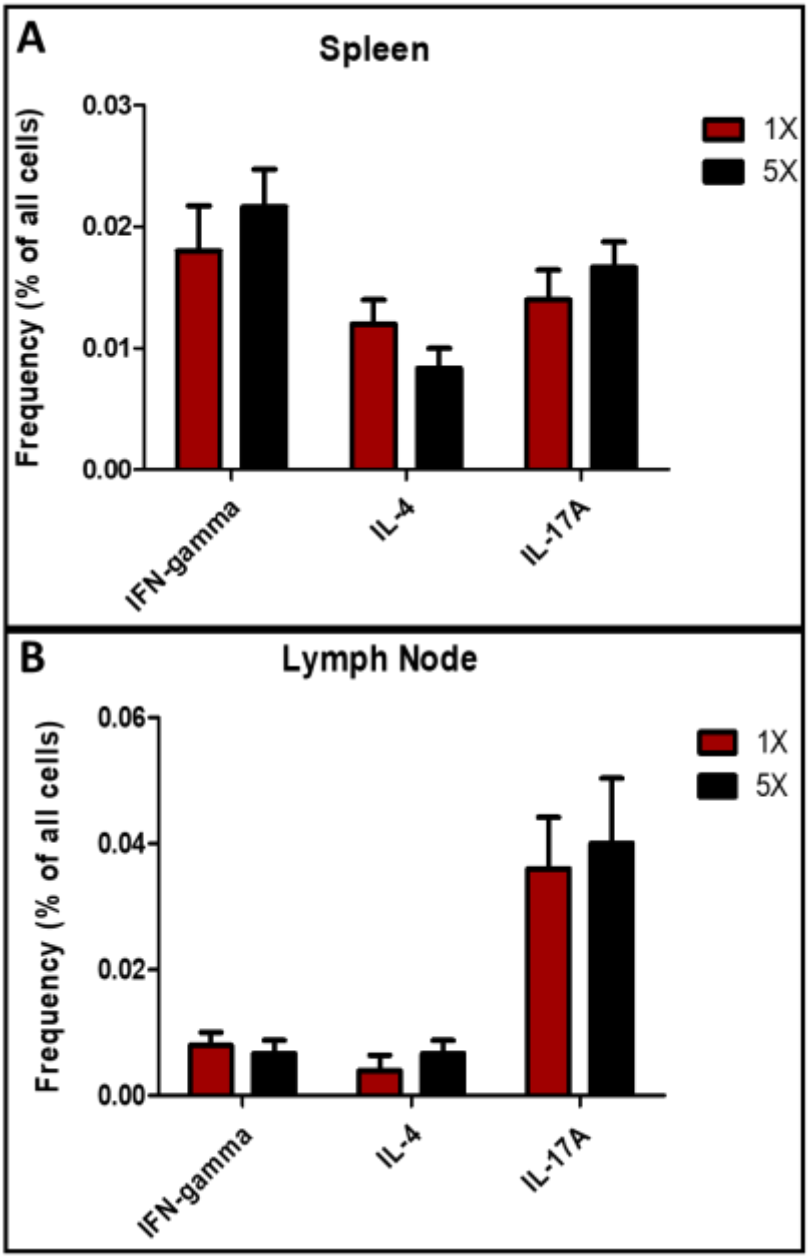

Figure 3.20: Prior *Cm* infection does not impact the induction of CD4+ T helper cell response cytokines during subsequent infection. C57BL/6 CD45.1 mice were intravaginally infected with one dose of *Cm* (6×10^5 IFU; 1X) (n=5 mice) or 5 low doses of *Cm* that are cumulatively equivalent to the 1X dose (1.2×10^5; 5X) (n=6 mice), then allowed to clear the infection prior to a single 1X dose re-challenge. Spleens (A) and lymph nodes (B) were excised 7 days after the re-infection, then intracellular cytokine expression was determined via flow cytometry. Data are presented as mean ± SEM of the frequency of the acquired cells and assessed for significance using a two-way ANOVA test with a Bonferroni *post hoc* test.

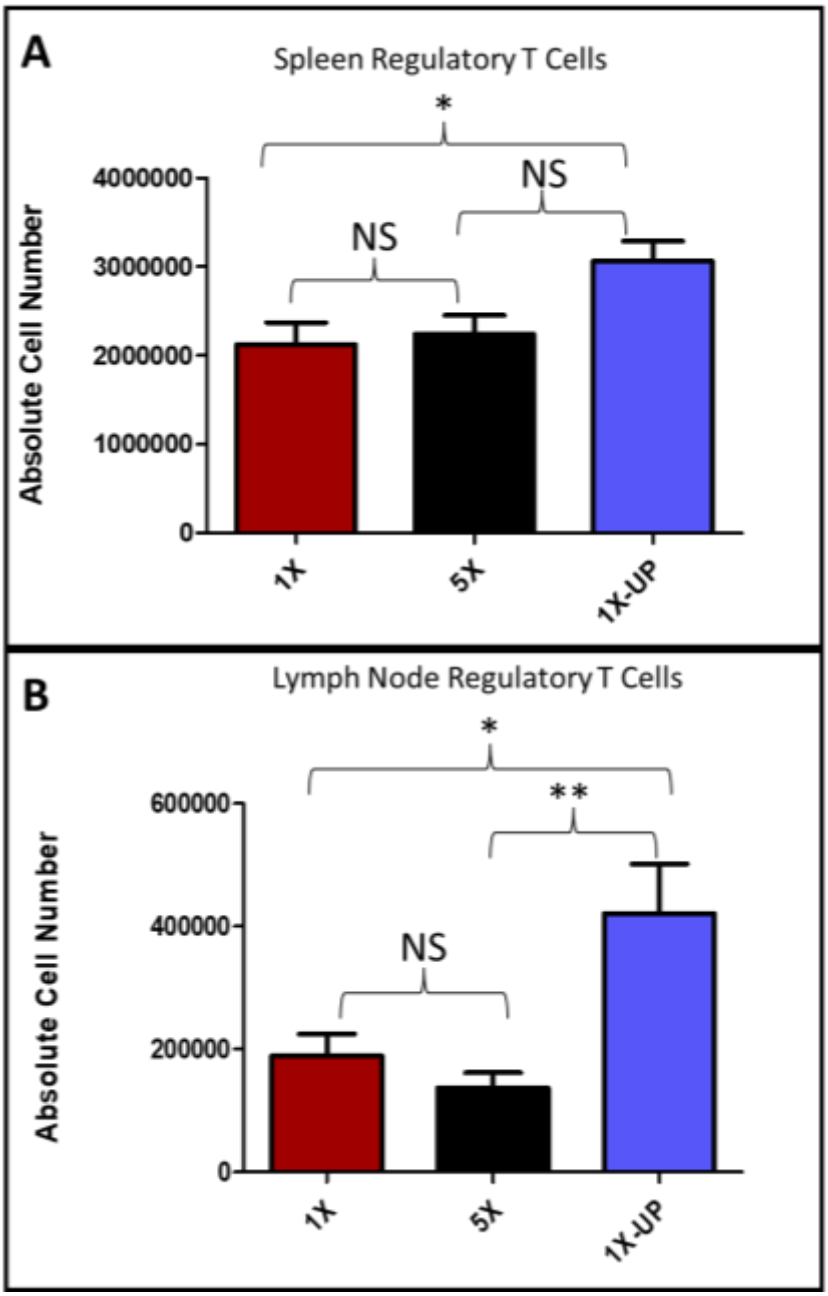

Figure 3.21: Prior *Cm* infection impacts the activation of regulatory T cells during subsequent *Cm* infection. C57BL/6 CD45.1 mice were intravaginally infected with one dose of *Cm* (6×10^5 IFU; 1X) (n=5 mice) or 5 low doses of *Cm* that are cumulatively equivalent to the 1X dose (1.2×10^5; 5X) (n=6 mice), then allowed to clear the infection prior to a single 1X dose re-challenge. An unprimed group of CD45.1 mice (n=5) were also infected with the single 1X dose as a control (1X-UP). Spleens (A) and lymph nodes (B) were excised 7 days after the re-infection, then intranuclear Foxp3 expression was determined via flow cytometry. Data are presented as mean ± SEM; *P≤0.05, **P≤0.01, using a one-way ANOVA test with a Bonferroni *post hoc* test.

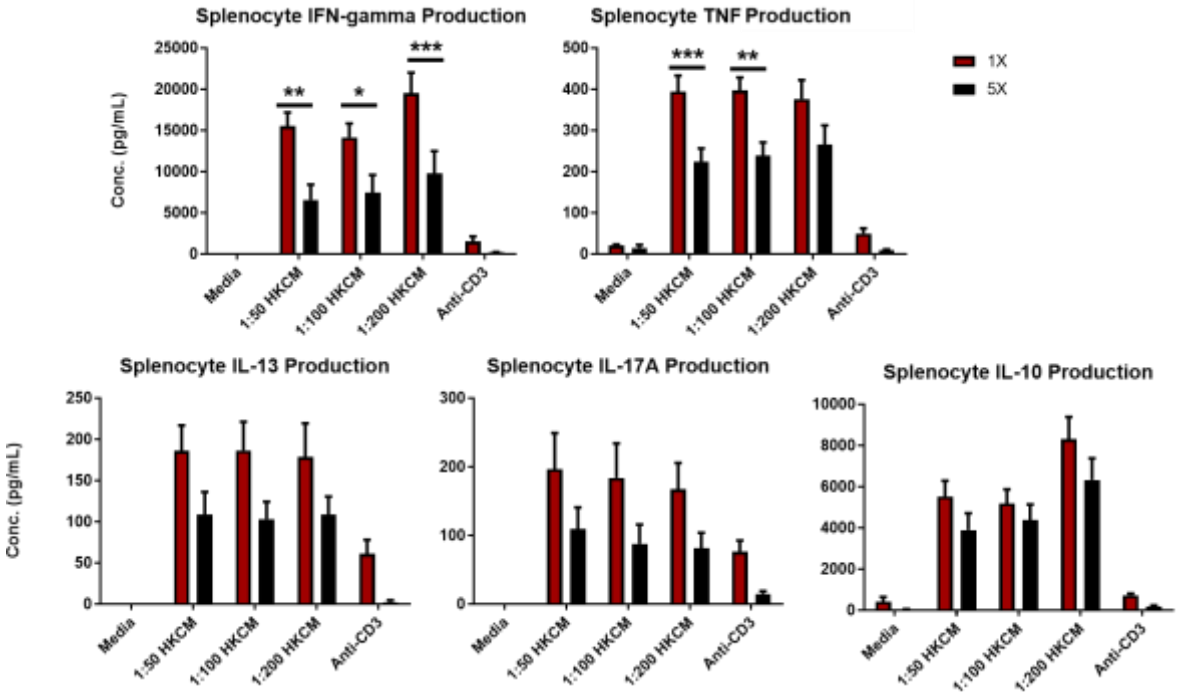

Figure 3.22: Splenocyte stimulation indicates prior 1X, but not 5X, *Cm* infection reinforces CD4+ Th1 responses. C57BL/6 Foxp3GFP mice were intravaginally infected with one dose of *Cm* (6×10^5 IFU; 1X) or 5 low doses of *Cm* that are cumulatively equivalent to the 1X dose (1.2×10^5; 5X), then allowed to clear the infection prior to a single 1X dose re-challenge. Splenocytes (n=4 mice/group pooled; n=3 technical replicates/group/stimulation) isolated 7 days after the re-infection were stimulated with media, heat killed *Cm* (HKCM), or anti-mouse CD3 antibody for 72 hours. Supernatants collected from the culture stimulations were assayed in a sandwich ELISA to measure production of IFN-γ, TNF, IL-13, IL-7A, and IL-10. Data are presented as mean ± SEM; *P≤0.05, **P≤0.01, ***P≤0.001, using a two-way ANOVA test with a Bonferroni *post hoc* test.

CHAPTER 4 DISCUSSION

4.1 Discussion of key findings

Animal models of chlamydial infections have yet to reveal full clarification of the infection course and sequelae following urogenital *Ct* infections in women. We developed a comparative mouse model of *Chlamydia* infection to account for human circumstances in *Ct* infection; our novel 5X mouse model involved five low dose infections with 1.2×10^5 IFU of *Cm*, which were compared to 1X mice that were infected with a single, 6×10^5 IFU dose of *Cm*. We hypothesized that the repeated, low dose infection schedule would disrupt the immune response that follows that of the classical single, high dose infection and produce an inflammation state that facilitates reproductive tissue damage. Through the use of this model, we aimed to identify whether the host responses would diverge following the two models of *Cm* infection, and if there were impacts to long term immunity during secondary infections.

4.1.1 Repeated, low dose *Cm* infections prime immune cell functioning that is inconsistent with those triggered by a single high dose *Cm* infection

In the literature, the conventional method of *Chlamydia* infection is a single, high inoculative dose given to ensure a productive infection (160). Other groups have recognized that animal models of *Chlamydia* infection may have deficits to parallels in human conditions and have attempted to manipulate the infectious dose accordingly. Rank and colleagues attempted to characterize whether there may be differences in outcomes between animal models of sexual *Chlamydia* transmission compared to a direct intravaginal infection (160). To this end, their group used a *C. psittaci* model of guinea pig infection, with inoculative doses ranging from 10^1, 10^2, 10^3, and 10^4 IFU (160). Rank and colleagues concluded that a lower inoculative dose, 10^2 IFU of *C. psittaci*, produced an infection state most similar to guinea pigs that had been confirmed to have an infection from sexual transmission (160). The scope of our findings of differential immune and host responses following repeated low doses of *Cm* infection compared to those following infection using a single high dose is consistent with the precedent report by Rank and colleagues.

The results from our study revealed that 5X *Cm* infections promote neutrophil infiltration into the genital tract and their subsequent polarization into inflammatory phenotypes at 30 d.p.i.i., which was not observed to the same degree during 1X *Cm* infection. This is not consistent with a 2009 report by Carey and colleagues; their group employed a range of IFU doses to assess the outcomes of *Cm* infection, using 5×10^2, 5×10^4, and 2.6×10^6 *Cm* IFU (162). Carey's group did see high levels of infiltrating neutrophils as a result of the *Cm* infection, as were observed during this study, but there were not differences between the numbers of neutrophils and lymphocytes infiltrating the uterine horns or oviducts (162). Yet another study assessing inoculative dose effects on chlamydial infection was undertaken by Maxion and colleagues, who used 1×10^4, 1.5×10^5, or 1×10^7 IFU of *Chlamydia* to establish an infection (161). Maxion's group found that not only were there neutrophil infiltration differences between the groups, but that the group receiving the highest IFU dose had the greatest elevation in neutrophil infiltration compared to the other infectious doses (161).

Such conflicts in the field make it difficult to evaluate our results in the context of single-dose models of *Chlamydia* infection. Yet, the critical factor of our work is that both groups received the same cumulative number of bacteria during the initiation of their primary infection. To our knowledge, no other studies have included this factor in their methodology of inoculative dose. Despite the discrepancies compared to preceding reports, our findings are consistent with clinical observations and histopathology studies, which have established the infiltration of neutrophils in the upper female reproductive tract during *Chlamydia* infection in human females (50, 156). Given the reports of recurrent *Ct* infections in human populations, our findings appear to mirror the elevated neutrophil infiltration that appears during PID complications.

Furthermore, we observed a pattern of upregulated expression of mediators associated with overall inflammation and the involvement of neutrophils at 23 d.p.i.i. in the 5X group genital tract. This is evidenced in the relatively higher expression of CXCL1, CXCL2, CCL3, CCL4, and CCL7; these chemokines are implicated in modulating neutrophil recruitment, activation, and functioning (76, 170-173). The enhanced expression of these factors provides a potential mechanism of supporting the

neutrophil kinetics we revealed through flow cytometry. However, in order to confirm this mechanism, we will need to produce additional data that can be assessed with appropriate statistical analyses, which were not employed in this work. To further validate our findings and produce a full characterization of the factors modulating neutrophil recruitment, it would be valuable to include a direct assessment of other mediators, such as complement fragments C3a and C5a, formyl peptides, and leukotrienes (76).

In addition to the upregulated molecules, it appeared that IL-9 expression was relatively reduced in the 5X group, as both the 1X and naïve mice had higher levels that appeared to be comparable to each other. Historically, IL-9 was associated with Th2 responses, although contemporary reports of an individual Th9 subset in the CD4+ T repertoire have led to endeavors to further characterize IL-9 and the related Th9 response (174). It appears that IL-9 expression provides some degree of protection during infections involving extracellular parasites (175-177). Despite this, it is not yet understood what the role of IL-9 is during *Chlamydia* infections; a report seeking to uncover the interactions between IL-9/Th9 and Th1/Th17 responses during a lung model of *Cm* infection observed brief IL-9 expression during early timepoints, but ultimately did not conclude that IL-9 had a tangible impact on the outcome of the infection (178). Nonetheless, the implications of reduced IL-9 expression during repeated *Cm* infections demonstrate another source of investigation that could be valuable in extending the *Chlamydia* literature.

We also found that the 5X group was distinct in its reduced expression of CXCL5, also known as epithelial neutrophil-activating peptide-78 (ENA-78) compared to the 1X group. The production of CXCL5 by the 1X group is akin to previous reports of chemokine upregulation during chlamydial infection. Previous studies of lung and genital infections in mouse models have revealed that *Cm* exposure will result in enhanced expression of CXCL5, although these reports have been observational in the context of CXCL5's role during infection (179, 180). To this end, CXCL5 is understood to operate as a promoter to neutrophil infiltration and effector functioning (181). As such, it is perplexing that the repeated infection did not also trigger the production of this molecule.

Given the differences between the groups, it would appear that the chemokine expression mediated by 5X *Cm* infection promotes a molecular environment that is not only unique to that of the 1X group, but may be inconsistent with some of the previously reported findings in *Chlamydia* studies. In this sense, the patterns in cellular and mediator expression that we have observed indicate the need for continued characterization of these responses following single and repeated *Cm* infection.

Overall, the diverging host responses we observed at 30 d.p.i.i. can be summarized by the appreciable differences in the populations present in the tSNE transformed plots, which underscore the variation in responses following the two models of *Cm* infection. Based on potential differences in the expression of Ly6C and CD11C, it is possible that the 1X and 5X infections promote the recruitment of distinct myeloid populations (182, 183) Future directions of this aspect of the project will include unravelling the identity of the uncharacterized, yet distinct, populations observed in the tSNE transformation. This work will also be supported by single cell RNA sequencing of select, sorted genital tract cells in order to reveal the variations between the 1X and 5X models at the transcriptomic level.

4.1.2 Repeated *Cm* infections in mice produce significantly altered immune responses that do not promote clearance of secondary *Cm* infections

In addition to the variations in innate effectors and mediator expression, we discovered at 30 d.p.i.i. that the host response following the 5X infection reduced B and T cell recruitment to the site of infection relative to that observed in the 1X infection. To this end, we determined the unique T cell features following the 1X or 5X infection. We assessed the cytokine production report that 1X infections preferentially prime CD4+ Th1 responses, which are known to contribute to chlamydial infection clearance in animals (120, 125, 184). The results from animal models have been established through observations in terms of cellular and molecular findings, and have been confirmed through the use of adoptive transfers, IFN-γ deficient animals, and CD4+ T cell depletion (124, 125, 127, 138). Our study is compatible with these established findings, as we observed some degree of CD4+ Th1 response with IFN-γ production in both the 1X and 5X groups. We determined that the CD4+ Th1 response appeared to be predominant in

the 1X group, based on relative IgG2a levels. Unlike the 1X group, we found evidence of enhanced CD4+ Th2, Th17, and Treg responses in the 5X group, based on cytokine production and antibody isotyping. We will explore the enhanced Th17 and Treg responses in conjunction with neutrophil-associated tissue damage.

In terms of the Th2 response, there is no consensus as to its outcome on host immunity and immunopathogenesis, including deficits in our understanding for animal and human studies. In humans, a prior report by Vicetti Miguel and colleagues determined that blood and endothelial tissues from *Ct* infection women had enhanced Th2, but not Th1, cytokine secretion (130). However, the patients from whom these samples were taken had already undergone anti-microbial treatment for *Ct*, so it is difficult to attribute the Th2 induction to responses stemming from the active infection and to determine the direct role of Th2 during *Ct* infection (133). Nonetheless, our findings on the upregulations in the Th2 response following 5X, but not 1X, infection are consistent with the report by Vicetti Miguel and colleagues (130).

Vicetti Miguel's group has utilized a mouse model to determine that *Ct* infection will enhance Th2 immunity and result in the induction of an eosinophil population that secretes IL-4 (63). Furthermore, Vicetti Miguel and colleagues found that these eosinophils were associated with reduced tissue damage in their animal model (63). While we observed increases in the relative tissue pathology in the Th2 predominant 5X group, we did discover that the 5X infection upregulates the relative expression of eotaxin, which is indicative of a potential for enhanced eosinophil component. Although we did not characterize the kinetics or cytokine profiles of eosinophils during our study, it is possible that our findings are inconsistent with the reports of other groups due to the differential host responses that we have observed to follow 5X *Cm* infections; this presents another avenue of investigation for future work related to our study.

In addition to the primary infection differences in T cell responses, we also observed that repeated, low doses of *Chlamydia* during a primary infection will prime distinct immunity during subsequent rechallenge that does not reflect that of single dose infection. The prior 5X infection did produce effective immunity that promoted infection clearance, but the 5X group's ability to control the subsequent infection lagged behind

that of the group with a prior 1X infection. In this case, the animals with a prior 1X infection produced significantly more IFN-γ compared to those that had received the prior 5X infection schedule. Our finding parallels that of a recent human study, which observed that the presence of CD4+ Th1 IFN-γ responses in the blood of human females was associated with improved protection against secondary infections with *Ct* (114).

While our observations are consistent with the findings of Bakshi and colleagues in humans, they are incompatible with previous animal model studies that assessed the outcome of different inoculative dose on memory responses in *Cm* infection. The use of 1×10^4, 1.5×10^5, or 1×10^7 IFU of *Chlamydia* to establish infection in mice revealed no differences in the effect of inoculating dose on adaptive responses (161). As Maxion and colleagues did not infect the animals with the same cumulative amount of bacteria, it is difficult to relate our findings to preceding work, underscoring the novelty of the 5X *Cm* infection model. Regardless of this, it is clear that the outcomes of acute and long-term adaptive immunity in the form of IFN-γ production through the CD4+ Th1 response that occur in the 1X group are consistent with the literature, which has repeatedly demonstrated that mice are able to develop protective immunity following a primary *Chlamydia* infection (119, 124-127). The CD4+ Th2 responses by the 5X group do not align with this dogma and instead indicate an irregularity from the typical, predominantly protective response that follows the standard initiation of *Cm* infection in mice via a single high IFU dose of the bacteria.

4.1.3 Repeated *Cm* infections dysregulate neutrophil and Th17/IL-17 responses, which is likely to contribute to the development of tissue damage

The divergent immune cell kinetics prompted us to delve into the protein and mediator expression profiles that followed the 1X and 5X infections. We have produced preliminary evidence that PDPN expression changes following *Chlamydia i*nfection. PDPN is a marker found on fibroblasts that could be associated with tissue fibrosis (74). We detected higher levels of PDPN at 23 d.p.i.i. in the genital tracts of 5X infected, but not 1X infected, animals. While PDPN has yet to be explored for its role in *Chlamydia* infections, our work is consistent with the findings of those in the field of cardiovascular and pulmonary diseases, as well as others. In regard to encapsulating peritoneal sclerosis,

which is characterized by fibrosis, a 2012 study found that PDPN-expressing cells were present in biopsies of patients with these conditions, but were not present in healthy controls (185, 186). Furthermore, PDPN-expressing cells, including MSCs, were associated with the development of fibrosis following myocardial infarctions (187). Of relevance to our findings, the use of podoplanin-depleting antibodies in LPS-induced inflammation models has suggested a link between PDPN expression and neutrophil functions in the context of host-mediated tissue damage (188). Indeed, the depletion of podoplanin resulted in reductions of neutrophil infiltration and improved the lung functioning following the LPS treatment (188). Our observations of both enhanced podoplanin expression and increases in neutrophil infiltration that occurred in the genital tract of animals with repeated, low dose *Cm* infections are compatible with previous reports, and indicate a potential connection to fibrosis that remains unexplored in the field.

When considering the significantly enhanced neutrophil infiltration in the 5X genital tract at 30 days following the induction of *Cm* infection, as well as the cytokine profiles that were consistent with skewed Th17 and Treg responses in the 5X group, it is apparent to us that the scope of divergence in the responses generated by the 1X and 5X infections extends outside of the much-researched Th1 paradigms. In the context of existing work regarding these factors, recent work by Vicetti Miguel and colleagues has demonstrated an upregulation in Th17 responses during mouse infection by *Ct*, without the same extent of Th2 immunity that they had observed in other reports (132). We used a similar infection schedule to that reported by Vicetti Miguel's group, which utilized a low dose infection series, using 9 doses of 10^4 IFU of *Ct* to reveal these enhanced Th17 responses, although this occurred in conjunction with IFN-γ depletion and there was not a direct comparison to the outcomes from a single high dose of an equivalent amount of bacteria (132). There was a reported concomitant increase of neutrophil infiltration following the anti-IFNγ treatment, as well as a marked elevation in the extent of tissue injury in the oviduct and uterine horn (132). While we did not utilize a treatment to inhibit the effect of the Th1 response in either the 1X or 5X infection, the results of the 5X infected mice described herein are remarkably consistent with the infection state reported by Vicetti Miguel and colleagues.

Peripheral agreement to Treg data from the 5X group are present in reports describing the balance between Th1 and Treg responses. One study assessing the interplay of CD4+ T cell responses in a mouse lung model of *C. pneumoniae* revealed that inhibition of NK cells compromised the power of Th1 responses during infection and instead primed a dominant IL-10/Treg response (100). This enrichment in the production of IL-10 and Treg functioning was connected to limitations in the ability of the host to control the infection, while also augmenting the histological damage associated with the infection relative to control animals (100). Likewise, we also observed both increased Treg expansion, evidenced by IL-10 production, and worsened tissue damage in the 5X group following the primary infection. Zhao and colleagues theorized that the pathology associated with the expanded Treg presence in the lung model of chlamydial infection was due to DC functions, which suggests an avenue of investigation that we may employ to further characterize our findings.

In the context of our data regarding Tregs, Th17 responses, and neutrophils, our findings are in consensus with past work by Dr. Wang's group, which has indicated an axis for Treg/Th17/neutrophil functioning during *Chlamydia* infection (83). During their work, Moore-Connors and colleagues found that *Cm* infection promoted the development of Tregs, which enhanced the development of the Th17 response (83). When Tregs were depleted, this produced a reduction in the observed Th17 response, measured by IL-17A production, as well as decreased the level of neutrophil infiltration; the overall observed result of these processes was an attenuation in the development of oviduct pathology (83). Our results appear to be consistent with this Treg/Th17/neutrophil axis, as we found that the 5X *Cm* infection resulted in enhanced neutrophil infiltration, elevated Th17 and Treg responses, and exacerbated tissue pathology.

Reflecting upon the data described by our group and by previous studies, it is plausible that the Treg/Th17/neutrophil axis is contributing to the development of tissue pathology in the infection state that we have induced with repeated, low dose exposures to *Cm*. There are numerous reports involving the depletion of neutrophils during *Chlamydia* infections, which has further underscored their association with the development of pathology. Indeed, previous studies have revealed that neutrophil

depletion during *Chlamydia* infection has a largely protective effect in terms of abrogating tissue damage, but does not impact the course of the infection (84, 85). Given the heightened neutrophilic responses elicited by the 5X infection, future directions for this work in the field of *Chlamydia* infection research would be significantly augmented by investigations that remove the neutrophil impact. Furthermore, as we observed elevations in both neutrophil influx and Th17 responses, the depletion of neutrophils may shed more light in elucidating the functioning of Th17/IL-17A during urogenital chlamydial infections. In this way, using the findings of repeated *Cm* infection that we have presented and further confirming these processes with neutrophil depletion could provide clarity on the cellular mechanisms that exacerbate tissue injury and sequelae during repeated *Ct* infections in women.

To this end, we theorize that this axis is especially pertinent in the context of neutrophil contributions to tissue fibrosis, which have been characterized in other fields (87, 189-192), but has yet to be established during chlamydial infections. In reports of fibrosis in a pulmonary model, the contributions of neutrophils in fibrosis have been characterized to occur through their strengthening of fibro- and myofibroblasts pro-fibrotic functions (190). Similarly, neutrophil influences on liver mesenchymal cells produced exacerbated hepatic fibrosis, which was demonstrated to be due to reactive oxygen species production by neutrophils (191). Our work aligns with these findings, given the significant neutrophil infiltration observed in the 5X genital tract and the implication of fibroblast activation, evidenced via enhanced PDPN expression at this site.

More notable in regard for the potential of the Treg/Th17/neutrophil axis in fibrosis are the reports that associate Th17-mediated fibrosis via fibroblast activity. This interaction has been reported for a range of fibrotic conditions, including inflammatory joint pathology (193), Crohn's disease (194), Graves' disease (195), and systemic sclerosis (196). Overall, these reports indicate the induction of pathogenic collagen deposition and matrix destruction during inflammation, leading to fibrosis that impairs functionality of the tissue (193-196). While we did observe the enhancement of Th17 responses in our 5X, but not 1X, animals that occurred following a potential upregulation of fibroblast protein expression, we have yet to pursue whether there are similar

histological findings in pathology samples generated from our work. Doing so could solidify a connection between the upregulated Th17 responses and tissue pathology generated following repeated, low dose *Cm* infection, while clarifying the relatively mild pathology we observed to after the single, high dose *Cm* infection.

A review of the literature did not reveal an overt association of neutrophil contributions to the dynamic of the Th17 response and fibroblasts in the development of fibrosis, despite the aforementioned reports characterizing the interactions between neutrophils and fibroblasts (87, 189-192), as well as Th17 responses and neutrophils (83, 132), that all appear to exert an impact on fibrosis pathology. However, our preliminary indications of PDPN expression and elevations in neutrophil and Th17 responses implicate a connection between these processes and the development of fibrosis during chlamydial infection. This apparent knowledge deficit further emphasizes the novelty of our findings, and suggests the applicability of the repeated, low dose infection on future investigations. Such usage of our 5X model could provide valuable perspectives for the development of treatments to clinically manage pelvic inflammatory disease and sequelae from patients infected with *Chlamydia*.

4.2 Future directions and limitations

Overall, we consistently found that the repeated, low dose *Cm* infections produced differential acute and chronic responses compared to the single high dose infection. Due to the nature of the infection schedules, we characterized the infection profiles at timepoints counted from the first day of infection. However, this resulted in a discrepancy between the time since the last infection between the two groups. Such a discrepancy limits our ability to assert that the results we observed are due exclusively to the single or repeated infection schedule. To amend this uncertainty, future work will include a third group in the model by delaying the single dose infection to occur on day 8, with SPG vehicle controls given for the days preceding to correspond with the first four infections in the 5X group. This will provide clarification as to whether the differences observed stem from the host responses primed from having a single or recurrent exposure, or if they are simply reflective of differences in the course of infection. Repeated modelling with an inverted 1X group in comparison to the conventional 1X

infection and our novel 5X schedule also presents an excellent opportunity to enhance the sample number. This is important for the PDPN and molecular mediator findings, as the pooled samples and low replicate number limit the statistical power of our data.

While an inverted 1X group could clarify the impact of repeated compared to single infections on host responses and outcomes following *Cm* infection, it is still unclear whether the 5X responses are part of the primary response to *Chlamydia*, or if they represent step-wise secondary, adaptive priming responses. We acknowledge that this gap is a limitation in our work. Unfortunately, this gap is inherent to the nature of comparing single and repeated infections and is not easily amenable. Furthermore, there is very limited research into comparing models of single and repeated infections in the field of *Chlamydia*, as well as for infections by other pathogens; therefore, it is difficult to propose a valid model to assess this limitation.

It may be valuable to use heat-inactivated *Cm* in place of the inert SPG as a vehicle model for the 1X group. Yet, the presence of inactive bacteria could further confound our findings, as it may prime a differential infection that is distinct from the responses induced by live *Chlamydia* infection in the 1X or 5X group (197). Furthermore, it could be possible that the exposure to heat-inactivated bacteria would be similar to an inoculation against the pathogen, as opposed to an exposure to initiate an infection (159). Prior work has attempted to use inactivated bacteria as a vaccination strategy against *Chlamydia*, with mixed results and limited success (159). Thus, there remains a need to determine the specific immunity phase induced following repeated, low dose *Cm* infections.

Another limitation inherent to our work is the use of progesterone to synchronize and control the mouse estrous cycle, which is conventional in most mouse models, but has been reported in several studies to favor the growth of *Chlamydia* (29). In human studies, there are conflicting reports regarding the effects of synthetic hormones on urogenital chlamydial infection, which extend to differences in outcomes following the use of progestin-only and combination progestin-estrogen contraceptives (29); our work would only be relevant to women using treatments with progestin alone. Furthermore, some women may not use hormonal contraceptives, underscoring another facet of this

limitation. While clarifying the impact of both the mouse estrous cycle and sex hormones is outside of the scope of this work, future directions could rectify this by utilizing the 1X and 5X infection schedules with additional hormone treatments. For example, progestin-estrogen treatment could be utilized for estrous cycle synchronization, while another condition with no estrous cycle synchronization could be included; both of these groups would improve the translational capacity of this work.

In terms of the pathology variations we found, there are other studies have found that different inoculative doses result in differences in bacterial ascension (161, 162). While we hypothesize that the differences in pathology observed are due primarily to host-mediated cell damages, we have yet to investigate whether this correlates with ascension into the upper genital tract. As the ascension paradigm of *Chlamydia* infection pathology is accepted as a possible mechanism of pathology (28), quantifying chlamydial gDNA from genital tract homogenates could readily reveal whether the dosage schedules we employ produce differences in ascension.

4.3 Proposed model of 1X and 5X *Cm* infections

We have determined substantial differences follow the initiation of a primary Cm infection with either a single, high dose or repeated, lower doses. Given the differential host responses primed by the 1X and 5X *Cm* infection, we propose a model to summarize the immune and local tissue outcomes following the primary infection (Figure 4.1).

Epithelial and local tissues responses to *Cm* infection support the priming of innate and adaptive effectors (Amjadi et al., 2014; Huttner & Bevins, 1999). Following a single exposure to high IFUs of *Cm*, the resultant molecular environment predominantly polarizes the induction of a CD4+ Th1 response. As revealed by decades of research, the production of IFN-γ mediated by CD4+ Th1 cells controls the spread of the infection and contributes to the resolution of chlamydial infection in mouse models (124, 125, 127, 138). Inflammation due to this response is associated with the development of some degree of oviduct tissue damage, which could impair reproductive function (155, 156). However, a protective CD4+ Th1 response will be induced again upon subsequent chlamydial infections (119, 124-127).

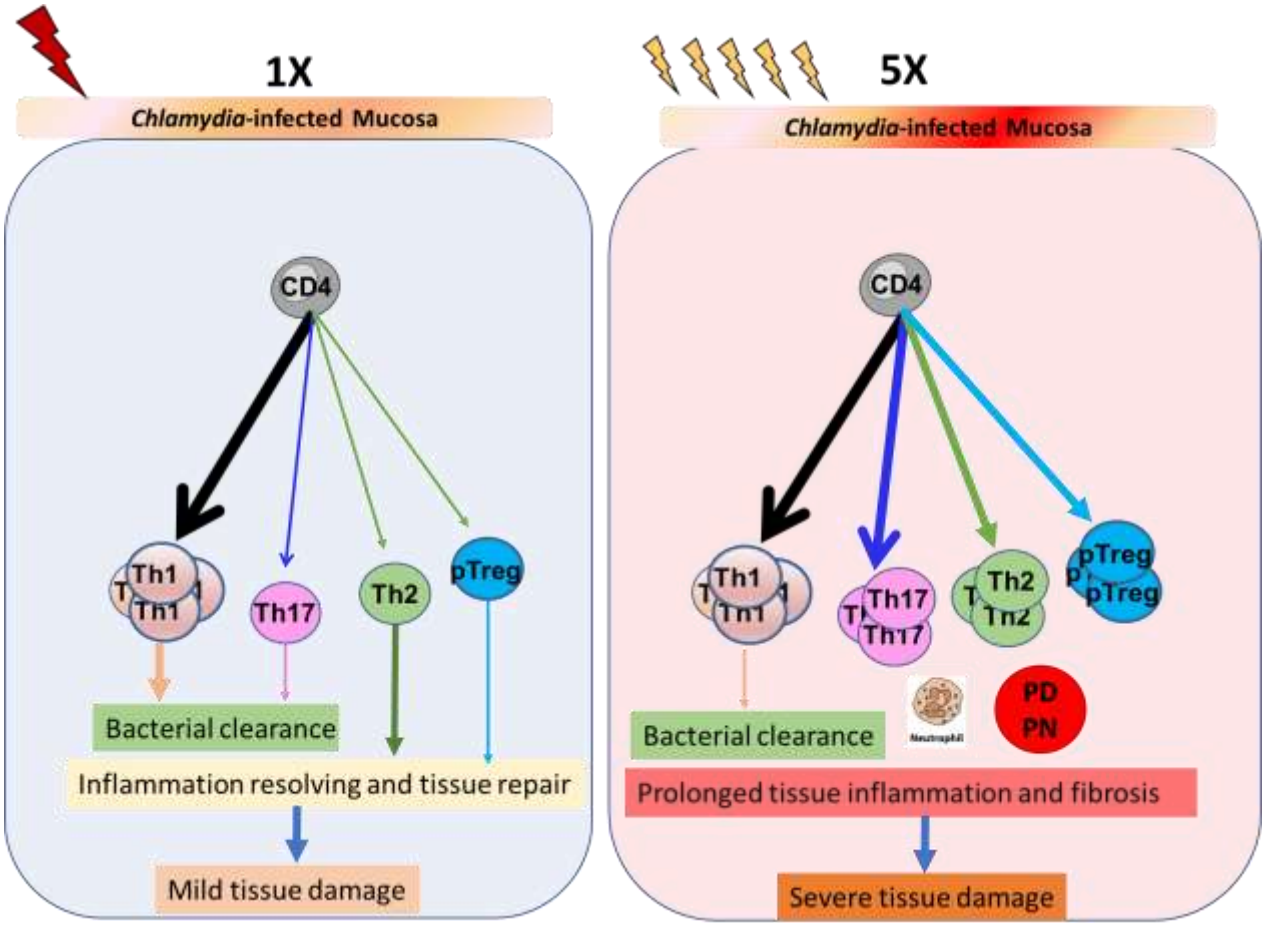

Figure 4.1: Proposed model of divergent host responses in mice infected with 1X and 5X doses of *Cm*. Conventional, 1X infection with *Cm* promotes the preferential activation of CD4+ Th1 responses, which supports the control and eventual resolution of the infection. Other CD4+ T response are not dominant, which minimizes the development of host-mediated tissue damage. These responses persist during subsequent infection and confer enhanced IFN-γ productions to promote infection clearance. The repeated, low dose 5X infection with *Cm* will also induce the CD4+ Th1 response, but in contrast to the 1X response, the 5X infection also results in amplified production of inflammatory molecules. This generates an atypical response characterized by enhanced neutrophilic infiltration, upregulated fibrosis, and abnormal CD4+ T responses, included Th17, Th2, and Tregs. These responses exacerbate the extent of oviduct pathology, without the robust protective immunity associated with conventional models of *Cm* infection.

Similarly to the 1X infection, the 5X infection will activate the development of the CD4+ Th1 response and the production of IFN-γ. However, other components of the initial response following the 5X infection diverge from those in the 1X infection. Neutrophil infiltration is significantly enhanced, inflammation is supported, and unconventional CD4+ Th2, Th17, and Treg responses are polarized in addition the activation of the Th1 response. Based on characterizations previously reported, we predict that these processes will contribute to significantly more severe tissue damage at the oviduct relative to 1X infection (83-85, 120, 132). Moreover, the protective immunity during subsequent chlamydial infection in mice with an initial *Cm* infection initiated by repeated, low IFU doses will be less robust in comparison to that primed by *Cm* infection initiated by a single, high IFU dose, further predisposing the host to tissue pathology.

4.4 Conclusions

The results generated by the repeated infection model in this study indicate that repeated low dose infections with *Chlamydia* dysregulate the immune response to the infection; the outcomes we observed parallel reports of human disease sequelae. These reductions in protective immunity during subsequent infections and enhancements in tissue severity present in the repeated infection group are not aligned with the overall protective immune state and minimalized tissue responses from the mice that received the classic single dose infection. Therefore, the data from this paper suggests that using a repeated, low dose infection to model *Chlamydia* in mice may provide more thorough insight into the response processes in human chlamydial infection.

REFERENCES

1. Dharamshi JE, Tamarit D, Eme L, Stairs CW, Martijn J, Homa F, Jørgensen SL, Spang A, Ettema TJG. Marine sediments illuminate Chlamydiae diversity and evolution. Curr Biol. 2020;30(6):1032.
2. Elwell C, Mirrashidi K, Engel J. Chlamydia cell biology and pathogenesis. Nat Rev Microbiol. 2016;14(6):385.
3. Borel N, Polkinghorne A, Pospischil A. A review on chlamydial diseases in animals: Still a challenge for pathologists? Vet Pathol. 2018;55(3):374.
4. Taylor HR. Doyne Lecture: trachoma, is it history? Eye (Lond). 2009;23(11):2007.
5. Stephens RS, Myers G, Eppinger M, Bavoil PM. Divergence without difference: phylogenetics and taxonomy of Chlamydia resolved. FEMS Immunol Med Microbiol. 2009;55(2):115.
6. Clarke IN. Evolution of Chlamydia trachomatis. Ann N Y Acad Sci. 2011;1230:e11.
7. Darville T, Rours GIJG. 167 - Chlamydia trachomatis. In: Long SS, Prober CG, Fischer M, editors. Principles and Practice of Pediatric Infectious Diseases (Fifth Edition): Elsevier; 2018. p.908.
8. Gautam J, Krawiec C. Chlamydia Pneumonia. StatPearls. Treasure Island (FL): StatPearls Publishing LLC.; 2022.
9. Gitsels A, Sanders N, Vanrompay D. Chlamydial infection from outside to inside. Front Microbiol. 2019;10:2329.
10. World Health Organization. WHO alliance for the global elimination of trachoma by 2020: progress report on elimination of trachoma, 2018/Alliance OMS pour l'elimination mondiale du trachome d'ici 2020: Rapport de situation sur l'elimination du trachome, 2018. World Health Organization; 2019. Report No.: 0049-8114 Contract No.: 29.

11. World Health Organization. Global health sector strategy on sexually transmitted infections 2016-2021. Geneva, Switzerland: World Health Organization; 2016.

12. Vande Weygaerde Y, Versteele C, Thijs E, De Spiegeleer A, Boelens J, Vanrompay D, Van Braeckel E, Vermaelen K. An unusual presentation of a case of human psittacosis. Respir Med Case Rep. 2018;23:138.

13. Nogueira AT, Braun KM, Carabeo RA. Characterization of the growth of Chlamydia trachomatis in in vitro-generated stratified epithelium. Front Cell Infect Microbiol. 2017;7:438.

14. Liu X, Afrane M, Clemmer DE, Zhong G, Nelson DE. Identification of Chlamydia trachomatis outer membrane complex proteins by differential proteomics. J Bacteriol. 2010;192(11):2852.

15. Fadel S, Eley A. Differential glycosaminoglycan binding of Chlamydia trachomatis OmcB protein from serovars E and LGV. J Med Microbiol. 2008;57(Pt 9):1058.

16. Su H, Watkins NG, Zhang YX, Caldwell HD. Chlamydia trachomatis-host cell interactions: role of the chlamydial major outer membrane protein as an adhesin. Infect Immun. 1990;58(4):1017.

17. Ouellette SP, Dorsey FC, Moshiach S, Cleveland JL, Carabeo RA. Chlamydia species-dependent differences in the growth requirement for lysosomes. PLoS One. 2011;6(3):e16783.

18. Saka HA, Valdivia RH. Acquisition of nutrients by Chlamydiae: unique challenges of living in an intracellular compartment. Curr Opin Microbiol. 2010;13(1):4.

19. Lee JK, Enciso GA, Boassa D, Chander CN, Lou TH, Pairawan SS, et al. Replication-dependent size reduction precedes differentiation in Chlamydia trachomatis. Nat Commun. 2018;9(1):45.

20. Sherrid AM, Hybiske K. Chlamydia trachomatis cellular exit alters interactions with host dendritic cells. Infect Immun. 2017;85(5):e00046.

21. Panzetta ME, Valdivia RH, Saka HA. Chlamydia persistence: a survival strategy to evade antimicrobial effects in-vitro and in-vivo. Front Microbiol. 2018;9:3101.

22. Rottenberg ME, Gigliotti-Rothfuchs A, Wigzell H. The role of IFN-gamma in the outcome of chlamydial infection. Curr Opin Immunol. 2002;14(4):444.

23. Mpiga P, Ravaoarinoro M. Chlamydia trachomatis persistence: an update. Microbiol Res. 2006;161(1):9.

24. Worboys M. Chlamydia: A disease without a history. In: Szreter S, editor. The hidden affliction: sexually transmitted infections and infertility in history. Rochester (NY): University of Rochester Press; 2019.

25. Centers for Disease Control and Prevention. Sexually transmitted infection treatment guidelines, 2021: chlamydial infection 2021 [April 11, 2022]. Available from: https://www.cdc.gov/std/treatment-guidelines/chlamydia.htm#.

26. Huai P, Li F, Chu T, Liu D, Liu J, Zhang F. Prevalence of genital Chlamydia trachomatis infection in the general population: a meta-analysis. BMC Infect Dis. 2020;20(1):589.

27. Lee V, Tobin JM, Foley E. Relationship of cervical ectopy to chlamydia infection in young women. J Fam Plann Reprod Health Care. 2006;32(2):104.

28. Menon S, Timms P, Allan JA, Alexander K, Rombauts L, Horner P, Keltz M, Hocking J, Huston WM. Human and pathogen factors associated with Chlamydia trachomatis-related infertility in women. Clin Microbiol Rev. 2015;28(4):969.

29. Berry A, Hall JV. The complexity of interactions between female sex hormones and Chlamydia trachomatis infections. Curr Clin Microbiol Rep. 2019;6(2):67.

30. Gratrix J, Plitt S, Turnbull L, Smyczek P, Brandley J, Scarrott R, Naidu P, Parker P, Blore B, Bull A, Shokoples S, Bertholet L, Martin I, Chernesky M, Read R, Singh A. Prevalence and antibiotic resistance of Mycoplasma genitalium among STI clinic attendees in Western Canada: a cross-sectional analysis. BMJ Open. 2017;7(7):e016300.

31. Werner RN, Gaskins M, Nast A, Dressler C. Incidence of sexually transmitted infections in men who have sex with men and who are at substantial risk of HIV infection - A meta-analysis of data from trials and observational studies of HIV pre-exposure prophylaxis. PLoS One. 2018;13(12):e0208107.

32. MacGregor L, Speare N, Nicholls J, Harryman L, Horwood J, Kesten JM, Lorenc A, Horner P, Edelman NL, Muir P, North P, Gompels M, Turner KME. Evidence of changing sexual behaviours and clinical attendance patterns, alongside increasing diagnoses of STIs in MSM and TPSM. Sex Transm Infect. 2021;97(7):507.

33. Boutrin MC, Williams DR. What racism has to do with it: Understanding and reducing sexually transmitted diseases in youth of color. Healthcare (Basel). 2021;9(6):673.

34. Mohseni M, Sung S, Takov V. Chlamydia. StatPearls. Treasure Island (FL): StatPearls Publishing LLC.; 2022.

35. Moore A, Traversy G, Reynolds DL, Riva JJ, Thériault G, Wilson BJ, Subnath M, Thombs BD. Recommendation on screening for chlamydia and gonorrhea in primary care for individuals not known to be at high risk. Cmaj. 2021;193(16):e549.

36. Johnson LF, Lewis DA. The effect of genital tract infections on HIV-1 shedding in the genital tract: a systematic review and meta-analysis. Sex Transm Dis. 2008;35(11):946.

37. Zhu H, Shen Z, Luo H, Zhang W, Zhu X. Chlamydia trachomatis infection-associated risk of cervical cancer: a meta-analysis. Medicine (Baltimore). 2016;95(13):e3077.

38. Fortner RT, Terry KL, Bender N, Brenner N, Hufnagel K, Butt J, Waterboer T, Tworoger SS. Sexually transmitted infections and risk of epithelial ovarian cancer: results from the Nurses' Health Studies. Br J Cancer. 2019;120(8):855.

39. Curry A, Williams T, Penny ML. Pelvic inflammatory disease: diagnosis, management, and prevention. Am Fam Physician. 2019;100(6):357.

40. Shaw JL, Dey SK, Critchley HO, Horne AW. Current knowledge of the aetiology of human tubal ectopic pregnancy. Hum Reprod Update. 2010;16(4):432.

41. Wallace TM, Hart WR. Acute chlamydial salpingitis with ascites and adnexal mass simulating a malignant neoplasm. Int J Gynecol Pathol. 1991;10(4):394.

42. Davies B, Turner KME, Frølund M, Ward H, May MT, Rasmussen S, Benfield T, Westh H. Risk of reproductive complications following chlamydia testing: a population-based retrospective cohort study in Denmark. Lancet Infect Dis. 2016;16(9):1057.

43. Bautista CT, Hollingsworth BP, Sanchez JL. Repeat Chlamydia diagnoses increase the hazard of pelvic inflammatory disease among US Army women: A retrospective cohort analysis. Sex Transm Dis. 2018;45(11):770.

44. Trent M, Bass D, Ness RB, Haggerty C. Recurrent PID, subsequent STI, and reproductive health outcomes: findings from the PID evaluation and clinical health (PEACH) study. Sex Transm Dis. 2011;38(9):879.

45. Hillis SD, Owens LM, Marchbanks PA, Amsterdam LF, Mac Kenzie WR. Recurrent chlamydial infections increase the risks of hospitalization for ectopic pregnancy and pelvic inflammatory disease. Am J Obstet Gynecol. 1997;176(1 Pt 1):103.

46. Mårdh PA, Møller BR, Ingerselv HJ, Nüssler E, Weström L, Wølner-Hanssen P. Endometritis caused by Chlamydia trachomatis. Br J Vener Dis. 1981;57(3):191.

47. Weström L, Mårdh PA. Chlamydial salpingitis. Br Med Bull. 1983;39(2):145.

48. Paavonen J, Aine R, Teisala K, Heinonen PK, Punnonen R, Lehtinen M, Miettinen A, Grönroos P. Chlamydial endometritis. J Clin Pathol. 1985;38(7):726.

49. Rezvani M, Shaaban AM. Fallopian tube disease in the nonpregnant patient. Radiographics. 2011;31(2):527.

50. Kiviat NB, Wølner-Hanssen P, Eschenbach DA, Wasserheit JN, Paavonen JA, Bell TA, Critchlow CW, Stamm WE, Moore DE, Holmes KK. Endometrial histopathology in patients with culture-proved upper genital tract infection and laparoscopically diagnosed acute salpingitis. Am J Surg Pathol. 1990;14(2):167.

51. Ajonuma LC, Ng EHY, Chan LN, Chow PH, Kung LS, Cheung ANY, Ho LS, Briton-Jones C, Lok IH, Haines CJ, Chan HC. Ultrastructural characterization of whole hydrosalpinx from infertile Chinese women. Cell Biol Int. 2005;29(10):849.

52. Huttner KM, Bevins CL. Antimicrobial peptides as mediators of epithelial host defense. Pediatr Res. 1999;45(6):785.

53. Amjadi F, Salehi E, Mehdizadeh M, Aflatoonian R. Role of the innate immunity in female reproductive tract. Adv Biomed Res. 2014;3:1.

54. Xu JZ, Kumar R, Gong H, Liu L, Ramos-Solis N, Li Y, Derbigny WA, Roy CR. Toll-like receptor 3 deficiency leads to altered immune responses to Chlamydia trachomatis infection in human oviduct epithelial cells. Infect Immun. 2019;87(10):e00483.

55. Zou Y, Lei W, He Z, Li Z. The role of NOD1 and NOD2 in host defense against chlamydial infection. FEMS Microbiol Lett. 2016;363(17):e170.

56. Wang Y, Liu Q, Chen D, Guan J, Ma L, Zhong G, Shu H, Wu X. Chlamydial lipoproteins stimulate toll-like receptors 1/2 mediated inflammatory responses through MyD88-dependent pathway. Front Microbiol. 2017;8:78.

57. Chen H, Wen Y, Li Z. Clear victory for Chlamydia: the subversion of host innate immunity. Front Microbiol. 2019;10:1412.

58. Rasmussen SJ, Eckmann L, Quayle AJ, Shen L, Zhang YX, Anderson DJ, Fierer J, Stephens RS, Kagnoff MF. Secretion of proinflammatory cytokines by epithelial cells in response to Chlamydia infection suggests a central role for epithelial cells in chlamydial pathogenesis. J Clin Invest. 1997;99(1):77.

59. Kessler M, Hoffmann K, Fritsche K, Brinkmann V, Mollenkopf HJ, Thieck O, Teixeira da Costa AR, Braicu EI, Sehouli J, Mangler M, Berger H, Meyer TF. Chronic Chlamydia infection in human organoids increases stemness and promotes age-dependent CpG methylation. Nat Commun. 2019;10(1):1194.

60. Xiang W, Yu N, Lei A, Li X, Tan S, Huang L, Zhou Z. Insights into host cell cytokines in Chlamydia infection. Front Immunol. 2021;12:639834.

61. Jolly AL, Rau S, Chadha AK, Abdulraheem EA, Dean D. Stromal fibroblasts drive host inflammatory responses that are dependent on Chlamydia trachomatis strain type and likely influence disease outcomes. mBio. 2019;10(2):e00225.

62. Giakoumelou S, Wheelhouse N, Brown J, Wade J, Simitsidellis I, Gibson D, Saunders PTK, Horner P, Entrican G, Howie SEM, Horne AW. Chlamydia trachomatis infection of human endometrial stromal cells induces defective decidualisation and chemokine release. Sci Rep. 2017;7(1):2001.

63. Vicetti Miguel RD, Quispe Calla NE, Dixon D, Foster RA, Gambotto A, Pavelko SD, Hall-Stoodley L, Cherpes TL. IL-4-secreting eosinophils promote endometrial stromal cell proliferation and prevent Chlamydia-induced upper genital tract damage. Proc Natl Acad Sci U S A. 2017;114(33):e6892.

64. Ayala-Cuellar AP, Kang JH, Jeung EB, Choi KC. Roles of mesenchymal stem cells in tissue regeneration and immunomodulation. Biomol Ther (Seoul). 2019;27(1):25.

65. Soundararajan M, Kannan S. Fibroblasts and mesenchymal stem cells: Two sides of the same coin? J Cell Physiol. 2018;233(12):9099.

66. Wang J, Zhao Y, Wu X, Yin S, Chuai Y, Wang A. The utility of human fallopian tube mucosa as a novel source of multipotent stem cells for the treatment of autologous reproductive tract injury. Stem Cell Res Ther. 2015;6(1):98.

67. Guler Z, Roovers JP. Role of fibroblasts and myofibroblasts on the pathogenesis and treatment of pelvic organ prolapse. Biomolecules. 2022;12(1):94.

68. Singh N, Prasad P, Das B, Rastogi S. Involvement of matrix metalloproteinases and their inhibitors in endometrial extracellular matrix turnover in Chlamydia trachomatis-infected recurrent spontaneous aborters. Pathog Dis. 2017;75(1).

69. Santos GC, Silva DN, Fortuna V, Silveira BM, Orge ID, de Santana TA, Sampaio GL, Paredes BD, Ribeiro-dos-Santos R, Soares MBP. Leukemia inhibitory factor (LIF) overexpression increases the angiogenic potential of bone marrow mesenchymal stem/stromal cells. Front Cell Dev Biol. 2020;8:778.

70. Nicola NA, Babon JJ. Leukemia inhibitory factor (LIF). Cytokine Growth Factor Rev. 2015;26(5):533.

71. Krishnan T, Winship A, Sonderegger S, Menkhorst E, Horne AW, Brown J, Zhang JG, Nicola NA, Tong S, Dimitriadis E. The role of leukemia inhibitory factor in tubal ectopic pregnancy. Placenta. 2013;34(11):1014.

72. Horner PJ, Flanagan H, Horne AW. Is there a hidden burden of disease as a result of epigenetic epithelial-to-mesenchymal transition following Chlamydia trachomatis genital tract infection? J Infect Dis. 2021;224(12 Suppl 2):S128.

73. Ward LSC, Sheriff L, Marshall JL, Manning JE, Brill A, Nash GB, McGettrick HM. Podoplanin regulates the migration of mesenchymal stromal cells and their interaction with platelets. J Cell Sci. 2019;132(5):e222067.

74. Cimini M, Garikipati VNS, de Lucia C, Cheng Z, Wang C, Truongcao MM, Lucchese AM, Roy R, Benedict C, Goukassian DA, Koch WJ, Kishore R. Podoplanin neutralization improves cardiac remodeling and function after acute myocardial infarction. JCI Insight. 2019;5(15):e126967.

75. Vasilevsky S, Greub G, Nardelli-Haefliger D, Baud D. Genital Chlamydia trachomatis: understanding the roles of innate and adaptive immunity in vaccine research. Clin Microbiol Rev. 2014;27(2):346.

76. Metzemaekers M, Gouwy M, Proost P. Neutrophil chemoattractant receptors in health and disease: double-edged swords. Cell Mol Immunol. 2020;17(5):433.

77. Yang H, Biermann MH, Brauner JM, Liu Y, Zhao Y, Herrmann M. New insights into neutrophil extracellular traps: Mechanisms of formation and role in inflammation. Front Immunol. 2016;7:302.

78. Wang J. Neutrophils in tissue injury and repair. Cell Tissue Res. 2018;371(3):531.

79. Barteneva N, Theodor I, Peterson EM, de la Maza LM. Role of neutrophils in controlling early stages of a Chlamydia trachomatis infection. Infect Immun. 1996;64(11):4830.

80. Frazer LC, O'Connell CM, Andrews CW Jr., Zurenski MA, Darville T. Enhanced neutrophil longevity and recruitment contribute to the severity of oviduct pathology during Chlamydia muridarum infection. Infect Immun. 2011;79(10):4029.

81. Rajeeve K, Das S, Prusty BK, Rudel T. Chlamydia trachomatis paralyses neutrophils to evade the host innate immune response. Nat Microbiol. 2018;3(7):824.

82. Ramsey KH, Sigar IM, Schripsema JH, Shaba N, Cohoon KP. Expression of matrix metalloproteinases subsequent to urogenital Chlamydia muridarum infection of mice. Infect Immun. 2005;73(10):6962.

83. Moore-Connors JM, Fraser R, Halperin SA, Wang J. $CD4^{+}CD25^{+}Foxp3^{+}$ regulatory T cells promote Th17 responses and genital tract inflammation upon intracellular Chlamydia muridarum infection. J Immunol. 2013;191(6):3430.

84. Lacy HM, Bowlin AK, Hennings L, Scurlock AM, Nagarajan UM, Rank RG. Essential role for neutrophils in pathogenesis and adaptive immunity in Chlamydia caviae ocular infections. Infect Immun. 2011;79(5):1889.

85. Lijek RS, Helble JD, Olive AJ, Seiger KW, Starnbach MN. Pathology after Chlamydia trachomatis infection is driven by nonprotective immune cells that are distinct from protective populations. Proc Natl Acad Sci U S A. 2018;115(9):2216.

86. Tsuda Y, Takahashi H, Kobayashi M, Hanafusa T, Herndon DN, Suzuki F. Three different neutrophil subsets exhibited in mice with different susceptibilities to infection by methicillin-resistant Staphylococcus aureus. Immunity. 2004;21(2):215.

87. Ding L, Yang J, Zhang C, Zhang X, Gao P. Neutrophils modulate fibrogenesis in chronic pulmonary diseases. Front Med (Lausanne). 2021;8:616200.

88. Ojcius DM, Bravo de Alba Y, Kanellopoulos JM, Hawkins RA, Kelly KA, Rank RG, Dautry-Varsat A. Internalization of Chlamydia by dendritic cells and stimulation of Chlamydia-specific T cells. J Immunol. 1998;160(3):1297.

89. Gervassi A, Alderson MR, Suchland R, Maisonneuve JF, Grabstein KH, Probst P. Differential regulation of inflammatory cytokine secretion by human dendritic cells upon Chlamydia trachomatis infection. Infect Immun. 2004;72(12):7231.

90. Lausen M, Christiansen G, Bouet Guldbæk Poulsen T, Birkelund S. Immunobiology of monocytes and macrophages during Chlamydia trachomatis infection. Microbes Infect. 2019;21(2):73.

91. Shi C, Pamer EG. Monocyte recruitment during infection and inflammation. Nat Rev Immunol. 2011;11(11):762.

92. Herweg JA, Rudel T. Interaction of Chlamydiae with human macrophages. Febs j. 2016;283(4):608.

93. Gracey E, Lin A, Akram A, Chiu B, Inman RD. Intracellular survival and persistence of Chlamydia muridarum is determined by macrophage polarization. PLoS One. 2013;8(8):e69421.

94. Rajaram K, Nelson DE. Chlamydia muridarum infection of macrophages elicits bactericidal nitric oxide production via reactive oxygen species and cathepsin B. Infect Immun. 2015;83(8):3164.

95. Zhang Y, Huang B. The development and diversity of ILCs, NK cells and their relevance in health and diseases. Adv Exp Med Biol. 2017;1024:225.

96. Shi FD, Ljunggren HG, La Cava A, Van Kaer L. Organ-specific features of natural killer cells. Nat Rev Immunol. 2011;11(10):658.

97. Wang H, Li J, Dong X, Zhou X, Zhao L, Wang X, Rashu R, Zhao W, Yang X. NK cells contribute to protective memory T cell mediated immunity to Chlamydia muridarum infection. Front Cell Infect Microbiol. 2020;10:296.

98. Tseng CT, Rank RG. Role of NK cells in early host response to chlamydial genital infection. Infect Immun. 1998;66(12):5867.

99. Hook CE, Matyszak MK, Gaston JS. Infection of epithelial and dendritic cells by Chlamydia trachomatis results in IL-18 and IL-12 production, leading to interferon-gamma production by human natural killer cells. FEMS Immunol Med Microbiol. 2005;45(2):113.

100. Zhao L, Wang H, Thomas R, Gao X, Bai H, Shekhar S, Wang S, Yang J, Zhao W, Yang X. NK cells modulate T cell responses via interaction with dendritic cells in Chlamydophila pneumoniae infection. Cell Immunol. 2020;353:104132.

101. Xu H, Su X, Zhao Y, Tang L, Chen J, Zhong G. Innate lymphoid cells are required for endometrial resistance to Chlamydia trachomatis infection. Infect Immun. 2020;88(7):e00152.

102. Toubal A, Nel I, Lotersztajn S, Lehuen A. Mucosal-associated invariant T cells and disease. Nat Rev Immunol. 2019;19(10):643.

103. Gibbs A, Leeansyah E, Introini A, Paquin-Proulx D, Hasselrot K, Andersson E, Broliden K, Sandberg JK, Tjernlund A. MAIT cells reside in the female genital mucosa and are biased towards IL-17 and IL-22 production in response to bacterial stimulation. Mucosal Immunol. 2017;10(1):35.

104. Ibana JA, Schust DJ, Sugimoto J, Nagamatsu T, Greene SJ, Quayle AJ. Chlamydia trachomatis immune evasion via downregulation of MHC class I surface expression involves direct and indirect mechanisms. Infect Dis Obstet Gynecol. 2011;2011:420905.

105. Del Balzo D, Capmany A, Cebrian I, Damiani MT. Chlamydia trachomatis infection impairs MHC-I intracellular trafficking and antigen cross-presentation by dendritic cells. Front Immunol. 2021;12:662096.

106. Kägebein D, Gutjahr M, Große C, Vogel AB, Rödel J, Knittler MR. Chlamydia trachomatis-infected epithelial cells and fibroblasts retain the ability to express surface-presented major histocompatibility complex class I molecules. Infect Immun. 2014;82(3):993.

107. Roche PA, Furuta K. The ins and outs of MHC class II-mediated antigen processing and presentation. Nat Rev Immunol. 2015;15(4):203.

108. Karunakaran KP, Yu H, Jiang X, Chan Q, Moon KM, Foster LJ, Brunham RC. Outer membrane proteins preferentially load MHC class II peptides: implications for a Chlamydia trachomatis T cell vaccine. Vaccine. 2015;33(18):2159.

109. Zhong G, Fan T, Liu L. Chlamydia inhibits interferon gamma-inducible major histocompatibility complex class II expression by degradation of upstream stimulatory factor 1. J Exp Med. 1999;189(12):1931.

110. Jiang X, Shen C, Rey-Ladino J, Yu H, Brunham RC. Characterization of murine dendritic cell line JAWS II and primary bone marrow-derived dendritic cells in Chlamydia muridarum antigen presentation and induction of protective immunity. Infect Immun. 2008;76(6):2392.

111. Moniz RJ, Chan AM, Kelly KA. Identification of dendritic cell subsets responding to genital infection by Chlamydia muridarum. FEMS Immunol Med Microbiol. 52009;55(2):226.

112. Darville T, Hiltke TJ. Pathogenesis of genital tract disease due to Chlamydia trachomatis. J Infect Dis. 2010;201 Suppl 2(Suppl 2):S114.

113. Seder RA, Ahmed R. Similarities and differences in CD4+ and CD8+ effector and memory T cell generation. Nat Immunol. 2003;4(9):835.

114. Bakshi RK, Gupta K, Jordan SJ, Chi X, Lensing SY, Press CG, Geisler WM. An adaptive Chlamydia trachomatis-specific IFN-γ-producing CD4(+) T cell response is associated with protection against Chlamydia reinfection in women. Front Immunol. 2018;9:1981.

115. Ibana JA, Myers L, Porretta C, Lewis M, Taylor SN, Martin DH, Quayle AJ. The major CD8 T cell effector memory subset in the normal and Chlamydia trachomatis-infected human endocervix is low in perforin. BMC Immunol. 2012;13:66.

116. Matyszak MK, Gaston JS. Chlamydia trachomatis-specific human CD8+ T cells show two patterns of antigen recognition. Infect Immun. 2004;72(8):4357.

117. Lampe MF, Wilson CB, Bevan MJ, Starnbach MN. Gamma interferon production by cytotoxic T lymphocytes is required for resolution of Chlamydia trachomatis infection. Infect Immun. 1998;66(11):5457.

118. Zhou Z, Tian Q, Wang L, Sun X, Zhang N, Xue M, Xu D, Zhong G, Roy CR. Characterization of pathogenic CD8(+) T cells in Chlamydia-infected OT1 mice. Infect Immun. 2022;90(1):e0045321.

119. Igietseme JU, Ramsey KH, Magee DM, Williams DM, Kincy TJ, Rank RG. Resolution of murine chlamydial genital infection by the adoptive transfer of a biovar-specific, Th1 lymphocyte clone. Reg Immunol. 1993;5(6):317.

120. Hawkins RA, Rank RG, Kelly KA. A Chlamydia trachomatis-specific Th2 clone does not provide protection against a genital infection and displays reduced trafficking to the infected genital mucosa. Infect Immun. 2002;70(9):5132.

121. Martinez-Sanchez ME, Huerta L, Alvarez-Buylla ER, Villarreal Luján C. Role of cytokine combinations on CD4+ T cell differentiation, partial polarization, and plasticity: continuous network modeling approach. Front Physiol. 2018;9:877.

122. Murphy KM, Stockinger B. Effector T cell plasticity: flexibility in the face of changing circumstances. Nat Immunol. 2010;11(8):674.

123. Zhu X, Zhu J. CD4 T helper cell subsets and related human immunological disorders. Int J Mol Sci. 2020;21(21):8011.

124. Su H, Caldwell HD. CD4+ T cells play a significant role in adoptive immunity to Chlamydia trachomatis infection of the mouse genital tract. Infect Immun. 1995;63(9):3302.

125. Gondek DC, Roan NR, Starnbach MN. T cell responses in the absence of IFN-gamma exacerbate uterine infection with Chlamydia trachomatis. J Immunol. 2009;183(2):1313.

126. Naglak EK, Morrison SG, Morrison RP. IFNγ is required for optimal antibody-mediated immunity against genital Chlamydia infection. Infect Immun. 2016;84(11):3232.

127. Helble JD, Gonzalez RJ, von Andrian UH, Starnbach MN. Gamma interferon is required for Chlamydia clearance but is dispensable for T cell homing to the genital tract. mBio. 2020;11(2):e00191.

128. Ibana JA, Belland RJ, Zea AH, Schust DJ, Nagamatsu T, AbdelRahman YM, Tate DJ, Beatty WL, Aiyar AA, Quayle AJ, Morrison RP. Inhibition of indoleamine 2,3-dioxygenase activity by levo-1-methyl tryptophan blocks gamma interferon-induced Chlamydia trachomatis persistence in human epithelial cells. Infect Immun. 2011;79(11):4425.

129. Rixon JA, Depew CE, McSorley SJ. Th1 cells are dispensable for primary clearance of Chlamydia from the female reproductive tract of mice. PLoS Pathog. 2022;18(2):e1010333.

130. Vicetti Miguel RD, Harvey SA, LaFramboise WA, Reighard SD, Matthews DB, Cherpes TL. Human female genital tract infection by the obligate intracellular bacterium Chlamydia trachomatis elicits robust Type 2 immunity. PLoS One. 2013;8(3):e58565.

131. Zhang M, Zhang S. T cells in fibrosis and fibrotic diseases. Front Immunol. 2020;11:1142.

132. Vicetti Miguel RD, Quispe Calla NE, Pavelko SD, Cherpes TL. Intravaginal Chlamydia trachomatis challenge infection elicits T_H1 and T_H17 immune responses in mice that promote pathogen clearance and genital tract damage. PLoS One. 2016;11(9):e0162445.

133. Labuda JC, McSorley SJ. Diversity in the T cell response to Chlamydia-sum are better than one. Immunol Lett. 2018;202:59.

134. Morrison SG, Farris CM, Sturdevant GL, Whitmire WM, Morrison RP. Murine Chlamydia trachomatis genital infection is unaltered by depletion of CD4+ T cells and diminished adaptive immunity. J Infect Dis. 2011;203(8):1120.

135. Li LX, McSorley SJ. A re-evaluation of the role of B cells in protective immunity to Chlamydia infection. Immunol Lett. 2015;164(2):88.

136. Ramsey KH, Soderberg LS, Rank RG. Resolution of chlamydial genital infection in B-cell-deficient mice and immunity to reinfection. Infect Immun. 1988;56(5):1320.

137. Rank RG, Batteiger BE, Soderberg LS. Susceptibility to reinfection after a primary chlamydial genital infection. Infect Immun. 1988;56(9):2243.

138. Morrison SG, Su H, Caldwell HD, Morrison RP. Immunity to murine Chlamydia trachomatis genital tract reinfection involves B cells and CD4(+) T cells but not CD8(+) T cells. Infect Immun. 2000;68(12):6979.

139. Morrison SG, Morrison RP. A predominant role for antibody in acquired immunity to chlamydial genital tract reinfection. J Immunol. 2005;175(11):7536.

140. Li LX, McSorley SJ. B cells enhance antigen-specific CD4 T cell priming and prevent bacteria dissemination following Chlamydia muridarum genital tract infection. PLoS Pathog. 2013;9(10):e1003707.

141. Naglak EK, Morrison SG, Morrison RP. Neutrophils are central to antibody-mediated protection against genital Chlamydia. Infect Immun. 2017;85(10): e00409.

142. Öhman H, Rantsi T, Joki-Korpela P, Tiitinen A, Surcel HM. Prevalence and persistence of Chlamydia trachomatis-specific antibodies after occasional and recurrent infections. Sex Transm Infect. 2020;96(4):277.

143. Murthy AK, Li W, Ramsey KH. Immunopathogenesis of chlamydial infections. Curr Top Microbiol Immunol. 2018;412:183.

144. Kol A, Bourcier T, Lichtman AH, Libby P. Chlamydial and human heat shock protein 60s activate human vascular endothelium, smooth muscle cells, and macrophages. J Clin Invest. 1999;103(4):571.

145. Huittinen T, Leinonen M, Tenkanen L, Mänttäri M, Virkkunen H, Pitkänen T, Wahlström E, Palosuo T, Manninen V, Saikku P. Autoimmunity to human heat shock protein 60, Chlamydia pneumoniae infection, and inflammation in predicting coronary risk. Arterioscler Thromb Vasc Biol. 2002;22(3):431.

146. Domeika M, Domeika K, Paavonen J, Mårdh PA, Witkin SS. Humoral immune response to conserved epitopes of Chlamydia trachomatis and human 60-kDa heat-shock protein in women with pelvic inflammatory disease. J Infect Dis. 1998;177(3):714.

147. Stephens RS. The cellular paradigm of chlamydial pathogenesis. Trends Microbiol. 2003;11(1):44.

148. Stacey C, Munday P, Thomas B, Gilchrist C, Taylor-Robinson D, Beard R. Chlamydia trachomatis in the fallopian tubes of women without laparoscopic evidence of salpingitis. Lancet. 1990;336(8721):960.

149. De Clercq E, Kalmar I, Vanrompay D. Animal models for studying female genital tract infection with Chlamydia trachomatis. Infect Immun. 2013;81(9):3060.

150. Bell JD, Bergin IL, Schmidt K, Zochowski MK, Aronoff DM, Patton DL. Nonhuman primate models used to study pelvic inflammatory disease caused by Chlamydia trachomatis. Infect Dis Obstet Gynecol. 2011;2011:675360.

151. Käser T, Renois F, Wilson HL, Cnudde T, Gerdts V, Dillon JR, Jungersen G, Agerholm JS, Meurens F. Contribution of the swine model in the study of human sexually transmitted infections. Infect Genet Evol. 2018;66:346.

152. de Jonge MI, Keizer SA, El Moussaoui HM, van Dorsten L, Azzawi R, van Zuilekom HI, Peters PPW, van Opzeeland FJH, van Dijk L, Nieuwland R, Roosenboom-Theunissen HWM, Vrijenhoel MP, van Duijnhoven WGF, van den Bosch JF, Nuijten PJM. A novel guinea pig model of Chlamydia trachomatis genital tract infection. Vaccine. 2011;29(35):5994.

153. Kaushic C, Zhou F, Murdin AD, Wira CR. Effects of estradiol and progesterone on susceptibility and early immune responses to Chlamydia trachomatis infection in the female reproductive tract. Infect Immun. 2000;68(7):4207.

154. Dockterman J, Coers J. Immunopathogenesis of genital Chlamydia infection: insights from mouse models. Pathog Dis. 2021;79(4):e012.

155. de la Maza LM, Pal S, Khamesipour A, Peterson EM. Intravaginal inoculation of mice with the Chlamydia trachomatis mouse pneumonitis biovar results in infertility. Infect Immun. 1994;62(5):2094.

156. Shah AA, Schripsema JH, Imtiaz MT, Sigar IM, Kasimos J, Matos PG, Inouye S, Ramsey KH. Histopathologic changes related to fibrotic oviduct occlusion after genital tract infection of mice with Chlamydia muridarum. Sex Transm Dis. 2005;32(1):49.

157. Sturdevant GL, Caldwell HD. Innate immunity is sufficient for the clearance of Chlamydia trachomatis from the female mouse genital tract. Pathog Dis. 2014;72(1):70.

158. Rank RG, Whittum-Hudson JA. Protective immunity to chlamydial genital infection: evidence from animal studies. J Infect Dis. 2010;201 Suppl 2:S168.

159. Phillips S, Quigley BL, Timms P. Seventy years of Chlamydia vaccine research - limitations of the past and directions for the future. Front Microbiol. 2019;10:70.

160. Rank RG, Bowlin AK, Reed RL, Darville T. Characterization of chlamydial genital infection resulting from sexual transmission from male to female guinea pigs and determination of infectious dose. Infect Immun. 2003;71(11):6148.

161. Maxion HK, Liu W, Chang MH, Kelly KA. The infecting dose of Chlamydia muridarum modulates the innate immune response and ascending infection. Infect Immun. 2004;72(11):6330.

162. Carey AJ, Cunningham KA, Hafner LM, Timms P, Beagley KW. Effects of inoculating dose on the kinetics of Chlamydia muridarum genital infection in female mice. Immunol Cell Biol. 2009;87(4):337.

163. Belij-Rammerstorfer S, Inic-Kanada A, Stojanovic M, Marinkovic E, Lukic I, Stein E, Montanaro J, Bintner N, Schürer N, Ghasemian E, Kundi M, Barisani-Asenbauer T. Infectious dose and repeated infections are key factors influencing immune response characteristics in guinea pig ocular chlamydial infection. Microbes Infect. 2016;18(4):254.

164. Geisler WM, Suchland RJ, Whittington WL, Stamm WE. Quantitative culture of Chlamydia trachomatis: relationship of inclusion-forming units produced in culture to clinical manifestations and acute inflammation in urogenital disease. J Infect Dis. 2001;184(10):1350.

165. Herbenick D, Rosenberg M, Golzarri-Arroyo L, Fortenberry JD, Fu TC. Changes in penile-vaginal intercourse frequency and sexual repertoire from 2009 to 2018: Findings from the National Survey of Sexual Health and Behavior. Arch Sex Behav. 2022;51(3):1419.

166. Schneider CA, Rasband WS, Eliceiri KW. NIH Image to ImageJ: 25 years of image analysis. Nat Methods. 2012;9(7):671.

167. Zeng H, Gong S, Hou S, Zou Q, Zhong G. Identification of antigen-specific antibody responses associated with upper genital tract pathology in mice infected with Chlamydia muridarum. Infect Immun. 2012;80(3):1098.

168. Sun X, Yang Z, Zhang H, Dai J, Chen J, Tang L, Rippentrop S, Xue M, Zhong G, Wu G, Morrison RP. Chlamydia muridarum induction of glandular duct dilation in mice. Infect Immun. 2015;83(6):2327.

169. Firacative C, Gressler AE, Schubert K, Schulze B, Müller U, Brombacher F, von Bergen M, Alber G. Identification of T helper (Th)1- and Th2-associated antigens of Cryptococcus neoformans in a murine model of pulmonary infection. Sci Rep. 2018;8(1):2681.

170. Belay T, Eko FO, Ananaba GA, Bowers S, Moore T, Lyn D, Igietseme JU. Chemokine and chemokine receptor dynamics during genital chlamydial infection. Infect Immun. 2002;70(2):844.

171. McDonald B, Kubes P. Chemokines: sirens of neutrophil recruitment-but is it just one song? Immunity. 2010;33(2):148.

172. Sawant KV, Poluri KM, Dutta AK, Sepuru KM, Troshkina A, Garofalo RP, Rajarathnam K. Chemokine CXCL1 mediated neutrophil recruitment: Role of glycosaminoglycan interactions. Sci Rep. 2016;6:33123.

173. Capucetti A, Albano F, Bonecchi R. Multiple roles for chemokines in neutrophil biology. Frontiers in Immunology. 2020;11:1259.

174. Chakraborty S, Kubatzky KF, Mitra DK. An update on interleukin-9: From its cellular source and signal transduction to its role in immunopathogenesis. Int J Mol Sci. 2019;20(9):2113.

175. Veldhoen M, Uyttenhove C, van Snick J, Helmby H, Westendorf A, Buer J, Martin B, Wilhelm C, Stockinger B. Transforming growth factor-beta 'reprograms' the differentiation of T helper 2 cells and promotes an interleukin 9-producing subset. Nat Immunol. 2008;9(12):1341.

176. Anuradha R, George PJ, Hanna LE, Chandrasekaran V, Kumaran P, Nutman TB, Babu S. IL-4-, TGF-β-, and IL-1-dependent expansion of parasite antigen-specific Th9 cells is associated with clinical pathology in human lymphatic filariasis. J Immunol. 2013;191(5):2466.

177. Licona-Limón P, Henao-Mejia J, Temann AU, Gagliani N, Licona-Limón I, Ishigame H, Hao L, Herbert DR, Flavell RA. Th9 cells drive host immunity against gastrointestinal worm infection. Immunity. 2013;39(4):744.

178. Peng Y, Gao X, Yang J, Shekhar S, Wang S, Fan Y, Yang X, Ojcius DM. Chlamydial lung infection induces transient IL-9 production which is redundant for host defense against primary infection. PLoS One. 2015;10(2):e0115195.

179. Rank RG, Lacy HM, Goodwin A, Sikes J, Whittimore J, Wyrick PB, Nagarajan UM. Host chemokine and cytokine response in the endocervix within the first developmental cycle of Chlamydia muridarum. Infect Immun. 2010;78(1):536.

180. Virok DP, Raffai T, Kókai D, Paróczai D, Bogdanov A, Veres G, Vécsei L, Poliska S, Tiszlavicz L, Somogyvári F, Endrész V, Burián K. Indoleamine 2,3-dioxygenase activity in Chlamydia muridarum and Chlamydia pneumoniae infected mouse lung tissues. Front Cell Infect Microbiol. 2019;9:192.

181. Walz A, Schmutz P, Mueller C, Schnyder-Candrian S. Regulation and function of the CXC chemokine ENA-78 in monocytes and its role in disease. J Leukoc Biol. 1997;62(5):604.

182. Hey YY, Tan JK, O'Neill HC. Redefining myeloid cell subsets in murine spleen. Front Immunol. 2015;6:652.

183. Yu YR, Hotten DF, Malakhau Y, Volker E, Ghio AJ, Noble PW, Kraft M, Hollingsworth JW, Gunn MD, Tighe RM. Flow cytometric analysis of myeloid cells in human blood, bronchoalveolar lavage, and lung tissues. Am J Respir Cell Mol Biol. 2016;54(1):13.

184. Cain TK, Rank RG. Local Th1-like responses are induced by intravaginal infection of mice with the mouse pneumonitis biovar of Chlamydia trachomatis. Infect Immun. 1995;63(5):1784.

185. Braun N, Alscher DM, Fritz P, Edenhofer I, Kimmel M, Gaspert A, Reimold F, Bode-Lesniewska B, Ziegler U, Biegger D, Wüthrich RP, Segerer S. Podoplanin-positive cells are a hallmark of encapsulating peritoneal sclerosis. Nephrol Dial Transplant. 2011;26(3):1033.

186. Braun N, Alscher MD, Fritz P, Latus J, Edenhofer I, Reimold F, Alper SL, Kimmel M, Biegger D, Lindenmeyer M, Cohen CD, Wüthrich RP, Segerer S, Kano MR. The spectrum of podoplanin expression in encapsulating peritoneal sclerosis. PLoS One. 2012;7(12):e53382.

187. Cimini M, Cannatá A, Pasquinelli G, Rota M, Goichberg P. Phenotypically heterogeneous podoplanin-expressing cell populations are associated with the lymphatic vessel growth and fibrogenic responses in the acutely and chronically infarcted myocardium. PLoS One. 2017;12(3):e0173927.

188. Lax S, Rayes J, Thickett DR, Watson SP. Effect of anti-podoplanin antibody administration during lipopolysaccharide-induced lung injury in mice. BMJ Open Respir Res. 2017;4(1):e000257.

189. Hasan SA, Eksteen B, Reid D, Paine HV, Alansary A, Johannson K, Gwozd C, Goring KR, Vo T, Proud D, Kelly MM. Role of IL-17A and neutrophils in fibrosis in experimental hypersensitivity pneumonitis. J Allergy Clin Immunol. 2013;131(6):1663.

190. Gregory AD, Kliment CR, Metz HE, Kim KH, Kargl J, Agostini BA, Crum LT, Oczypok EA, Oury TA, Houghton AM. Neutrophil elastase promotes myofibroblast differentiation in lung fibrosis. J Leukoc Biol. 2015;98(2):143.

191. Zhou Z, Xu MJ, Cai Y, Wang W, Jiang JX, Varga ZV, Feng D, Pacher P, Kunos G, Torok NJ, Gao Bin. Neutrophil-hepatic stellate cell interactions promote fibrosis in experimental steatohepatitis. Cell Mol Gastroenterol Hepatol. 2018;5(3):399.

192. Tang J, Yan Z, Feng Q, Yu L, Wang H. The roles of neutrophils in the pathogenesis of liver diseases. Front Immunol. 2021;12:625472.

193. Akbar M, Crowe LAN, McLean M, Garcia-Melchor E, MacDonald L, Carter K, Fazzi UG, Martin D, Arthur A, Reilly JH, McInnes IB, Millar NL. Translational targeting of inflammation and fibrosis in frozen shoulder: Molecular dissection of the T cell/IL-17A axis. Proc Natl Acad Sci U S A. 2021;118(39): e2102715118.

194. Biancheri P, Pender SL, Ammoscato F, Giuffrida P, Sampietro G, Ardizzone S, Ghanbari A, Curciarello R, Pasini A, Monteleone G, Corazza GR, Macdonald TT, Di Sabatino A. The role of interleukin 17 in Crohn's disease-associated intestinal fibrosis. Fibrogenesis Tissue Repair. 2013;6(1):13.

195. Fang S, Huang Y, Zhong S, Li Y, Zhang Y, Li Y, Sun J, Liu X, Wang Y, Zhang S, Xu T, Sun X, Gu P, Li D, Zhou H, Li B, Fan X. Regulation of orbital fibrosis and adipogenesis by pathogenic Th17 cells in Graves orbitopathy. J Clin Endocrinol Metab. 2017;102(11):4273.

196. Park MJ, Moon SJ, Lee EJ, Jung KA, Kim EK, Kim DS, Lee JH, Kwok SK, Min JK, Park SH, Cho ML. IL-1-IL-17 signaling axis contributes to fibrosis and inflammation in two different murine models of systemic sclerosis. Front Immunol. 2018;9:1611.

197. Ugolini M, Sander LE. Dead or alive: how the immune system detects microbial viability. Curr Opin Immunol. 2019;56:60.